UNIVERSITY OF BELGRADE

FACULTY OF MEDICINE

Aleksandar V. Ćirović

Microstructural basis of increased bone fragility in the femoral neck of individuals with type 2 diabetes mellitus

Doctoral dissertation

Belgrade, 2023

UNIVERSITY OF BELGRADE

FACULTY OF MEDICINE

Aleksandar V. Ćirović

Microstructural basis of increased bone fragility in the femoral neck of individuals with type 2 diabetes mellitus

Doctoral dissertation

Belgrade, 2023

UNIVERZITET U BEOGRADU

MEDICINSKI FAKULTET

Aleksandar V. Ćirović

Promene u mikrostrukturi kao osnova povećane fragilnosti vrata butne kosti osoba sa tip 2 dijabetesom

Doktorska disertacija

Beograd, 2023

PhD Advisor:

Prof. Dr. Petar Milovanović, Associate Professor, Faculty of Medicine, University of Belgrade

Members of the Committee:

Prof. Dr. Marija Đurić, Full Professor, Faculty of Medicine, University of Belgrade

Prof. Dr. Zoran Baščarević, Full Professor, Faculty of Medicine, University of Belgrade

Prof. Dr. Radmila Matijević, Associate Professor, Faculty of Medicine, University of Novi Sad

Date of Defense:

……

Ментор:

Проф. др Петар Миловановић, ванредни професор, Медицински факултет, Универзитет у Београду

Чланови Комисије:

Проф. др Марија Ђурић, редовни професор, Медицински факултет, Универзитет у Београду

Проф. др Зоран Башчаревић, редовни професор, Медицински факултет, Универзитет у Београду

Проф. др Радмила Матијевић, ванредни професор, Медицински факултет, Универзитет у Новом Саду

Датум одбране:

.....

At first, I would like to express my deepest gratitude to Dr. Petar Milovanović for his exceptional guidance and unwavering support throughout the completion of my thesis. The invaluable contributions and expertise provided by Dr. Milovanović have played a pivotal role in shaping the trajectory of my research journey. I am truly grateful for the immense dedication and time invested in providing mentorship. Dr. Milovanović's insightful feedback, constructive criticism, and thoughtful suggestions have consistently challenged me to reach new heights of academic excellence. The guidance and support offered have not only expanded my understanding of the subject matter but have also fostered personal and professional growth. Beyond the academic realm, Dr. Milovanović has exemplified the highest standards of integrity, passion for research, and commitment to lifelong learning. These qualities have not only shaped my research endeavors but have also instilled in me a deep appreciation for the pursuit of knowledge. Furthermore, I am grateful for the vibrant academic community created under Dr. Milovanović's guidance. The emphasis on collaboration, intellectual curiosity, and open dialogue has enriched my overall experience as a researcher.

First and foremost, I would like to express my sincere gratitude to Professor Marija Đurić for her comprehensive and selfless support throughout the entire process. I am immensely grateful for the valuable assistance she provided. Additionally, I would like to acknowledge the significant contributions made by Professor Danijela Đonić and Dr. Jelena Jadžić, whose diligent efforts greatly contributed to the success of this PhD thesis. I am truly indebted to all the individuals associated with the Center for Bone Biology, as this thesis is a collective outcome of their dedication and hard work.

I would also like to extend a special thank you to Professor Slobodan Nikolić, Professor Vladimir Živković, Dr. Danica Đukić, Professor Zoran Baščarević, Dr. Marko Vujačić, and Dr. Bojan Petrović for their invaluable support during the demanding sample collection phase. Your expertise and assistance were instrumental in the completion of this research.

I would like to express my sincere appreciation and gratitude to Dr. Felix N. Schmidt, Bashar Yazigi, Dr. Praveer Sihota, and Prof. Björn Busse for their invaluable contribution to my PhD thesis. Their expertise and diligent analysis of scanning femoral neck images using Quantitative Backscattered Electron Imaging (qBEI) have significantly enhanced the quality and depth of my research.

Lastly, I dedicate this thesis to my beloved family—my wife Ana, my daughter Mila, my brother Nikola, and my parents Marija and Veroljub. Your unwavering love and encouragement have been my greatest source of inspiration throughout this journey

Belgrade, 2023

Microstructural basis of increased bone fragility in the femoral neck of individuals with type 2 diabetes mellitus

Summary

Introduction: The number of individuals with type 2 diabetes (T2DM) has reached alarming levels worldwide, with projections indicating that it will assume pandemic proportions in the future. Physicians and scientists are becoming increasingly aware of the elevated fracture risk in individuals with T2DM compared with non-diabetic individuals. However, the fracture mechanisms associated with T2DM are not yet fully understood, and preventive programs remain underdeveloped.

Aim: This thesis aimed to investigate the alterations in cortical and trabecular bone caused by the presence of T2DM in the femoral neck, a common site of fracture in diabetic subjects. In parallel with this investigation, we conducted a detailed analysis of the microarchitecture along the superolateral femoral neck in elderly individuals for two reasons. First, it is a common site for the initiation of fractures, and second, if the microarchitecture of the superolateral femoral neck is non-uniform, the areas with weaker microarchitecture might experience additional deterioration in the presence of diabetes.

Material and methods: We performed densitometric (DXA) measurements, microarchitectural analyses, bone mineral density distribution, osteocyte lacunar density, and microhardness measurements in the trabeculae of the femoral head (18 individuals with T2DM and fracture, and 25 non-T2DM individuals without fracture), as well as DXA measurements, microarchitectural analyses, osteocyte lacunar density, and microhardness measurements in the regions of the superolateral femoral neck (8 individuals with T2DM without fracture, and 8 non-T2DM individuals without fracture). The surgical samples of the femoral heads from individuals who had sustained fragility fractures and had been diagnosed with T2DM prior to the appearance of the fracture were collected at surgery (Institute for Orthopedic Surgery Banjica), while their appropriate control specimens and specimens of the superolateral femoral neck (both T2DM and control) were collected during autopsies (Institute of Forensic Medicine, Belgrade).

Results: The femoral neck T-score was similar between T2DM individuals and controls without fractures. However, we observed a lower femoral neck T-score in T2DM individuals who had sustained fragility fractures compared with controls. The presence of T2DM was associated with lower cortical porosity and thickness in the superolateral femoral neck, indicating weaker cortical bone. Although the trabecular microarchitecture was similar between T2DM individuals and controls at the examined sites, the presence of vascular complications in T2DM subjects contributed to the deterioration of trabecular microarchitecture. The microhardness measurements revealed lower values in both cortical and trabecular bone of the superolateral femoral neck, as well as in the trabeculae of the femoral head, in individuals with T2DM. This suggests a reduction in the overall hardness and mechanical strength of bone in T2DM. Bone mineral density distribution analysis revealed decreased calcium heterogeneity in the trabeculae of the femoral head in T2DM individuals. There were no significant differences in osteocyte lacunar density parameters between T2DM individuals and controls for the trabeculae of the femoral head and femoral neck, but the cortex of the superolateral femoral neck exhibited an altered pattern of osteocyte distribution. Specifically, T2DM individuals showed a lower number of non-mineralized lacunae per bone area in the endocortical and periosteal regions of the superolateral femoral neck in the T2DM group compared with the corresponding regions in the

control group. Although the number of mineralized lacunae per bone area was similar between the two groups, the ratio of mineralized to total lacunae tended to be higher in the T2DM group. Cortical porosity varied significantly along the superolateral femoral neck, with highest percent of critical areas (low cortical thickness and/or high cortical porosity) located in the subcapital part of superolateral femoral neck. Among the three subregions of the superolateral femoral neck, the basicervical part had better microarchitecture of both cortical and trabecular compartments.

Conclusions: In summary, the results of this study demonstrate that T2DM is associated with significant alterations in the bone structure and quality of the superolateral femoral neck and trabeculae of the femoral head. The findings indicate that individuals with T2DM have weaker cortical bone, impaired trabecular microarchitecture in the presence of vascular complications, reduced microhardness, and altered patterns of osteocyte lacunar density in the superolateral femoral neck. These findings highlight the negative impact of diabetes on bone health and emphasize the need for further research and the development of preventive strategies and interventions to mitigate the increased fracture risk in individuals with T2DM.

Key words: diabetes; bone quality; microarchitecture; DXA; osteocyte lacunar density

Scientific field: Medicine

Scientific subfield: Skeletal biology

UDK Nr: ……

Promene u mikrostrukturi kao osnova povećane fragilnosti vrata butne kosti osoba sa tip 2 dijabetesom

Sažetak

Uvod: Broj obolelih od dijabetesa tipa 2 (T2DM) je dostigao alarmantne razmere širom sveta, sa projekcijama koje ukazuju da će ovo hronično nezarazno oboljenje u budućnosti dostići pandemijske razmere. Sa druge strane, lekari i naučnici sve više postaju svesni povećanog rizika od preloma kod osoba sa T2DM u poređenju sa osobama bez dijabetesa. Međutim, mehanizmi koji dovode do povećane koštane fragilnosti kod osoba sa T2DM još uvek nisu potpuno razjašnjeni, a preventivni programi su nedovoljno razvijeni.

Cilj: Stoga, cilj ovog istraživanja je bio da se ispitaju promene koje T2DM izaziva kako u kortikalnom tako i u trabekularnom delu vrata butne kosti, uobičajenom mestu nastanka preloma. Paralelno sa ovim istraživanjem, detaljno smo analizirali mikroarhitekturne varijacije duž superolateralnog dela vrata butne kosti iz dva razloga. Prvo, superolateralni deo vrata je uobičajeno mesto za inicijaciju frakture prilikom pada na bok, a drugo, ako mikroarhitektura superolateralnog dela vrata nije uniformna, područja sa slabijom mikroarhitekturom mogu biti dodatno oslabljena u prisustvu dijabetesa.

Materijal i metode: Za potrebe ovog rada, izvršili smo denzitometrijska merenja, analizu mikroarhitekture, stepena mineralizacije koštanog tkiva, gustine mineralizovanih i nemineralizovanih osteocitnih lakuna, kao i merenje mikrotvrdoće na trabekulama glave femura (18 osoba sa T2DM i frakturom, i 25 osoba bez T2DM i frakture); obavili smo i denzitometrijska merenja, analizu mikroarhitekture, gustine mineralizovanih i nemineralizovanih osteocitnih lakuna, kao i merenje mikrotvrdoće u regionima superolateralnog dela vrata femura (8 osoba sa T2DM bez frakture i 8 osoba bez T2DM i frakture). Uzorci glave femura su dobijeni sa operacija (na Institutu za ortopedskohirurške bolesti „Banjica“) osoba sa prelomom vrata butne kosti kod kojih je pre pojave preloma postavljena dijagnoza T2DM, dok su adekvatni kontrolni uzorci i uzorci superolateralnog dela vrata femura (i T2DM i kontrolna grupa) prikupljeni tokom rutinskih obdukcija na Institutu za sudsku medicinu u Beogradu.

Rezultati: T-skor vrata femura je bio sličan između osoba sa T2DM i kontrolne grupe (obe grupe bez preloma), dok smo uočili niži T-skor vrata femura kod osoba sa T2DM sa prelomom kuka u poređenju sa kontrolnom grupom. Grupa sa T2DM je pokazala manju kortikalnu poroznost i debljinu superolateralnog dela vrata butne kosti, što je ukazalo na smanjenu mehaničku otpornost kosti. Iako je generalno trabekularna mikroarhitektura bila slična kod osoba sa T2DM i kontrolne grupe na oba ispitivana mesta, prisustvo vaskularnih komplikacija kod osoba sa T2DM je dovelo i do pogoršanja trabekularne mikroarhitekture glave butne kosti. Mikrotvrdoća je bila niža i u kortikalnoj i u trabekularnoj kosti superolateralnog dela butne kosti, kao i u trabekulama glave butne kosti, što ukazuje na smanjenje ukupne tvrdoće i mehaničke otpornosti kostiju kod T2DM. Analiza mineralizacije koštanog matriksa je pokazala homogeniju raspodelu kalcijuma u trabekulama glave butne kosti kod osoba sa T2DM. Gustina osteocitnih lakuna je bila slična kod osoba sa T2DM i kontrolne grupe u trabekulama glave butne kosti. Međutim, kortikalna kost superolateralnog dela vrata butne kosti je pokazala promene u gustini osteocitnih lakuna. Konkretno, pronađen je manji broj nemineralizovanih osteocitnih lakuna po koštanoj površini u endokortikalnim i periostealnim regijama superolateralnog dela vrata butne kosti kod grupe sa T2DM u poređenju sa odgovarajućim regijama u kontrolnoj grupi. Iako je broj mineralizovanih osteocitnih lakuna po površini kosti bio sličan između dve grupe, procenat mineralizovanih

lakuna u odnosu na ukupan broj lakuna je bio viši kod T2DM grupe. Kao i debljina korteksa, kortikalna poroznost je značajno varirala duž superolateralnog dela vrata butne kosti, sa najvećim procentom kritičnih područja (zona sa malom kortikalnom debljinom i/ili visokom kortikalnom poroznošću) u subkapitalnom delu superolateralnog dela vrata butne kosti. Od tri podregiona superolateralnog dela butne kosti, bazicervikalni deo je pokazao bolju mikroarhitekturu kako u kortikalnom tako i u trabekularnom odeljku. Promene na vratu femura nastale usled prisustva dijabetesa ustvari predstavljaju pogoršanje kvaliteta kostiju na različitim nivoima organizaje. Kortikalna poroznost je pokazala značajnu varijaciju duž superolateralnog dela butne kosti, sa najvećim procentom kritičnih područja (karakterisanih niskom kortikalnom debljinom i/ili visokom kortikalnom poroznošću) zapaženim u subkapitalnom delu superolateralnog dela butne kosti.

Zaključci: Ukratko, rezultati ove studije pokazuju da T2DM dovodi do značajnih promena u koštanoj strukturi i kvalitetu superolateralnog dela vrata butne kosti i trabekulama glave butne kosti. Nalazi ukazuju da osobe sa T2DM imaju slabiju kortikalnu kost, oštećenu trabekularnu mikroarhitekturu u prisustvu vaskularnih komplikacija, smanjenu mikrotvrdoću i izmenjen obrazac gustine osteocitnih lakuna u superolateralnom delu vrata butne kosti. Ovi rezultati ističu negativan uticaj dijabetesa na zdravlje kostiju i naglašavaju potrebu za daljim istraživanjima i razvojem preventivnih strategija i intervencija radi smanjenja povećanog rizika od preloma kod osoba sa T2DM.

Ključne reči: dijabetes, kvalitet kosti, mikroarhitektura, osteodenzitometrija, osteocitne lakune

Naučna oblast: Medicina

Uža naučna oblast: Biologija skeleta

UDK broj: ……

CONTENTS

SECTION 1

Introduction

Type 2 diabetes mellitus (T2DM) is a non-communicable disease characterized by chronically high blood glucose levels. Projections for the number of new cases in the near future are discouraging; it is expected that by the beginning of the next decade, more than 550 million individuals worldwide will be affected by T2DM (Aschner et al., 2021). Hyperglycemia often causes damage to small blood vessels, leading to tissue damage and numerous complications that can affect almost any organ, including bones. Diabetic complications may appear more rapidly if the disease is not well controlled, and it is estimated that more than 70% of subjects with T2DM have insufficiently controlled blood glucose levels (Alzaheb and Altemani, 2018). In addition to well-known complications of diabetes, such as diabetic nephropathy, neuropathy, and retinopathy, increased bone fracture risk has recently been recognized as another complication of T2DM and has been attracting broad research attention.

Osteoporosis represents another significant public health problem. The World Health Organization provides a clear distinction between osteoporosis and osteopenia. Specifically, according to the World Health Organization's definition, osteoporosis is characterized by a bone mineral density (BMD) that falls more than 2.5 standard deviations below the average BMD of young individuals. On the other hand, osteopenia is identified as a BMD that ranges between 1 and 2.5 standard deviations below the average BMD of young individuals. It is primarily a bone disease that, if unrecognized, inevitably leads to fractures. In addition to spine and wrist fractures, hip fractures are common in individuals with osteoporosis (Hanusch et al., 2017; Oyen et al., 2011; Warriner et al., 2011). Although the majority of fractures occur in women (Alswat, 2017; Kim et al., 2010), osteoporosis is also a substantial health problem for men. A number of factors could influence bone quality, such as the status of bone microarchitecture, the amount and characteristics of collagen fibers and other extracellular proteins (e.g., osteopontin, osteonectin, protein C), the degree of bone extracellular matrix mineralization, and the total and mineralized osteocyte lacunar numbers. While bone microarchitecture can be roughly examined with computed tomography (CT) (Poole et al., 2012), micro-CT and peripheral quantitative computed tomography (pQCT) can provide much more accurate data about all trabecular and cortical parameters. In the past two decades, microarchitecture of the proximal femur has been extensively studied (Chen et al., 2010; Djuric et al., 2010; Milovanovic et al., 2012). It is known that the superolateral femoral neck presents poorer bone microarchitecture than the inferomedial femoral neck, especially in aged individuals (Milovanovic et al., 2012), which is why the superolateral femoral neck is the most common starting site of an age-related hip fracture (de Bakker et al., 2009; Zani et al., 2015). However, data regarding microarchitectural variability within the superolateral femoral neck are still limited. Anatomical classification of the femoral neck fractures distinguishes between three main types, namely, subcapital, transcervical, and basicervical fractures, depending on which subregion of the superolateral femoral neck specifically is broken, but it is unknown whether there is microstructural basis for the preferential fracture occurrence at a certain subregion of the femoral neck.

Although bone mineral density (BMD) is a surrogate marker of bone strength (Jiang et al. 2000), and individuals with lower BMD are considered to have a higher risk of osteoporotic fractures, individuals with T2DM often have higher BMD compared with controls (Nilsson et al., 2017). The Fracture Risk Assessment Tool (FRAX), another method designed to predict general and hip fracture risk in subjects between 40 and 90 years, is also not sufficiently reliable in subjects with T2DM, given that it partly relies on BMD, which may be higher in T2DM subjects than in controls (Valentini et al., 2018). Indeed, the results of densitometric studies alone cannot explain the epidemiological data showing a substantially increased fracture risk among subjects with diabetes (Fan et al., 2016). Even after stratifying the risk by the type of diabetes (T1DM and T2DM), the susceptibility to fractures remains substantial in T2DM subjects (relative risk, RR=1.34) (Fan et al., 2016). Therefore, it is essential to

comprehensively explore bone characteristics in individuals with T2DM at both the macroscopic and the microscopic levels (Cirovic and Milovanovic, 2023).

In a recent study, Schousboe et al. (2022) analyzed incidence of fracture in 80,238 individuals, including 8,676 with diagnosed T2DM, and showed that subjects with T2DM had an increased risk of sustaining hip fracture and proximal humeral fractures, while the risk of forearm fractures was not associated with T2DM. However, the majority of studies that assessed cortical and trabecular microarchitecture of T2DM subjects have focused on the distal radius and distal tibia (Samakkarnthai et al., 2020; Shanbhogue et al., 2016), which are not frequent fracture sites in individuals with T2DM. For these regions, if subjects with T2DM have no history of vascular complications or fragility fractures, bone microarchitecture does not seem to differ between T2DM and control groups (Samakkarnthai et al., 2020). Evaluation of bone microarchitecture at the femoral neck—the typical fracture location—in T2DM individuals has been rare, and even when examined, T2DM subjects have shown equally good (Karim et al., 2018) or even better microarchitecture than controls (Osima et al., 2017). However, microarchitectural examination of the femoral neck has usually been conducted at a relatively poor resolution (over 600 μm) (Osima et al., 2017), which does not provide sufficient quality for the quantitative assessment of bone microstructure. Consequently, data on the microstructural basis of bone fragility at the femoral neck in T2DM remain scarce.

While other features that generally contribute to bone strength, such as the osteocyte lacunar number, characteristics of collagen fibers, osteon density, or the degree of cortical and trabecular mineralization, may be affected by T2DM, there are insufficient data in the literature to show whether they are responsible for bone fragility in T2DM. Wölfel et al. (2020) demonstrated that individuals with T2DM and high cortical porosity had lower osteon density at the subtrochanteric region of the femoral diaphysis compared with T2DM subjects with normal cortical porosity and the control group. It is known that bone matrix composition changes with aging, i.e., there are changes in the mineral and organic components of the bone matrix (Zimmermann et al. 2011), which may be related to the reduction in bone mechanical competence (Zimmermann et al. 2011). However, there are limited data on the bone composition changes in individuals with T2DM and their association with the increased fracture risk. For example, accumulation of advanced glycation end-products (AGEs), often marked as non-enzymatic cross-links, physiologically occurs during aging; when accumulated in abundance, AGEs cause increased bone stiffness and consequently lower resistance to fracture (Zimmermann et al., 2011). The existing studies present conflicting findings regarding the levels of advanced glycation end-products (AGEs) in the bones of individuals with T2DM. Some studies, such as those by Karim et al. (2018) and Wölfel et al. (2020), have reported similar levels of bone AGEs in T2DM subjects compared with controls. On the other hand, Sihota et al. (2021) found increased AGEs levels in T2DM subjects. Consequently, it remains uncertain whether the composition of the bone matrix in T2DM is significantly altered.

In addition to AGEs, other aspects of bone quality may also be affected by T2DM. Milovanovic et al. (2015) observed an increased number of hypermineralized osteocyte lacunae in individuals with osteoporosis, but there are no data in individuals with T2DM. Wölfel et al. (2020) demonstrated an altered pattern of mineralization in the cortical regions (endocortical and periosteal regions) of the femur diaphysis in individuals with T2DM, but there are still no data at the regions of the femoral neck.

Considering the increased fracture risk in individuals with T2DM, it is apparent that analyzing only one aspect of bone quality is largely insufficient. It is likely that T2DM affects bone quality in multiple ways. Therefore, further examination of various aspects of the bone matrix at the femoral neck is necessary to gain a comprehensive understanding of the origins of bone fragility in T2DM subjects. Such knowledge can be valuable in developing strategies for preventing fractures in individuals

SECTION 2

The objectives and outline of the research

Considering that the increased hip fracture risk in individuals with T2DM cannot be explained by analyzing only one aspect of bone quality, it is necessary to profoundly examine bone tissue specimens in T2DM subjects, so that the origins of bone fragility in these patients can be understood and appropriate preventive and therapeutic measures can be designed.

In this context, the **overall aim** of this thesis was to investigate how T2DM alters various microarchitectural, cellular, compositional, and micromechanical features of clinically and biomechanically relevant bone regions of the femoral neck, and whether these changes could explain the increased fracture risk at these sites in individuals with T2DM.

In **Section 3**, we examined the trabecular bone specimens from the femoral head in individuals with T2DM who have sustained a fragility hip fracture and in a control, non-fracture group of non-T2DM individuals of similar age and sex. Our aim was to investigate whether the fracture susceptibility in individuals with T2DM-related hip fracture is reflected in trabecular bone microarchitecture of the femoral head region. Considering that the specimens of T2DM individuals were obtained at surgery in individuals who broke their femoral neck at variable subregions, in order to analyze consistent bone specimens and ensure reliable comparisons with the control group (autopsy specimens), here we explored the femoral head trabeculae that are directly adjacent and continuous with the inferomedial femoral neck compartment. The main goal of this study was to determine whether T2DM influences trabecular microarchitecture and whether there is a link between fracture appearance and microarchitectural parameters. This study represents an important first step in understanding the adverse effects of T2DM on bone quality. In view of the general expectation that T2DM may have heterogenous effects in different individuals, given that clinical data were available for T2DM patients, we also analyzed whether the bone microarchitecture in T2DM individuals was related to the various clinical parameters, such as T score, FRAX, and presence of vascular complications, which could be helpful in clinical practice.

In **Section 4**, we analyzed the microarchitectural parameters and micromechanical characteristics (microhardness) of the cortical and trabecular compartments at the superolateral femoral neck in individuals with T2DM (without fracture) and control group of similar age, sex, and body mass index (BMI). With this study, we have taken a step further in examining the potential influence of T2DM on bone quality, given that the superolateral femoral neck is the typical site where hip fractures initiate. Moreover, although the individuals with T2DM included in this study hadnot yet sustained a hip fracture, the biomechanical relevance of the investigated T2DM-related microarchitectural deterioration was possible to evaluate considering that we measured the micromechanical properties of the examined bony regions as a surrogate for bone strength. Therefore, clarifying whether T2DM causes any changes in the microarchitecture and microhardness of the bone at the superolateral femoral neck is beneficial for a better understanding of the fracture mechanism in individuals with T2DM.

We next focused on the superolateral femoral neck in non-T2DM individuals and investigated whether there were any cortical and trabecular microarchitectural differences (variations) within this region, which could make some parts of the superolateral femoral neck more vulnerable and prone to fracture. Our starting point for this study was the assumption that the superolateral femoral neck microarchitecture is nonuniform, although previous studies have insufficiently considered this important question. In general, anatomical classification distinguishes three types of femoral neck fractures, depending on the exact site of the fracture line: subcapital, transcervical (midcervical), and basicervical. Most previous studies examined the midcervical part of the femoral neck only, where as subcapital and basicervical regions remained largely unexplored. Therefore, in **Section 5**, we compared the bone microarchitecture of the subcapital and basicervical parts of the superolateral femoral neck.

After revealing the variations in bone microarchitecture between the subregions of the superolateral femoral neck and considering that hip fractures may originate at any subregion of the femoral neck (though with different likelihood and frequency), in **Section 6** we further mapped cortical porosity and cortical thickness along the superolateral femoral neck, hypothesizing that areas with a particularly low thickness and high porosity of the cortex may be the "weak spots" where the fracture may initiate. This analysis was conducted preferentially in women because two-thirds of osteoporotic fractures occur in older females.

With the results obtained in Sections 5 and 6, we concluded that the division of the superolateral femoral neck to the subcapital, midcervical, and basicervical subregions is meaningful for fracture risk stratification. Therefore, in **Section 7**, we divided the superolateral femoral neck to the subcapital, midcervical, and basicervical subregions both in T2DM and in control specimens. Specifically, to further understand the origins of bone fragility in T2DM, our aim was to investigate the effects of T2DM on other relevant bone quality indexes, such as the density of osteocyte lacunae (total, mineralized, and non-mineralized) in cortical and trabecular compartments of the superolateral femoral neck and its subregions. Furthermore, in trabecular bone specimens adjacent to the femoral neck, we analyzed parameters related to matrix mineralization to determine whether T2DM could change the mineralization patterns. Such a multiscale assessment of the specimens with T2DM and non-T2DM provided deeper insights into the fundamental origins of bone fragility related to T2DM.

SECTION 3

Vascular complications in individuals with type 2 diabetes mellitus additionally increase the risk of femoral neck fractures due to deteriorated trabecular microarchitecture

The results presented in this Section were first published in: Cirovic A, Vujacic M, Petrovic B, Cirovic A, Zivkovic V, Nikolic S, Djonic D, Bascarevic Z, Djuric M, Milovanovic P. Vascular Complications in Individuals with Type 2 Diabetes Mellitus Additionally Increase the Risk of Femoral Neck Fractures Due to Deteriorated Trabecular Microarchitecture. Calcif Tissue Int. 2022 Jan;110(1):65-73. doi: 10.1007/s00223-021-00894-5, and are reproduced with permission from Springer.

3.1. Abstract

Individuals with diabetes mellitus type 2 (T2DM) have an increased risk of hip fracture, especially if vascular complications are present. However, microstructural origins of increased bone fragility in T2DM are still controversial. DXA measurement of the contralateral hip and three-dimensional microCT analyses of femoral neck trabecular microarchitecture were performed in 32 individuals (26 women and 6 men, 78±7 years). The specimens were divided to two groups: T2DM individuals with hip fracture (DMFx, n=18) and healthy controls (CTL, n=14). DMFx group consisted of individuals with vascular complications (DMFx_VD, n=8) and those without vascular complications (DMFx_NVD, n=10).T score was significantly lower in DMFx_VD and DMFx_NVD than in controls ($p<0.001$). BV/TV, Tb.N, Tb.Sp, SMI, and FD varied among DMFx_NVD, DMFx_VD, and CTL groups ($p=0.023$, $p=0.004$, $p=0.008$, $p=0.001$, $p=0.007$, respectively). Specifically, BV/TV of DMFx_VD was significantly lower than that of DMFx_NVD group ($p=0.020$); DMFx_NVD group had higher Tb.N and lower Tb.Sp compared with DMFx_VD ($p=0.006$, $p=0.012$, respectively) and CTL ($p=0.026$, $p=0.035$, respectively). DMFx group and healthy controls showed similar BV/TV, Tb.Th, Tb.N, Tb.Sp, Conn.D, DA, and FD ($p=0.771$, $p=0.503$, $p=0.285$, $p=0.266$, $p=0.208$, $p=0.235$, $p=0.688$, respectively), while SMI was significantly higher in controls ($p=0.005$). Two distinct phenotypes of bone fragility were identified in T2DM patients: patients with vascular complications showed impaired trabecular microarchitecture, whereas bone fragility in the group without vascular complications was independent on trabecular microarchitecture pattern. Such heterogeneity among T2DM patients may explain contradicting literature data, and may set a basis for further studies to evaluate fracture risk related to T2DM.

Keywords: T2DM; fracture; femoral neck; microarchitecture; trabeculae

3.2. Introduction

Diabetes mellitus (DM) is one of the fastest expanding, public health problems of the 21st century. According to World Health Organization (WHO), DM occurs in every twelfth non-pediatric individual, and it is estimated that in 2045 there will be 700 million individuals with DM worldwide (Saeedi et al. 2019). Poorly controlled glucose levels accelerate the development of diabetic complications, such as diabetic neuropathy, diabetic retinopathy, etc. Moreover, patients with DM complications are at an increased risk of falls and higher risk of bone fracture (Napoli et al. 2017; Vestergaard et al. 2009; Yokomoto-Umakoshi et al. 2017). Despite frequently having normal or even a higher bone mineral density (BMD) (Bonds et al. 2006; Lipscombe et al. 2007; Nilsson et al. 2017a; Schwartz et al. 2002), patients with type 2 DM (T2DM) are at an increased risk of sustaining hip fracture (Bonds et al. 2006; Dede et al. 2014; Fan et al. 2016; Janghorbani et al. 2007; Schwartz et al. 2002; Tebe et al. 2019; Vestergaard et al. 2009). Almost a third of patients with hip fracture die within the first year after fracture (Panula et al. 2011), while mortality after hip fracture in patients with coexisting DM is approximately two times higher (Dubey et al. 2000; Gulcelik et al. 2011; Tebe et al. 2019).

Studies of bone microarchitecture were conducted to try to unravel the reasons for higher bone fragility in spite of BMD out of osteoporotic range. According to studies which used high-resolution peripheral quantitative computed tomography (HR-pQCT), cortical and trabecular microarchitecture of distal tibia and radius is at least equally good or even slightly improved in T2DM individuals with no vascular complications or history of hip fracture compared with healthy controls (Nilsson et al. 2017b; Patsch et al. 2013; Shanbhogue et al. 2016). In contrast, some studies suggested deteriorated microarchitecture of distal radius and tibia in T2DM individuals with microvascular complications such as diabetic retinopathy, neuropathy or nephropathy (Shanbhogue et al. 2016) or who had previously sustained hip fracture (Patsch et al. 2013) compared with controls.

Although hip fractures are more common in T2DM patients (Janghorbani et al. 2007; Lipscombe et al. 2007), data on femoral microarchitecture in those patients are still limited. Wölfel et al. recently identified a subgroup of T2DM individuals with increased subtrochanteric cortical porosity and a subgroup with normal cortical porosity (Wölfel et al. 2020). Osima et al. (Osima et al. 2017) also examined subtrochanteric region of the femoral diaphysis using low-resolution computed tomography (CT), and showed lower cortical porosity in postmenopausal women with T2DM compared with those without DM. In contrast, Karim et al. did not find any significant differences in cortical or trabecular bone microarchitecture of the femoral neck and head between T2DM and non-diabetic patients undergoing total hip replacement surgery for osteoarthritis (Karim et al. 2018). Hunt et al. (Hunt et al. 2019) reported that in men undergoing total hip arthroplasty for osteoarthritis, a lower trabecular separation and a trend to higher trabecular number were observed at the femoral neck of T2DM patients compared with non-DM controls. However, those studies of femoral microarchitecture did not include T2DM patients who sustained a hip fracture, and most of them analyzed specimens with osteoarthritis. Considering an overall trend of improved microarchitecture of the femoral neck in individuals with hip osteoarthritis (Djuric et al. 2013) and likely reduced hip fracture risk (Chudyk et al. 2012; Franklin et al. 2010), assessment of patients with severe osteoarthritis has a limited value for understanding the real fracture risk. Therefore, it is important to assess femoral bone microarchitecture in DM patients who sustained a hip fracture. Moreover, considering that it was suggested that DM patients with cardiovascular complications have a greater fracture risk (Napoli et al. 2017; Vestergaard et al. 2009), it should be analyzed whether the presence of vascular complications influence bone microarchitecture in T2DM patients. Considering lack of microarchitectural assessments of the femoral neck in T2DM patients with hip fracture as well as contradicting results obtained in previous HR-pQCT and micro-CT studies, the aims of our study were to examine whether there is microarchitectural basis for bone fragility in patients with T2DM and to determine whether trabecular microarchitecture in T2DM patients is affected by the presence of vascular complications. Therefore, here we compared trabecular microarchitecture of the femoral neck between T2DM patients who sustained a hip fracture and had confirmed vascular complications, T2DM patients with hip fracture and no positive history of vascular complications, and age-matched healthy controls; moreover, we pooled all individuals with T2DM to compare trabecular microarchitecture of the femoral neck between T2DM subjects with fracture and healthy controls.

3.3. Material and methods

3.3.1. Groups of individuals

For this study we obtained the femoral neck specimens of 32 individuals (age 78 ± 7 years; 26 women and 6 men). The specimens were divided to two groups: T2DM individuals with hip fracture (DMFx, n=18) and healthy controls (CTL, n=14). In DMFx group, we identified two subgroups: individuals with vascular complications (DMFx_VD, n=8) and individuals without vascular complications (DMFx_NVD, n=10) (Table 1).

The DMFx group encompassed patients with T2DM who were undergoing total hip arthroplasty due to hip fracture at a tertiary-level, orthopedic university hospital (Institute for Orthopedic Surgery "Banjica", Belgrade). This was a consecutive group of patients treated during 2019, until the Institute was turned to a COVID-19 hospital as a governmental measure in securing enough beds for COVID-19 patients with moderately severe disease. The inclusion criteria were as follows: i) T2DM treated with oral antidiabetic medications (documented in clinical records and medical history); ii) unilateral fracture of the femoral neck caused by fall at the same level; iii) clinical decision to treat the fracture surgically using hip arthroplasty; iv) patient's consent to surgery; v) patient's informed consent to be included in the study. The exclusion criteria encompassed the presence of other diseases or treatments with significant effects on bone metabolism or structure, as follows: i) rheumatoid arthritis; ii) inborn

skeletal anomalies; iii) chronic liver disease; iv) any type of malignancy; v) endocrine diseases such as acromegaly, hypo- or hyperparathyroidism; vi) treatment with bisphosphonates, glucocorticoids, estrogen, anticonvulsants, or antipsychotics; vii) hip osteoarthritis. All included patients had intracapsular fracture of the femoral neck, whereas patients with trochanteric fracture were not included in the study. Before arthroplasty, DXA of the spine and contralateral hip was conducted, and HbA1c level was measured. Data about patients' health status, including vascular complications and medications used, were collected from anamnesis, clinical records, and medical history. All the individuals with vascular complications had mainly macrovascular complications such as peripheral artery disease, stroke, ischemic heart disease including myocardial infarction, or carotid artery (Table 2). We calculated the FRAX score for each patient who underwent total hip arthroplasty. Characteristics of patients with T2DM and non-diabetic controls are summarized in Table 1.

Table 1. Characteristics of T2DM individuals with fracture and no known vascular complications (DMFx_NVD), T2DM individuals with fracture and known vascular complications (DMFx_VD), and nondiabetic controls (CTL).

Characteristics	**DMFx_NVD (N=10)**	**DMFx_VD (N=8)**	**CTL (N=14)**	**p**	**Post-hoc analyses**
Demographic					
Age (years)[¥]	75.1±6.7	80.87±5.1	77.93±6.8	0.179	NA
Sex (women)[#]	9 (90%)	6 (75%)	11 (78.6%)	0.729	NA
Duration of T2DM (years)*	6.4±7.3	13.8±10.5	NA	0.158	NA
Duration of menopause (years)*	24.2±6.1	29.2±1.3	NA	0.08	NA
Anthropometry					
Body mass index (kg/m^2)[¥]	26.3±3.5	24.7±2	25.5±5.7	0.814	NA
Biochemical					
Hemoglobin A1c (HbA1c, %)*	6±1.4	6.2±1.6	NA	0.801	NA
Creatinine*	93.5±19.5	107.6±47.7	NA	0.437	NA
Diabetes medications					
Metformin[#]	9/10 (90%)	5/8 (62.5%)	NA	0.274	NA
Sulfonylureas[#]	4/10 (40%)	4/8 (50%)	NA	1	NA
FRAX score[¥]	2.5±1.7	2.5±1.1	3.9±3.2	0.536	NA
T-score femoral neck[¥]	-2.1±0.7	-2.2±0.6	1.6±0.5	<0.001	<0.001 (DMFx_NVD vs CTL) <0.001 (DMFx_VD vs CTL)
T-score lumbar spine*	-1.33±1.1	-1.4±0.6	NA	0.886	NA

**T* test for independent samples

[¥] One-way ANOVA

[#] Fisher's exact test

Table 2. List of vascular complications in T2DM patients (DMFx_VD).

DMFx_VD subjects	Age	Sex	Vascular complication
Subject 1	81	Male	Coronary artery disease
Subject 2	75	Female	Stroke
Subject 3	87	Female	Carotid artery disease
Subject 4	74	Male	Myocardial infarction
Subject 5	80	Female	Coronary artery disease
Subject 6	78	Female	Neuropathy
Subject 7	86	Female	Coronary artery disease
Subject 8	86	Female	Coronary artery disease

T2DM was relatively well-controlled at the time before fracture, considering that HbA1c values were on average 6.07% ± 1.42% [range 4.3%–8.4%]. The patients signed informed consent and the procedures were approved by the institutional review board of the Institute for Orthopedic Surgery "Banjica".

To ensure having the same and consistent bony part available for the micro-CT analysis, control group (CTL) included individuals who were admitted to the Institute of Forensic Medicine in Belgrade for autopsy. Their main causes of death were natural or sudden deaths, such as cardiac arrest, respiratory failure, car accidents with preserved hip region, and violent death. Inclusion criteria were as follows: i) no T1DM and T2DM; ii) no history of hip fracture. Exclusion criteria were based on medical history and autopsy reports, and they encompassed the following: i) rheumatoid arthritis; ii) inborn skeletal anomalies; iii) chronic kidney disease; iv) chronic liver disease; v) any type of malignancy in the moment of death; vi) acromegaly, and hypo- or hyperparathyroidism; vii) known treatment with bisphosphonates, glucocorticoids, estrogen, anticonvulsants, or antipsychotics; viii) hip osteoarthritis; ix) manifest vascular complications. For each individual in the control group, postmortem DXA measurement was performed and FRAX score was calculated. All the procedures were approved by the Ethics Committee of the Faculty of Medicine, University of Belgrade.

3.3.2. Collection and preparation of bone specimens

Immediately after removal at surgery or autopsy, the femoral neck samples were stored in 4% formaldehyde solution at 4°C. From each of the 32 samples, an approximately 10 mm x 10 mm trabecular bone cube was cut directly inferior to the epiphyseal line of the femoral head/neck interface in the direction of the femoral head fovea, as suggested in a previous study (Ciarelli et al. 2000), by using a water-cooled low-speed diamond saw. The excised trabecular region was chosen due to following reasons: (i) it represents the continuation of the inferomedial femoral neck compartment at the base of the femoral head, and (ii) the examined bone cube was not affected by the fracture line, so the samples could be harvested and analyzed in a consistent manner.

3.3.3. Microcomputed tomography

Each specimen was placed on a sample holder in a consistent orientation and scanned using Skyscan 1172 micro-computed tomography system (Bruker microCT, Skyscan, Belgium) with the following scanning conditions and parameters: 80 kV, 124 μA, 1200 ms exposure time. A combined aluminum and copper filter was used. 2K camera binning was used, leading to 10 μm isotropic resolution. Rotation step of 0.40° and triple frame averaging were chosen. We reconstructed the obtained projection images using NRecon software (Bruker microCT, Belgium) on InstaRecon platform (InstaRecon, USA) with Gaussian smoothing of 3, thermal drift correction, misalignment compensation, ring artifact and beam hardening corrections as needed. A global gray-level threshold of

95/255 was selected to distinguish between the mineralized and non-mineralized tissue. We manually marked the region of interest (ROI) for each slice to obtain the volume of interest (VOI). We analyzed at least 1000 slices per sample, meaning that the sample thickness of at least 1 cm per subject was evaluated. After importing all 32 VOIs to CT.An software (ver. 1.16.4.1: Skyscan, Belgium), we analyzed the following trabecular bone parameters: trabecular bone volume fraction (BV/TV, %), trabecular number (Tb.N, 1/mm), trabecular thickness (Tb.Th, mm), trabecular separation (Tb.Sp, mm), connectivity density ($1/mm^3$), structure model index (SMI, dimensionless), fractal dimension (FD, dimensionless), degree of anisotropy (DA, dimensionless).

3.3.4. Statistical analysis

The Kolmogorov-Smirnov test was used to verify that all measured parameters complied with the normal distribution. One-way ANOVA was performed to check for overall differences in age, BMI, femoral neck and lumbar spine T-scores, FRAX scores, and microarchitectural bone parameters between DMFx_VD, DMFx_NVD, and CTL groups; when overall ANOVA showed p value <0.05, pairwise comparisons (post-hoc tests) under Bonferroni correction for multiple testing were conducted. *T* tests for independent samples were used to compare microarchitectural bone parameters between DMFx and CTL, as well as quantitative parameters between the two DMFx subgroups (disease duration, menopause duration, hemoglobin A1c level, creatinine level). Fisher's exact probability test was used to evaluate the difference in sex distribution and medications between the groups. All analyses were performed two-tailed in SPSS software ver. 15 at the significance level of 0.05.

3.4. Results

We compared femoral trabecular microarchitecture among individuals with T2DM who experienced hip fracture and had confirmed vascular complications (DMFx_VD, n=8), individuals with T2DM who sustained hip fracture and had no vascular complications (DMFx_NVD, n=10), and healthy controls (CTL, n=14).

DMFx_NVD, DMFx_VD, and CTL groups did not differ in age (p=0.179), sex (p=0.701), and BMI (p=0.814). FRAX score for hip fracture was similar between the groups (p=0.536); nevertheless, we found a significantly reduced femoral neck T-score in DMFx_VD and DMFx_NVD groups compared with CTL group (p<0.001). DMFx_VD and DMFx_NVD groups did not differ in HbA1c (p=0.801), duration of disease (p=0.158), or creatinine level (p=0.437). Moreover, T-score of the femoral neck and lumbar spine did not vary significantly between the DMFx subgroups (p=0.906, p=0.886, respectively).

3.4.1. Microarchitectural analyses of DMFx and CTL groups

Comparison between DMFx and CTL groups revealed no significant differences in BV/TV, Tb.Th, Tb.N, Tb.Sp, Conn.D, DA, and FD (p=0.771, p=0.503, p=0.285, p=0.266, p=0.208, p=0.235, p=0.688, respectively), whereas SMI was slightly but significantly higher in controls (p=0.005) (Table 3).

Table 3. Trabecular microarchitectural parameters of T2DM individuals with fracture (DMFx) and nondiabetic control group (CTL).

Parameter	***Groups***	***n***	***Mean***	***SD***	***p-value***
BV/TV [%]	DMFx	18	25.52	3.45	p=0.771
	CTL	14	25.04	5.79	
Tb.Th [mm]	DMFx	18	0.20	0.02	p=0.503
	CTL	14	0.21	0.03	
Tb.N [1/mm]	DMFx	18	1.27	0.15	p=0.285
	CTL	14	1.20	0.19	
Tb.Sp [mm]	DMFx	18	0.66	0.07	p=0.266
	CTL	14	0.70	0.10	
Conn.D [1/mm^3]	DMFx	18	12.57	4.39	p=0.208
	CTL	14	14.47	3.80	
DA	DMFx	18	1.96	0.18	p=0.235
	CTL	14	2.05	0.24	
FD	DMFx	18	2.55	0.05	p=0.688
	CTL	14	2.54	0.06	
SMI	DMFx	18	0.85	0.42	p=0.005*
	CTL	14	1.35	0.51	

T test for independent samples, * p<0.05

3.4.2. Microarchitectural analyses of DMFx_VD, DMF_NVD, and CTL groups

We found that BV/TV, Tb.N, Tb.Sp, SMI, and FD (p=0.023, p=0.004, p=0.008, p=0.001, p=0.007, respectively) varied between the examined groups (Table 4). Tb.Th, Conn.D, and DA were similar between the groups (p=0.586, p=0.106, p=0.286, respectively). Furthermore, post-hoc analyses showed significantly lower BV/TV in DMFx_VD group compared with DMFx_NVD group (p=0.020), whereas no significant differences in BV/TV were found between CTL and any of the T2DM groups (DMFx_VD, p=0.450; DMF_NVD, p=0.260). We found significantly higher Tb.N in DMFx_NVD compared with CTL (p=0.026) and DMFx_VD (p=0.006) groups. DMFx_NVD showed the lowest Tb.Sp (vs. CTL: p=0.035; vs. DMFx_VD, p=0.012). Although SMI was significantly lower in DMFx_NVD compared with CTL (p<0.001) and DMFx_VD (p=0.046) groups, it reflected predominance of trabecular plates over rods in all groups. FD was lower in DMFx_NVD compared with DMFx_VD group (p=0.006) (Table 4).

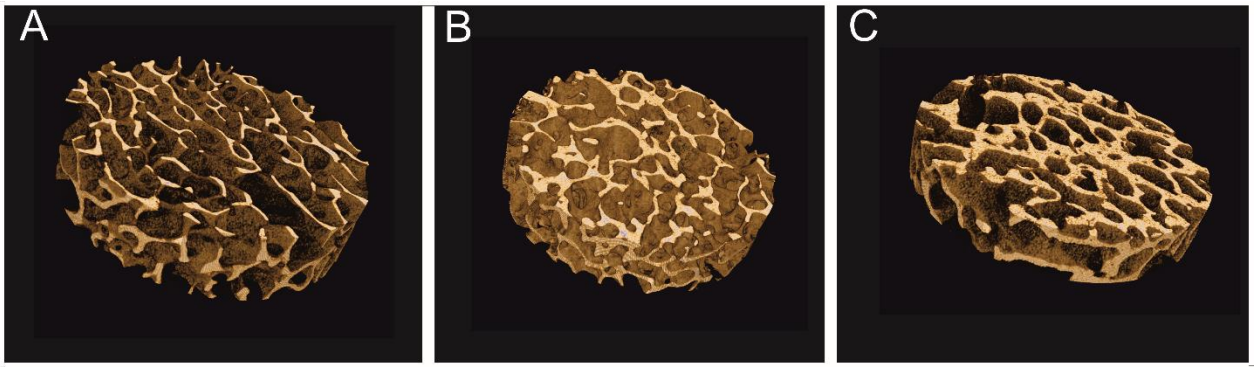

Figure 1. Representative 3D reconstructions of femoral neck trabecular bone in T2DM individuals with hip fracture and with vascular complications (DMFx_VD), T2DM individuals with hip fracture and without vascular complications (DMFx_NVD), and healthy controls (CTL).

Table 4. Trabecular microarchitectural parameters of T2DM individuals with fracture and no known vascular complications (DMFx_NVD), T2DM individuals with fracture and known vascular complications (DMFx_VD), and nondiabetic controls (CTL).

Parameter	*Groups*	*n*	*Mean*	*SD*	*p-value*	*Post-hoc analyses (Bonferroni)*
BV/TV [%]	DMFx_NVD	10	28.07	1.90	p=0.023*	p=0.020 (DMFx_NVD vs DMFx_VD)
	DMFx_VD	8	22.34	1.85		
	CTL	14	25.04	5.79		
Tb.Th [mm]	DMFx_NVD	10	0.20	0.02	p=0.586	NA
	DMFx_VD	8	0.20	0.01		
	CTL	14	0.21	0.03		
Tb.N [1/mm]	DMFx_NVD	10	1.37	0.08	p=0.004*	p=0.006 (DMFx_NVD vs DMFx_VD); p=0.030 (DMFx_NVD vs CTL)
	DMFx_VD	8	1.14	0.10		
	CTL	14	1.20	0.19		
Tb.Sp [mm]	DMFx_NVD	10	0.61	0.05	p=0.008*	p=0.012 (DMFx_NVD vs DMFx_VD); p=0.035 (DMFx_NVD vs CTL)
	DMFx_VD	8	0.73	0.04		
	CTL	14	0.70	0.10		
Conn.D [1/mm^3]	DMFx_NVD	10	14.05	5.14	p=0.106	NA
	DMFx_VD	8	10.71	2.43		
	CTL	14	14.47	3.80		
DA	DMFx_NVD	10	1.91	0.19	p=0.286	NA
	DMFx_VD	8	2.01	0.14		
	CTL	14	2.05	0.24		
FD	DMFx_NVD	10	2.58	0.03	p=0.007*	p=0.006 (DMFx_NVD vs DMFx_VD)
	DMFx_VD	8	2.51	0.02		
	CTL	14	2.54	0.06		
SMI	DMFx_NVD	10	0.62	0.34	p=0.001*	p=0.046 (DMFx_NVD vs DMFx_VD); p<0.001 (DMFx_NVD vs CTL)
	DMFx_VD	8	1.14	0.34		
	CTL	14	1.35	0.51		

One-way ANOVA, * $p<0.05$

3.5. Discussion

Our analysis showed the poorest femoral trabecular microarchitecture in T2DM patients with vascular complications. In particular, these patients clearly showed worse microarchitectural parameters than T2DM patients without vascular complications, although these subgroups of T2DM individuals did not differ in any of the relevant demographic factors (sex, age, BMI), disease-related factors (duration of the disease, HbA1c level, creatinine level), and type of therapy. Hence, clear variability in the femoral trabecular microarchitecture that is related to the presence or absence of vascular complications indicates that patients with T2DM should not be considered a single and uniform group in studies of the fracture risk.

Some of the microarchitectural parameters in T2DM patients who experienced fracture and did not have vascular complications were even better than those in the control group. However, after

pooling both DMFx subgroups, there were no differences in trabecular microarchitecture of the femoral neck compared with CTL group. Considering that DMFx_NVD group experienced hip fracture despite having similar femoral BV/TV and even higher Tb.N compared with the CTL group, it is apparent that the reasons for increased fragility in T2DM patients may also lie beyond trabecular microarchitecture. Of note, by examining cortical microarchitecture of subtrochanteric region, Osima et al. (Osima et al. 2017) assumed that the reason for increased fragility in T2DM individuals is probably beyond cortical microarchitecture. Since trabecular compartment also significantly contributes to femoral neck strength (Manske et al. 2009), we examined trabecular bone microarchitecture; clearly, although both DMFx_VD and DMFx_NVD groups experienced fracture, they displayed quite different microarchitecture patterns, also highlighting that the risk of fracture does not correlate fully with microarchitecture in all patients, and other determinants of bone fragility should be considered.

Although DXA was able to identify an increased fracture risk in both DMFx subgroups (DMFx_VD, DMFx_NVD) compared with controls, we showed that DXA measurement was "blind" for the additional risk observed in individuals with vascular complications. A previous study suggested that diabetic complications such as diabetic nephropathy and vascular diseases may increase the risk of fracture in DM individuals (Vestergaard et al. 2009). A large, retrospective study on more than 600,000 men (Lee et al. 2019) showed a higher prevalence of vascular and cerebrovascular diseases in DM patients who sustained hip fracture than in DM patients without a fracture. Leanza and colleagues (Leanza et al. 2019) suggested that among T1DM patients, those with vascular diseases more often sustained two or more non-vertebral fractures than those without cardiovascular diseases. Likewise, Miao et al. (Miao et al. 2005) reported that T1DM patients hospitalized due to microvascular complications (diabetic retinopathy and neuropathy) or cardiovascular diseases had a much greater relative risk of fracture than individuals without cardiovascular disease or diabetic complications. However, there is limited evidence for the microarchitectural origins of such trends. So far, only an HR-pQCT based study showed that, compared with T2DM patients without microvascular complications (retinopathy, nephropathy, or neuropathy), T2DM patients with complications showed a higher cortical porosity of distal radius (Shanbhogue et al. 2016), but no data are available for the femoral neck, the frequent fracture site. Here, we showed notable differences in femoral trabecular bone microarchitecture between the group of T2DM patients with and without vascular complications. Considering that both groups of T2DM patients sustained a low-energy hip fracture, it is obvious that they had a reduction in femoral bone mechanical competence. In T2DM patients without vascular complications, the fracture occurred despite good trabecular bone microarchitecture reflected in higher Tb.N and similar BV/TV to controls. In contrast, the fracture occurrence in T2DM patients with vascular complications likely stems from deterioration in trabecular bone microarchitecture, probably in addition to other bone changes that occur in patients without complications as well, but further studies are needed to unravel those changes.

Wölfel et al. analyzed subtrochanteric region of T2DM patients; beside deteriorated microarchitecture, they found additional weaknesses, such as impaired mineralization profile and reduced osteon density of endocortical region, mirroring impaired bone quality in T2DM individuals with high cortical porosity. Oren et al. obtained a 32% higher content of pentosidine in tibial plateau of 10 T2DM patients compared with controls (Oren et al. 2011). In vivo studies in T2DM patients confirmed excessive skin accumulation of advanced glycation end products (AGEs) (Furst et al. 2016), and content of AGEs in the skin positively correlated with quantum of AGEs accumulated in bone (Kida et al. 2019; Sell and Monnier 1989). AGEs tend to accumulate more severely in cortical bone (Odetti et al. 2005), and cortical AGEs content is a solid marker of normal bone aging. AGEs could be one of the reasons for bone fragility in DM individuals since accumulation of AGEs is more pronounced in T2DM patients and excessive AGEs tend to deteriorate bone quality directly via

interference with osteoblast function (Sanguineti et al. 2008) and indirectly via non-enzymatic glycosylation of collagen fibers (Katayama et al. 1996).

In our sample, based on the mean HbA1c value among the included T2DM patients, mid-term glucoregulation was relatively good. However, all the patients sustained the fracture, indicating that bone strength was suboptimal despite having almost desirable levels of HbA1c (<6.5%). Our microstructural phenotyping of T2DM patients with "favorable" HbA1c levels supports the findings from a large prospective study on the relationship between glycemic control and fracture risk, which showed that persons with diabetes and HbA1c values below 6.5% had similar risk to individuals with HbA1c levels between 7% and 7.9% (Conway et al. 2016).

This study had several limitations. First, it was limited by investigating only trabecular bone, which was chosen as it could be consistently obtained from surgical specimens of hip fracture cases, whereas cortical bone of the femoral neck is rarely and inconsistently obtained at the surgery. Further studies are needed to elucidate other determinants of bone fragility beyond bone microarchitecture, such as bone matrix characteristics and bone cell phenotypes. Next, our sample size was limited, suggesting that the study may be underpowered to detect all intergroup differences, especially in ANOVA with Bonferroni correction; nevertheless, it is of the same order of magnitude like many micro-CT studies. With larger sample size, some of the insignificant differences may become significant. Third, the values of HbA1c in our sample may not be representative of the entire population of T2DM patients because the value of HbA1c indicated that the disease was relatively well-controlled. However, it should be noted that we included only those patients in whom the medical team estimated that surgical treatment of the fracture is possible, with reasonable level of risk, which may have caused such a distribution of HbA1c values. Nevertheless, our data are valuable as this is the first study documenting microstructure of the femoral neck in individuals with "favorable" HbA1c levels and a fracture. Finally, there may be differences in the level of details and accuracy in diagnosing comorbidities between clinical patients and autopsy individuals. Moreover, complete medical history for cadaver donors is often difficult to obtain, especially the data regarding medications used. Nevertheless, control group was selected at autopsies to ensure consistent harvesting of the same bony region for the analyses and to avoid osteoarthritis as a potential factor influencing femoral neck microarchitecture.

Our study suggested that trabecular bone microarchitecture of the femoral neck in T2DM patients without vascular complications does not explain the fracture risk. Considering that both T2DM groups of patients sustained hip fracture, our data may suggest two distinct mechanisms of bone fragility in T2DM patients, depending on the presence of vascular complications. Namely, despite having experienced a fracture, patients without manifest diabetic complications did not show significant differences in microarchitecture compared with the control group; however, deterioration of trabecular microarchitecture was evident in patients with vascular complications compared with those without. Our data further highlight that consideration of diabetic complications is needed for proper understanding of the mechanisms of bone fragility in T2DM patients, and they may partly explain some of the inconsistencies observed in previous studies. Physicians should be aware of the higher fracture risk in T2DM individuals with vascular complications, even if HbA1c values are below 6.5%. Here, we observed bone microarchitecture at the common location for fragility fractures, and therefore, our findings may contribute to better understanding of the fracture risk in diabetic patients.

SECTION 4

Increased cortical porosity, reduced cortical thickness, and reduced trabecular and cortical microhardness of the superolateral femoral neck confer the increased hip fracture risk in individuals with type 2 diabetes

The results presented in this Section were first published in: Cirovic A, Jadzic J, Djukic D, Djonic D, Zivkovic V, Nikolic S, Djuric M, Milovanovic P. Increased Cortical Porosity, Reduced Cortical Thickness, and Reduced Trabecular and Cortical Microhardness of the Superolateral Femoral Neck Confer the Increased Hip Fracture Risk in Individuals with Type 2 Diabetes. Calcif Tissue Int. 2022 Nov;111(5):457-465. doi: 10.1007/s00223-022-01007-6, and are reproduced with permission from Springer.

4.1. Abstract

Individuals with diabetes mellitus type 2 (T2DM) have approximately 30% increased risk of hip fracture; however, the main cause of the elevated fracture risk in those subjects remains unclear. Moreover, micromechanical and microarchitectural properties of the superolateral femoral neck—the common fracture-initiating site—are still unknown. We collected proximal femora of 16 men (eight with T2DM and eight controls; age: 61±10 years) at autopsy. After performing post-mortem bone densitometry (DXA), the superolateral neck was excised and scanned with microcomputed tomography (microCT). We also conducted Vickers microindentation testing. T2DM and control subjects did not differ in age (p=0.605), body mass index (p=0.114), and femoral neck bone mineral density (BMD) (p=0.841). Cortical porosity (Ct.Po) was higher and cortical thickness (Ct.Th) was lower in T2DM (p=0.044, p=0.007, respectively). Of trabecular microarchitectural parameters, only structure model index (p=0.022) was significantly different between T2DM subjects and controls. Control group showed higher cortical (p=0.002) and trabecular bone microhardness (p=0.005). Increased Ct.Po and decreased Ct.Th in T2DM subjects increase the propensity to femoral neck fracture. Apart from the deteriorated cortical microarchitecture, decreased cortical and trabecular microhardness suggests altered bone composition of the superolateral femoral neck cortex and trabeculae in T2DM. Significantly deteriorated cortical microarchitecture of the superolateral femoral neck is not recognized by standard DXA measurement of the femoral neck.

Key words: T2DM; microarchitecture; microhardness; DXA; femoral neck; cortical porosity

4.2. Introduction

In 2017, it was estimated that 6.28% of the world population had diabetes mellitus (DM), and over one million deaths were associated with DM (Khan et al. 2020). If the current trends remain, it is expected that more than 10% of the global population will have DM by 2030 (Saeedi et al. 2019). Individuals with type 2 diabetes mellitus (T2DM) have a 1.34-fold higher risk of hip fracture (Fan et al. 2016); however, it remains unknown how T2DM increases the fracture risk.

Bone microarchitecture of individuals with T2DM was broadly studied in previous two decades. When scientific community has become aware of the increased fracture risk in T2DM individuals, one more challenge appeared. Namely, it has been shown that dual-energy X-ray absorptiometry (DXA) is not a sufficiently reliable tool to predict the fracture risk in T2DM since bone mineral density (BMD) has often been reported to be equally good (Holloway-Kew et al. 2021) as in controls or even higher (Samakkarnthai et al. 2020). Since BMD does not reliably predict the fracture risk, examination of bone microarchitecture was a natural approach to further understand the origins of the increased fracture risk in T2DM. High-resolution peripheral quantitative computed tomography (HR-pQCT) has frequently been used for the assessment of bone microarchitecture at distal tibia and radius (Burghardt et al. 2010; Nilsson et al. 2017; Patsch et al. 2013; Samakkarnthai et al. 2020; Shanbhogue et al. 2016). While increased cortical porosity in T2DM is often found in these clinical studies of bone microarchitecture, this is not a consistent finding, particularly in T2DM subjects without microvascular disease (Samakkarnthai et al. 2020; Shanbhogue et al. 2016). Another issue is that tibia, which is highly accessible for examination by HR-pQCT, is not a typical fracture site in T2DM subjects (Schousboe et al. 2022). As the femoral neck microarchitecture can only be crudely examined by conventional computed tomography (Osima et al. 2017), the majority of studies used bone samples for microcomputed tomography (microCT) assessment (Cirovic et al. 2022; Karim et al. 2018; Piccoli et al. 2020; Sihota et al. 2021). However, the available microCT studies that examined the femoral neck have evaluated trabecular (Karim et al. 2018; Piccoli et al. 2020; Sihota et al. 2021) or cortical bone of the inferomedial femoral neck (Karim et al. 2018). The femoral head trabecular core

(Cirovic et al. 2022; Karim et al. 2018), which has also been often examined, represents a distal continuation of the inferomedial neck trabeculae. However, trabeculae of the inferomedial femoral neck have different aging-related changes (Djuric et al. 2010) and fracture patterns (Milovanovic et al. 2012) compared with trabeculae of the superolateral neck. Therefore, it is crucial to investigate cortex and trabeculae of the superolateral femoral neck, particularly considering that the superolateral femoral neck is a site where a hip fracture usually starts.

Mechanical testing techniques such as and OsteoProbe indentation and Vickers microindentation may offer information about bone micromechanical properties, which are largely related to bone matrix composition. Bone matrix is a highly complex environment, which is mainly composed of collagen fibers; however, many other proteins are also present, such as protein S (Maillard et al. 1992), osteocalcin, osteopontin, bone sialoprotein, and others (Bellows et al. 1999). Even a subtle imbalance in any of the components, which could be induced by DM, may lead to deteriorated matrix composition, resulting in reduced bone capability to resist fracture. If DM is able to induce changes in bone matrix, it is expected that they would be possible to detect by microindentation measurements, which may evaluate some aspects of bone quality. According to Khosla et al., results of clinical studies have revealed that two most consistent impairments of bone quality in patients with T2DM are altered bone material properties and increased cortical porosity (Farr et al. 2014; Khosla et al. 2021). By using OsteoProbe, Holloway-Kew et al. have recently shown that individuals with T2DM have a lower BMSi compared with non-DM subjects (individuals with normoglycemia and those with impaired fasting glucose), but femoral neck BMD did not differ between the groups (Holloway-Kew et al. 2021). Equal or higher femoral BMD in T2DM individuals is a common finding in BMD studies (Burghardt et al. 2010; Holloway-Kew et al. 2021). The reduced BMSi in individuals with T2DM has been confirmed by other studies (Nilsson et al. 2017), definitely linking the increased bone fragility in T2DM individuals with the impaired bone material properties. In contrast, Samakkarnthai et al. did not find differences in BMSi between T2DM and controls (Samakkarnthai et al. 2020). However, all of the studies that examined BMSi in T2DM individuals have used a clinical microindentation testing device and have focused exclusively on the mid-shaft of tibia (Holloway-Kew et al. 2021; Samakkarnthai et al. 2020). As a laboratory method, Vickers microindentation can be applied on bone specimens, which allows for the examination of clinically more relevant skeletal sites that would otherwise be inaccessible to OsteoProbe-based indentation in a clinical context. While Vickers microindentation has not yet been applied in bone specimens of individuals with diabetes, the technique has been successfully used to probe iliac bone biopsies, showing reduced microhardness in osteoporosis compared with control subjects (Boivin et al. 2008).

Nevertheless, typical fractures in T2DM individuals are actually fractures of the hip and proximal humerus (Schousboe et al. 2022). To date, one study has reported lower hardness of the femoral neck trabeculae in T2DM (Sihota et al. 2021); however, it remains uninvestigated whether hardness of the superolateral femoral neck—a common fracture-originating site (Zani et al. 2015)—is lower in T2DM subjects than in non-DM subjects.

The aim of this study was to determine the origins of the increased fracture risk in older individuals with T2DM by analyzing bone microarchitecture and microhardness of the superolateral femoral neck trabecular and cortical compartments in T2DM subjects and age- and sex-matched controls.

4.3. Materials and methods

4.3.1. Sample selection and preparation

Sixteen proximal femora were obtained postmortem from male donors at the Institute of Forensic Medicine in Belgrade. Eight samples belonged to individuals who had received diagnosis of T2DM prior to death, and eight belonged to control subjects without DM. The sample contained the proximal

femora of 16 male individuals (age range, 47 to 83 years; mean age, 61±10.41 years). The principal causes of death, as obtained from autopsy reports, included diabetic ketoacidosis, acute cardiac failure, stroke or cerebral hemorrhage, motor vehicle accidents, other sudden traumatic injuries, or natural death. None of the individuals had a history of a bone fracture, metabolic bone disease, chronic liver disease, or cancer.

The inclusion criteria for the T2DM group were as follows: (1) T2DM diagnosed prior to death; (2) no positive history of hip fracture. The exclusion criteria were based on the autopsy reports, and they included the presence of the following: (1) rheumatoid arthritis; (2) inborn skeletal anomalies; (3) chronic kidney or liver disease; (4) any type of malignancy in the moment of death; (5) acromegaly, hypo- or hyperparathyroidism; (6) known treatment with bisphosphonates, glucocorticoids, anticonvulsants, or antipsychotics; (7) hip osteoarthritis; (8) alcoholism. The inclusion criteria for the control group were as follows: (1) absence of T1DM or T2DM; ii) no history of a hip fracture. The exclusion criteria were the same as those for the T2DM group.

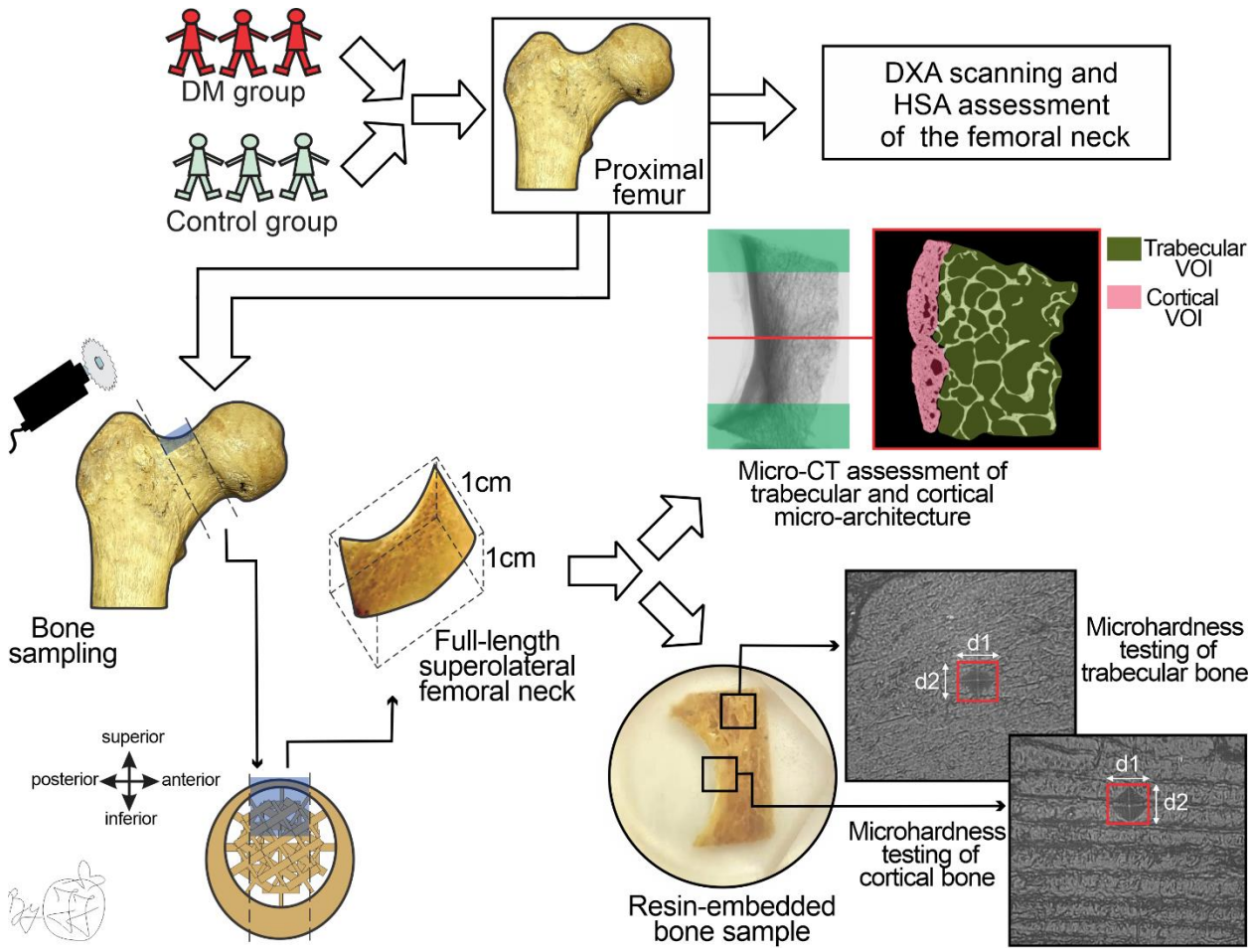

Figure 1. Methodological approach in our study. The blue portion of femoral neck cross-section indicates the area evaluated in this study.

Using a water-cooled low-speed diamond saw, we separated the superolateral neck from the rest of the specimen with several precise cuts, as described previously (Cirovic et al. 2020). The approval for the collection of the sample was granted by the institutional Ethics Committee.

4.3.2. DXA measurement

We conducted ex vivo DXA scanning on 14 out of 16 partially excised proximal femora (Figure 1) using Hologic QDR 1000/W DXA apparatus (Hologic, USA). Following previous recommendations (Jadzic et al. 2021), these bony samples were water-immersed during scanning to simulate the effects of surrounding soft tissues. The assessment of areal bone mineral density (BMD, g/cm2) of the femoral neck was done using built-in APEX software (version 2.0, Hologic, USA). In addition, we used hip structure analysis (HSA) plug-in to estimate cross-sectional area (CSA; cm2), cross-sectional moment of inertia (CSMI; cm4), buckling ratio (BR, dimensionless), cortical thickness (CTh.n, mm), and section modulus (Zn, cm3) in the standardized region of interest (narrow neck—located at the thinnest part of the femoral neck).

4.3.3. MicroCT

We scanned all of the specimens using a Skyscan 1172 micro-computed tomography system (Bruker microCT, Skyscan, Belgium) under the scanning conditions and parameters previously established: 80 kV, 124 µA, 1200 ms exposure time, aluminum and copper filter, 2 K camera binning, 10 µm voxel size (isotropic), rotation step of 0.40 degrees, and triple frame averaging (Cirovic et al. 2020). The reconstruction of the projection images obtained during the scanning was performed in NRecon software (Bruker microCT, Belgium) on InstaRecon platform (InstaRecon, USA) with suitable thermal drift correction, misalignment compensation, Gaussian smoothing of 3, and appropriate ring artifact and beam hardening corrections. To ensure representativeness of the evaluated bone volume, analyze consistent bone region, and avoid inter-site differences along the superolateral femoral neck (Cirovic et al. 2020), we analyzed the middle 60% of the superolateral femoral neck. Namely, if the length of the superolateral femoral neck parallel to longitudinal axis was about 3 cm, in this study we evaluated trabecular and cortical microarchitecture of about 1.8 cm. Volumes of interest (VOIs) were manually marked for cortex and trabeculae separately (Figure 1). Each VOI included about 1800 slices per sample (middle 60% of the superolateral neck).

The following cortical and trabecular parameters were evaluated using automatic 3D analysis in Ct.An (Skyscan, ver. 1.16.4.1): cortical thickness (Ct.Th, mm), cortical porosity (Ct.Po); trabecular bone volume fraction (BV/TV, %), trabecular number (Tb.N, 1/mm), trabecular thickness (Tb.Th, mm), trabecular separation (Tb.Sp, mm), structure model index (SMI, dimensionless), connectivity density(Conn.D, 1/mm3), fractal dimension (FD), and degree of anisotropy (DA, dimensionless).

Microindentation testing

To assess tissue-level micromechanical properties of cortical and trabecular bone, we used Vickers microhardness tester (HMV-G version, Schimadzu, Japan). Measurements were conducted under the previously established conditions for microhardness measurement (Jadzic et al. 2021) with the load of 50 g and 12 s of indentation time for both the cortical and trabecular regions (Figure 1). In order to prepare specimens for microindentation testing, all of the samples were embedded in resin and polished. In each specimen, using a 40× magnifying lens, we made five separate and valid measurements of the cortical compartment and five measurements of the trabecular compartment, and average values were used for intergroup comparisons. For both the cortical and the trabecular compartments, we ensured that the indentations were at least 2.5 diagonals from the margins to avoid boundary effects and that there were at least 2.5 diagonals between adjacent indentations to avoid overlapping of artificial depressions from one indentation to another (Yin et al. 2019). The measurements were performed by two researchers independently of each other, and the average value was taken for the analysis.

4.3.4. Statistical analysis

The Kolmogorov–Smirnov test was used to verify that all of the measured parameters complied with normal distribution. The t test for independent samples was used to check for differences in age, BMI, femoral neck BMD, CSAn, microarchitectural bone parameters, and microhardness between the investigated groups (T2DM and controls). To account for possible effects of age and BMI, we conducted analysis of covariance (ANCOVA) for the examined cortical parameters. Linear regression analysis was used to examine the associations between cortical microhardness and cortical porosity. All analyses were performed two-tailed in SPSS software ver. 15 at the significance level of 0.05. The effect size was calculated for each of the microCT parameters in accordance with the guidelines provided by Joseph A. Durlak (Durlak 2009); we used the Effect Size Calculator for T-Test (https://www.socscistatistics.com/effectsize/default3.aspx).

4.4. Results

T2DM and control subjects did not differ in age (p=0.605) or BMI (p=0.114). Femoral neck BMD did not differ between the examined groups either (p=0.841). CSAn, BR, CSMI, CTh.n, and Zn also did not differ between the investigated groups (p=0.357, p=0.465, p=0.140, p=0.722, and p=0.274, respectively) (Table 1).

Table 1. Characteristics and DXA results of individuals with T2DM and non-diabetic controls.

Characteristics	**T2DM (N=8)**	**Controls (N=8)**	p
Demographic			
Age (years)	60±8.93	62±12.25	0.605
Sex (men)	8(100%)	8(100%)	NA
Anthropometry			
Body mass index (kg/m^2)	26.83±2.81	23.42±4.6	0.114
Densitometry			
Femoral neck BMD (g/cm^2)	0.74±0.07	0.73±0.13	0.841
CSAn (cm^2)	3.1±0.27	2.85±0.6	0.357
BR (dimensionless)	12.4±1.75	11.59± 2.15	0.465
CSMI (cm^4)	3.84±0.31	3.17±1.0	0.140
CTh.n (cm)	0.17±0.02	0.16±0.03	0.722
Zn (cm^3)	1.86±0.14	1.64±0.44	0.274

4.4.1. Cortical microarchitecture and microindentation

We found that Ct.Po was significantly increased in T2DM subjects compared with controls (p=0.044). Moreover, Ct.Th was significantly lower in T2DM than in control individuals (p=0.007) (Table 2). After adjusting for BMI and age, the significant intergroup difference in Ct.Po was lost, but P-values were still close to significance (p=0.090). Even after adjusting for age and BMI, Ct.Th remained significantly lower in T2DM (p=0.032). Microindentation testing revealed that control specimens had higher cortical bone microhardness compared with T2DM specimens (p=0.002) (Figure 2).

We next used linear regression analysis to examine the associations of cortical microhardness and cortical porosity, and showed that cortical microhardness negatively correlated with Co.Po (r=-0.6, p=0.039).

4.4.2. Trabecular microarchitecture and microindentation

Majority of trabecular microarchitectural parameters were not significantly different between T2DM and control groups. Specifically, BV/TV, Tb.N, Tb.Th, Tb.Sp, DA, FD, and Conn.D did not vary between the groups (p=0.695, p=0.581, p=0.930, p=0.234, p=0.355, p=0.516, and p=0.124, respectively) (Table 2). Only SMI was significantly lower in T2DM than in control group (p=0.022). Control specimens had higher trabecular bone microhardness than T2DM specimens (p=0.005) (Figure 2).

Table 2. Trabecular and cortical microarchitectural parameters of T2DM and control groups.

Parameter	***Groups***	***n***	***Mean***	***SD***	***p-value***	***Effect size (Cohen d)***
BV/TV [%]	T2DM	8	13.32	3.02	p=0.695	
	Control	8	13.99	3.61		-0.20132
Tb.Th [mm]	T2DM	8	0.15	0.03	p=0.930	
	Control	8	0.15	0.03		0
Tb.N [1/mm]	T2DM	8	0.90	0.19	p=0.581	
	Control	8	0.87	0.14		0.179766
Tb.Sp [mm]	T2DM	8	0.97	0.10	p=0.234	
	Control	8	0.89	0.15		0.627572
Conn.D [1/mm^3]	T2DM	8	5.45	2.37	p=0.124	
	Control	8	8.56	4.82		-0.81886
DA [dimensionless]	T2DM	8	2.68	0.33	p=0.355	
	Control	8	2.50	0.41		0.483668
FD [dimensionless]	T2DM	8	2.35	0.07	p=0.516	
	Control	8	2.37	0.07		-0.28571
SMI [dimensionless]	T2DM	8	0.93	0.22	p=0.022*	
	Control	8	1.46	0.54		**-1.28544**
Ct.Po [%]	T2DM	8	31.48	8.88	p=0.044*	
	Control	8	22.87	6.47		1.108248
Ct.Th [mm]	T2DM	8	0.24	0.03	p=0.007*	
	Control	8	0.33	0.07		**-1.67126**

T test for independent samples, * p<0.05

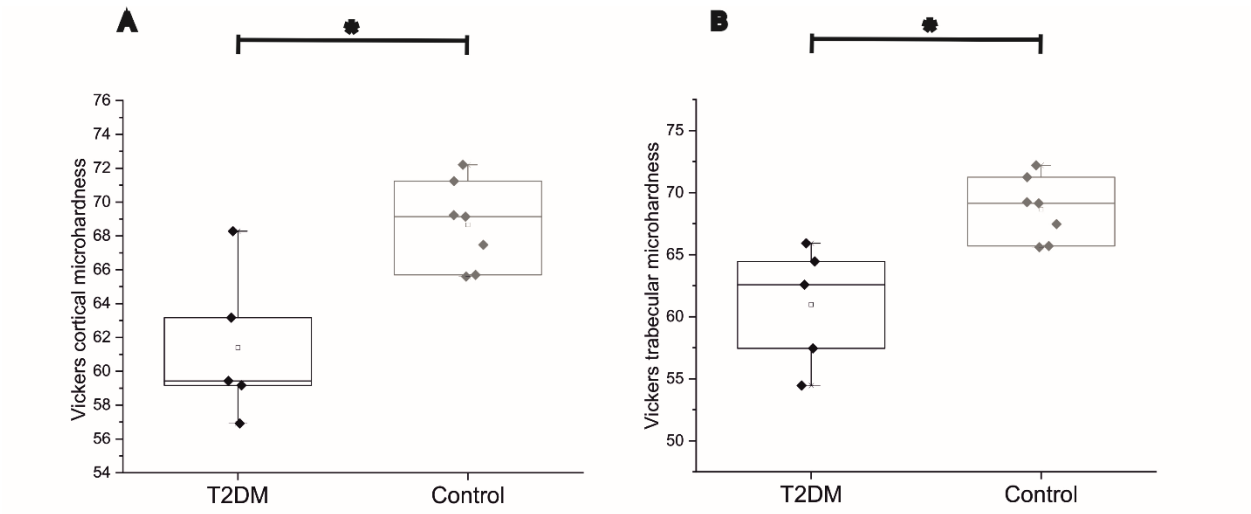

Figure 2. Micromechanical evaluation of bone specimens. A) Vickers cortical microhardness of T2DM and control groups; B) Vickers trabecular microhardness of T2DM and control groups.
* $p<0.05$

4.5. Discussion

To the best of our knowledge, this is the first evaluation of bone micromechanical properties and microarchitecture of cortical and trabecular compartments of the superolateral femoral neck in individuals with T2DM. Investigations of the superolateral femoral neck are particularly relevant considering that simulations of a sideways fall in fresh frozen human cadaveric femora unequivocally confirmed that a fracture most often initiated at the superolateral femoral neck (de Bakker et al. 2009). Therefore, it is essential to evaluate T2DM effects at this region of the skeleton so as to better understand the basis for the increased hip fracture risk in T2DM. We found that individuals with T2DM have impaired bone micromechanical properties of cortical and trabecular compartments of the superolateral neck, coupled with deteriorated cortical microarchitecture, indicating the microstructural origins of an increased fracture risk in subjects with T2DM. However, none of the DXA and HSA parameters differed between the examined groups. Indeed, bone fractures occur when the applied force exceeds bone strength. Therefore, apart from the magnitude and direction of a force, bone intrinsic characteristics are essential to understand the individual's bone fracture risk. Two fundamental components of cortical bone strength are cortical thickness and cortical porosity (Kral et al. 2017; McCalden et al. 1993). For example, in a CT-based finite element study based on 44 right femora from female individuals, Endo et al. showed that the reduced cortical bone thickness caused powerful stresses and strains, finally resulting in an increased risk of hip fracture (Endo et al. 2020). Also, two HR-pQCT studies conducted by Sundh et al. emphasized that increased cortical porosity was associated with a higher prevalence of multiple osteoporotic fractures in men (Sundh et al. 2015) and women (Sundh et al. 2017). Hence, our findings reflect an increased fracture risk in individuals with T2DM.

Recently, Wölfel et al. have analyzed hardness of the femoral mid-shaft cortex in T2DM, high-porosity T2DM, and control groups (Wölfel et al. 2020). Those subjects were older than our subjects and included both sexes; however, nanoindentation analyses did not reveal any variations in hardness between the groups. Even the group consisting of T2DM subjects with high Ct.Po did not differ in nanohardness from the other two groups (Wölfel et al. 2020), which may indicate that the deterioration of bone microarchitecture is independent of changes in nanostructure. Recently, Holloway-Kew et al. have speculated that the assessment of bone material properties is better than DXA for bone quality evaluation in T2DM individuals; their hypothesis was based on the fact that in their study on 340 men,

no differences in femoral neck BMD were found, while distal tibia BMSi was lower in T2DM individuals than in non-DM group (Holloway-Kew et al. 2021). Similar to Holloway-Kew et al., we also analyzed only male subjects, and found that femoral neck BMD was similar between the investigated groups; in our study, microhardness was reduced in T2DM, but we examined the femoral neck of individuals with T2DM, whereas Holloway-Kew et al. investigated the distal tibia (Holloway-Kew et al. 2021). Samakkarnthai et al. conducted a series of analyses, including measuring BMSi (using microindentation of the distal tibia), measurement of skin advanced glycation end-products (AGEs) (using autofluorescence), and HR-pQCT of the distal radius and tibia, in 171 T2DM patients and 108 age-matched non-DM subjects (Samakkarnthai et al. 2020). However, they showed that BMSi of the distal tibia did not vary between the investigated groups. Samakkarnthai et al. also showed that T2DM subjects with vascular complications had a significantly more porous cortex of the distal tibia compared with controls, whereas the presence of vascular complications did not affect BMSi (Samakkarnthai et al. 2020). Farr et al. conducted a study on BMSi and microarchitecture of the distal tibia and radius in 60 postmenopausal women; they found that T2DM patients had a significantly lower BMSi than controls, which was coupled with a higher cortical thickness of the distal radius and tibia. Farr et al. also found improved trabecular microarchitecture of the distal radius in T2DM individuals, before adjusting for BMI. However, after adjusting the data for BMI, Tb.N was no longer higher and Tb.Sp was not lower in T2DM subjects (Farr et al. 2014). Nilsson et al. performed a cross-sectional study that assessed microarchitecture of the distal tibia and radius in 99 women with T2DM and 954 control subjects (Nilsson et al. 2017). They reported a significantly higher trabecular BV/TV in T2DM group at both skeletal sites. While Ct.Po in the tibia did not differ between the groups, Ct.Po of the radius was either better (at a more proximal site) or worse (at a standard site) in T2DM compared with controls (Nilsson et al. 2017). Finite element analysis revealed significantly higher failure loads in T2DM than in control group (Nilsson et al. 2017), and BMSi by reference point indentation was lower in T2DM (Nilsson et al. 2017). By using microCT, Karim et al. analyzed trabecular microarchitecture of the femoral core of the head in 20 T2DM subjects undergoing elective total hip replacement surgery and 33 non-DM controls (Karim et al. 2018). Trabecular microarchitecture did not differ between the groups for any of the examined parameters (Karim et al. 2018). The authors also found that T2DM group demonstrated impaired cortical bone biomechanical properties, as evidenced by some cyclic reference point indentation properties (Karim et al. 2018). Our findings regarding the femoral neck trabecular microarchitecture in T2DM subjects are mostly in agreement with previous studies (Cirovic et al. 2022). Namely, previous studies that examined trabecular microarchitecture of the femoral head (trabecular cores that are actually derived from inferomedial trabeculae of the femoral neck) did not find significant intergroup differences for any of the investigated parameters (Cirovic et al. 2022; Karim et al. 2018; Piccoli et al. 2020). However, Sihota et al. reported deteriorated trabecular microarchitecture of the femoral head (lower BV/TV, Tb.N, and Tb.Th; higher SMI and Tb.Sp) as well as lower modulus and hardness obtained by nanoindentation testing (Sihota et al. 2021). This could be partly explained by the choice of the examination site given that Sihota et al. examined trabeculae from subchondral compartment of the femoral head—the compartment located on the opposite part of the femoral head than the trabecular cores examined by the previously mentioned studies (Cirovic et al. 2022; Karim et al. 2018; Piccoli et al. 2020). To summarize, regardless of the used methodology (microCT or pQCT), the results of the previous studies that examined bone microarchitecture (T2DM vs controls) are not uniform, but the majority of the studies agree that bone microstructure and mechanical properties are altered in T2DM individuals.

To the best of our knowledge, our study was the first to examine micromechanical and microarchitectural properties of the superolateral femoral neck trabeculae, and examination of the cortical compartment of the superolateral femoral neck may be considered the main strength of our study. Particularly, our assessment of cortical bone is important because its deterioration was not

detectable by clinical tools, considering that we found similar BMD and hip geometry parameters between the groups with the current sample size.

Here, we showed that 36% of the variability in cortical microhardness was explainable by the variability in cortical porosity. As for the remaining portion of the variability in mechanical properties in T2DM, it could be dependent on other aspects of bone quality that could be affected by the disease. On iliac crest biopsies of osteoporosis and control subjects, Boivin et al. showed that Vickers microhardness positively correlated with the degree of bone mineralization (DMB); nevertheless, the lower microhardness in individuals with osteoporosis cannot be fully explained by DMB alone (Boivin et al. 2008). In this context, organic matrix was also shown to partly determine microhardness values (about 30%) (Boivin et al. 2008). The reduced Vickers microhardness in individuals with T2DM in our study may reflect the higher fracture risk in these individuals, particularly having in mind that the reduced microhardness is determined by the alterations to both inorganic and organic components of the bone matrix and that Vickers microhardness correlates with tissue-level Young's modulus (Boivin et al. 2008). Of note, there are also other potential contributors to the increased fracture risk in T2DM that may or may not be captured by microindentation. For example, in addition to the altered mineralization pattern, T2DM individuals may present lower osteon density compared with control subjects (Wölfel et al. 2020), as well as low bone turnover coupled with a decreased number of osteoblast precursors and increased number of osteoclast precursors (Sassi et al. 2018). Indeed, additional research is warranted to comprehensively study the effects of T2DM on other aspects of bone quality and further clarify the mechanisms of the increased fracture risk.

However, there are few limitations, such as missing data regarding the duration of disease and HbA1c, and a relatively small number of samples. The sample size was conditioned by the COVID-19 outbreak and avoidance of autopsies in COVID-19–positive individuals; nevertheless, our study was sensitive enough to demonstrate that cortical microarchitecture and cortical and trabecular microhardness are significantly reduced in older individuals with T2DM. While clinical studies have used OsteoProbe for microindentation, here we used Vickers microhardness testing as a traditional and standardized method that has been broadly used for material testing and has been also used for the evaluation of bone specimens (Boivin et al. 2008; Jadzic et al. 2021; Yin et al. 2019). We used standardized forces as suggested in previous studies on bones, which were able to measure the tissue-level hardness of the examined bone specimens. Although different, both of these methods are obviously able to distinguish between diabetes and controls specimens. Moreover, it has recently been shown that the BMSi, as measured by OsteoProbe indentation, is a valid measurement of hardness (Ly et al. 2020), and correlates strongly and significantly with Vickers and Rockwell microhardness values (r=0.94, r=0.93, respectively) (Ly et al. 2020). However, it should be noted that OsteoProbe assesses the outer cortical surface only, as this is the only possible testing direction in a clinical setting; in contrast, Vickers microindentation on the excised bone specimens allowed us to examine the cross-section material properties of the superolateral femoral neck, which allowed us to separately evaluate its cortical and trabecular bony compartments. The superolateral femoral neck—the typical fracture-initiating site—is nonaccessible to the clinical indentation methods, so gaining direct knowledge on the superolateral femoral neck micromechanical properties is only possible on excised bone specimens obtained from surgery or autopsy.

4.6. Conclusions

T2DM individuals have deteriorated cortical microarchitecture of the superolateral femoral neck, and cortical and trabecular micromechanical properties are impaired in T2DM subjects as well. These findings offer explanation for the increased hip fracture risk in T2DM subjects. Considering that the significantly deteriorated cortical microarchitecture of the superolateral femoral neck is not recognized

by DXA measurement, analyses of bone microarchitecture and bone material properties offer better understanding of the reduced bone strength in T2DM subjects.

SECTION 5

Three-dimensional microstructural basis for differential occurrence of subcapital vs. basicervical hip fractures in men

The results presented in this Section were first published in: Cirovic A, Cirovic A, Djonic D, Zivkovic V, Nikolic S, Djuric M, Milovanovic P. Three-Dimensional Microstructural Basis for Differential Occurrence of Subcapital versus Basicervical Hip Fractures in Men. Calcif Tissue Int. 2020 Sep;107(3):240-248. doi: 10.1007/s00223-020-00717-z, and are reproduced here with permission from Springer.

5.1. Abstract

We analyzed the bone microarchitecture of the subcapital and basicervical subregions of the femoral neck in men, to determine whether microarchitectural differences of cortical or trabecular bone can explain differential frequency of subcapital vs. basicervical fractures, especially in aged persons. The study sample encompassed twenty male proximal femora obtained during autopsy. They were divided in two age groups: young (<40 years, n=10) and aged (>60 years, n=10). Microcomputed tomography was used to evaluate cortical and trabecular microarchitecture of the subcapital and basicervical regions of the superolateral femoral neck–typical fracture initiation site. Basicervical region showed significantly thicker and less porous cortex than subcapital region ($p=0.02$, $p<0.001$, respectively), along with increased distance between cortical pores ($p=0.004$) and smaller pore diameters ($p=0.069$). Higher trabecular number (Tb.N: $p=0.042$), lower trabecular thickness (Tb.Th: $p<0.001$), and lower trabecular separation ($p=0.003$) were also hallmarks of the basicervical compared to subcapital region, although BV/TV was similar in both regions ($p=0.133$). Age-related deterioration was mostly visible in trabecular bone (for BV/TV, Tb.Th, Tb.N and fractal dimension: $p=0.026$, $p=0.049$, $p=0.059$, $p=0.009$, respectively). Moreover, there were tendencies to age-specific patterns of trabecular separation (more pronounced inter-site differences in aged) and cortical thickness (more pronounced inter-site differences in young). Trabecular microarchitecture corresponded to cortical characteristics of each region. Our study revealed the microarchitectural basis for higher incidence of subcapital than basicervical fractures of the femoral neck. This is essential for better understanding of the fracture risk, as well as for future strategies to prevent hip fractures and their complications.

Keywords: hip fracture, basicervical, subcapital, microarchitecture, men

5.2. Introduction

Osteoporosis is a chronic progressive condition accompanied with increased risk of bone fractures (Alswat 2017; Svedbom et al. 2013; Wright et al. 2012). Although more frequent in women, hip fractures are also an important and growing problem in men (Wright et al. 2012). After the age of 65 years, the risk of mortality after hip fracture increases threefold, especially in men (Panula et al. 2011), and men sustain hip fracture generally in more advanced age than women (Tanner et al. 2010). Among the typical osteoporotic fractures (vertebral, distal radius, and fractures of the proximal femur) (Vogt et al. 2002; Warriner et al. 2011), the fractures of the femoral neck are particularly frequent and associated with a notably high morbidity and mortality rates (Wright et al. 2012).

In orthopedic practice, hip fractures can be classified in several ways. However, often neglected is anatomical classification, which highlights the subregions of the superolateral and/or inferomedial neck where the fracture line passes. In this context, the anatomical classification of hip fractures distinguishes between subcapital, transcervical, and basicervical types. Subcapital and transcervical are intracapsular fractures, while basicervical are usually extracapsular and are typically treated like intertrochanteric fractures (Chen et al. 2008; Saarenpää et al. 2002). The fracture typically linked with nonunion and avascular necrosis is the subcapital fracture of the femoral neck (Dedrick et al. 1986; Mayhew et al. 2005), whereas the occurrence of these complications is much less frequent in transcervical and basicervical fractures (Jo et al. 2016). Although empirical data shows that subcapital fractures are more common than other two types (Jo et al. 2016; Magu et al. 2014), there have been no studies on the origins of such distribution of femoral neck fractures.

Disruption of the superolateral cortex is typically the beginning component of a femoral neck fracture (de Bakker et al. 2009). This is also reflected in Garden's classification, one of the most frequently used in orthopedic practice, where the first type is defined as an incomplete fracture where only the superolateral neck is broken (Kazley et al. 2018). Among microstructural studies, Djuric et al. (Djuric et al. 2010) showed an age-related reduction in trabecular bone volume fraction (BV/TV) and

connectivity density (Conn.D) in the superolateral neck region in both men and women, suggesting the microstructural reasons for its particular fragility; however, that study investigated the mid-portion of the superolateral neck. Likewise, Chen et al. (Chen et al. 2010) and Lochmüller et al. (Lochmüller et al. 2008) analyzed the mid-portion of the femoral neck, demonstrating trabecular deterioration in aged individuals. Impaired trabecular microarchitecture in advanced age is accompanied by age-related thinning of the superolateral cortex in females, but not in males (Johannesdottir et al. 2011; Mayhew et al. 2005). Hence, previous studies explored the mid-portion of the femoral neck, and there were no reports on bone microarchitecture in subcapital and basicervical regions of the femoral neck. Nevertheless, age-related changes in proximal femur's microarchitecture in so far investigated regions are not uniform (Cui et al. 2008; Djuric et al. 2010). Therefore, considering also that distribution of fractures is not uniform among the regions of the femoral neck, we hypothesized that differential occurrence of subcapital vs. basicervical fractures may have origins in different bone microarchitecture in those two subregions. Given that the superolateral neck is particularly affected by aging in men (Djuric et al. 2010) and that it is the initiating region of hip fracture (de Bakker et al. 2009), it would be of great importance to investigate spatial heterogeneity of its microarchitecture.

Therefore, the aims of this study were: 1) to analyze microarchitecture of the subcapital and basicervical subregions of the superolateral femoral neck trabecular compartment in men, 2) to analyze bone microarchitecture of the subcapital and basicervical subregions of the superolateral femoral neck cortical bone in men, and 3) to determine whether microarchitectual differences in these femoral neck subregions can explain differential frequency of subcapital vs. basicervical fractures, especially in aged persons.

5.3. Material and methods

5.3.1. Sample selection and preparation

Twenty right proximal femora were collected during autopsies from male postmortem human subjects at the Institute of Forensic Medicine. The approval for collection of the sample was granted by the institutional Ethics Committee. The sample contained the proximal femora of 20 male individuals (age range from 19 to 84 years; mean, 52.25 ± 25.42 years) whose principal causes of death, as obtained from autopsy reports included acute cardiac failure, stroke or cerebral hemorrhage, motor vehicle accidents, and other sudden, traumatic injuries or natural death. Any individuals with a history of musculoskeletal diseases, metabolic bone disease or cancer were automatically ineligible for this study. The obtained samples we divided into two age categories: young (age <40 years, n=10) and aged group (age >60 years, n=10).

The full circumference of the femoral neck could be divided into the following four regions: superolateral, inferomedial, anterior, and posterior neck. Further division per longitudinal axis of the femoral neck divides each of these regions to three subregions: basicervical region (the third of the neck closer to the trochanter, midcervical region (middle third), and subcapital subregion (the third closer to the femoral head). The full length of the superolateral femoral neck was obtained by cutting at the base of the femoral head and at the base of femoral neck (Figure 1A), using a water-cooled low-speed diamond saw. In further preparation, we cut the samples in coronal planes parallel to the longitudinal axis of femoral neck (Figure 1B), removing the anterior and posterior cortex with adjacent trabecular bone. The remaining part of the neck (approximately 10 mm wide) consisted of the superolateral and inferomedial cortex and the trabecular bone between them (Figure 1B, 1C). We separated the superolateral neck from the rest of the specimen by another cut (Figure 1C).

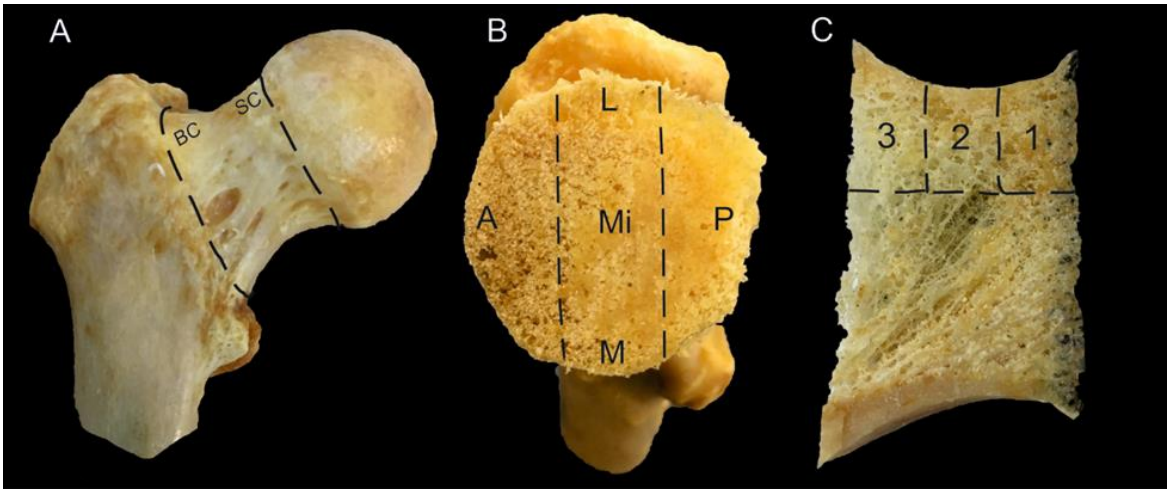

Figure 1. Regions of the proximal femur. (A) Anterior view: dashed lines denote the borders of the femoral neck (BC=basicervical region, SC=subcapital region); (B) Medial view on the femoral neck after removing the femoral head: L – superolateral neck, A - anterior neck, P- posterior neck, M - inferomedial neck, Mi - mid- portion of femoral neck (dashed lines indicate the cutting lines to remove anterior and posterior neck regions); (C) Division of the superolateral neck: 1- subcapital part of superolateral neck, 2 - mid-portion of superolateral neck, 3 - basicervical part of superolateral neck.

5.3.2. Micro-computed tomography

Fixed on a sample holder, the specimens were scanned using Skyscan 1172 micro-computed tomography system (Bruker microCT, Skyscan, Belgium) under the following scanning conditions and parameters: 80 kV, 124 µA, 1200 ms exposure time, aluminum and copper filter, 2K camera binning, 10 µm voxel size (isotropic), rotation step of 0.40 degrees, and triple frame averaging. The reconstruction of the projection images was performed in NRecon software (Bruker microCT, Belgium) on InstaRecon platform (InstaRecon, USA) with suitable thermal drift correction, misalignment compensation, Gaussian smoothing of 3, and appropriate ring artifact and beam hardening corrections.

During the scanning, all samples were vertically positioned with subcapital region oriented upward. Each superolateral neck specimen was approximately 25 mm in length. Considering the isotropic voxel size of 10 µm, a total of approximately 2,500 slices were obtained and divided to three equal stacks of slices (basicervical, midcervical, and subcapital). For this study, basicervical and subcapital regions were further analyzed (Figure 1C). We manually segmented the cortical and trabecular volumes of interest (VOI) of each region, yielding a total of 80 VOIs for the entire sample of 20 femora. Each of the 80 VOIs consisted of at least 500 slices, resulting in analysis of at least 5 mm-thick VOIs of each subregion. The global threshold of 95/255 was chosen to discriminate between the mineralized bone and marrow spaces. The same threshold was applied for all VOIs to allow inter-individual and inter-site comparisons of microarchitectual parameters.

The following trabecular parameters were evaluated using automatic 3D analysis in Ct.An (Skyscan, ver. 1.16.4.1): trabecular bone volume fraction (BV/TV, %), trabecular number (Tb.N, 1/mm), trabecular thickness (Tb.Th, mm), trabecular separation (Tb.Sp, mm), structure model index (SMI, dimensionless), connectivity density (Conn.D, $1/mm^3$), fractal dimension (FD) and degree of anisotropy (DA, dimensionless). In cortical bone, we determined the bone volume fraction (BV/TV, %), pore diameter (Po.Dm, mm), pore spacing (Po.Sp, mm), closed pores' number per bone volume (Po.N/BV, $1/mm^3$), cortical thickness (Ct.Th, mm), open porosity (Po.op, %), total porosity (Po.tot, %), closed porosity (Po.cl, %), standard deviation of pore separation (SD_Po.Sp, mm), and standard deviation of pore diameter (SD_Po.Dm, mm).

5.3.3. Statistical analysis

The Kolmogorov-Smirnov test was used to verify that all measured parameters complied with the normal distribution. Analysis of variance for repeated measurements was performed to check for differences in microarchitectual bone parameters between the investigated regions (basicervical and subcapital) and groups (young and aged) as well as their interaction (region * group). All analyses were performed two-tailed in SPSS software ver. 15 at the significance level of 0.05.

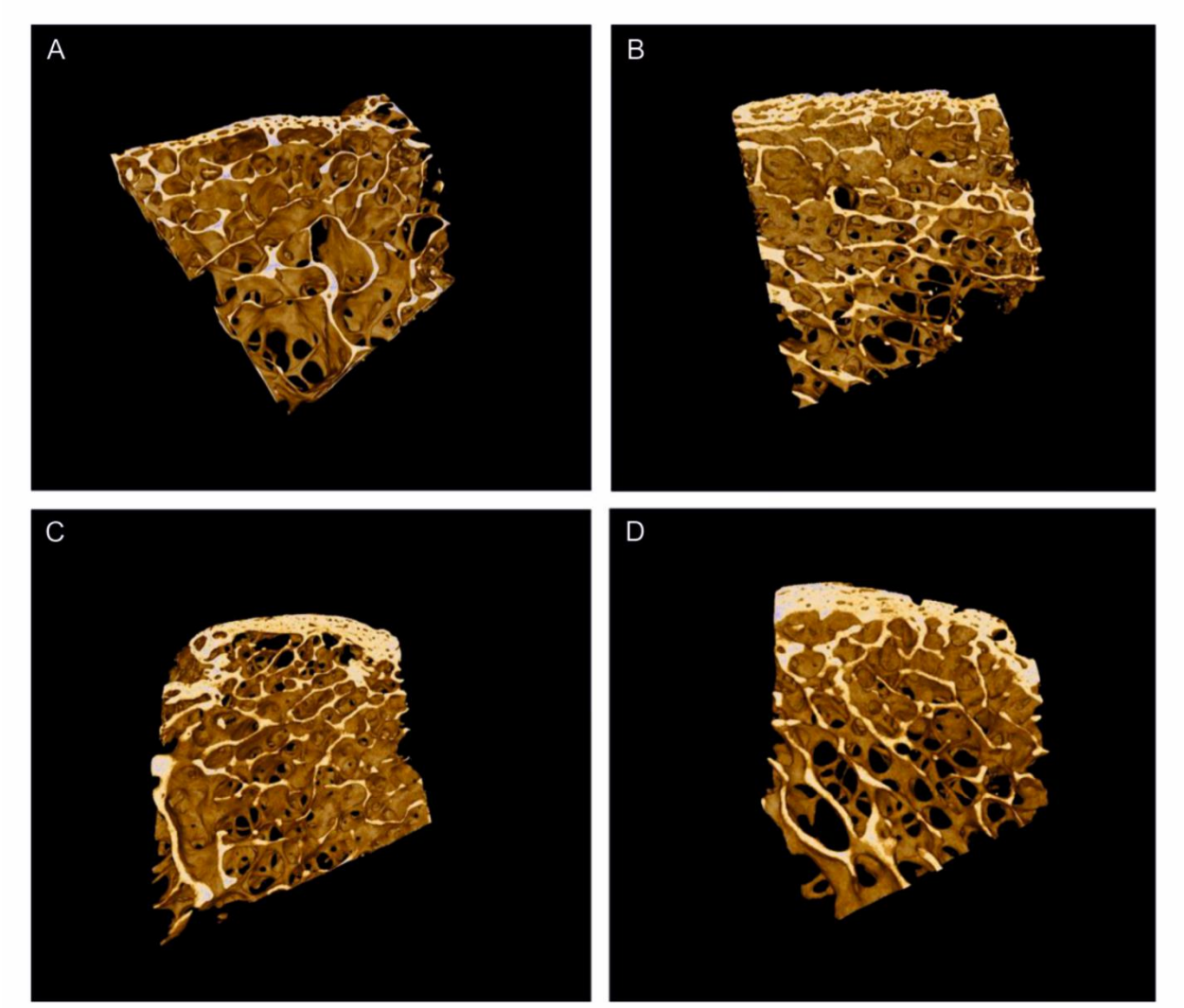

Figure 2. Representative 3D reconstructions of cortical and trabecular bone. (A) Subcapital region in an aged individual, (B) Basicervical region in an aged individual, (C) Subcapital region in a young individual, (D) Basicervical region in a young individual.

5.4. Results

We have investigated bone microarchitecture of subcapital and basicervical subregions of the superolateral region of the human femoral neck in young and aged men (Figure 2).

Table 1. Trabecular microarchitectural parameters of subcapital and basicervical regions in young and aged group**.**

Parameter	*Location*	*n*	*Mean*	*SD*	*p-value*
Trabecular bone volume fraction [%]	Subcapital young	10	21.44	6.25	Site*Group p=0.629
	Subcapital aged	10	15.44	2.88	
	Basicervical young	10	20.06	7.85	Site p=0.133
	Basicervical aged	10	14.72	2.92	Group p=0.026*
Trabecular number [1/mm]	Subcapital young	10	1.02	0.19	Site*Group p=0.273
	Subcapital aged	10	0.84	0.12	
	Basicervical young	10	1.05	0.20	Site p=0.042*
	Basicervical aged	10	0.94	0.16	Group p=0.059
Trabecular thickness [mm]	Subcapital young	10	0.21	0.03	Site*Group p=0.616
	Subcapital aged	10	0.18	0.02	
	Basicervical young	10	0.19	0.04	Site p <0.01*
	Basicervical aged	10	0.16	0.03	Group p=0.049*
Trabecular separation [mm]	Subcapital young	10	0.86	0.14	Site*Group p=0.077*
	Subcapital aged	10	0.95	0.13	
	Basicervical young	10	0.81	0.15	Site P=0.003*
	Basicervical aged	10	0.81	0.12	Group p=0.455
Structure model Index	Subcapital young	10	0.91	0.78	Site*Group p=0.915
	Subcapital aged	10	1.06	0.26	
	Basicervical young	10	1.00	0.53	Site p=0.278
	Basicervical aged	10	1.13	0.30	Group p=0.523
Connectivity density [1/mm^3]	Subcapital young	10	6.44	2.22	Site*Group p=0.425
	Subcapital aged	10	5.38	1.93	
	Basicervical young	10	6.29	2.28	Site p=0.639
	Basicervical aged	10	5.94	2.35	Group p=0.437
Degree of anisotropy	Subcapital young	10	2.20	0.29	Site*Group p=0.319
	Subcapital aged	10	2.48	0.24	
	Basicervical young	10	2.48	0.51	Site p=0.072
	Basicervical aged	10	2.56	0.49	Group p=0.247
Fractal dimension	Subcapital young	10	2.40	0.05	Site*Group p=0.138
	Subcapital aged	10	2.32	0.04	
	Basicervical young	10	2.38	0.05	Site p=0.826
	Basicervical aged	10	2.34	0.06	Group p=0.009*

*Repeated-measures ANOVA: * p< 0.05*

5.4.1. Trabecular bone microarchitecture

We found significantly lower BV/TV in aged than in young men (p=0.026), but no significant variation was evident between the sites (p=0.133). Structure model index (SMI) did not show any differences either between the sites (p=0.278) or age groups (p=0.523). Further, trabeculae were thicker in subcapital compared to basicervical subregion (p<0.001) (Figure 2 and 3), and the values of trabecular thickness significantly declined with advanced age (p=0.049) (Table 1). In contrast to trabecular thickness, trabeculae were more numerous in basicervical region (p=0.042) and trabecular number decreased in both regions with almost significant age-trend (p=0.059). We found significantly lower values of distance between adjacent trabeculae in basicervical compared to subcapital region (p=0.003), although no clear age trend was observed (p=0.455). However, interaction of age and region for

trabecular separation showed a trend (p=0.077) reflecting pronounced inter-site differences in the aged group (lower values in basicervical region) in contrast to the young group where both regions showed quite uniform Tb.Sp. Significantly lower values of fractal dimension values we observed in the aged group compared to the young (p=0.009), while no differences were observed between the sites. No statistical inter-group and inter-site difference was observed in connectivity density and degree of anisotropy (p>0.05).

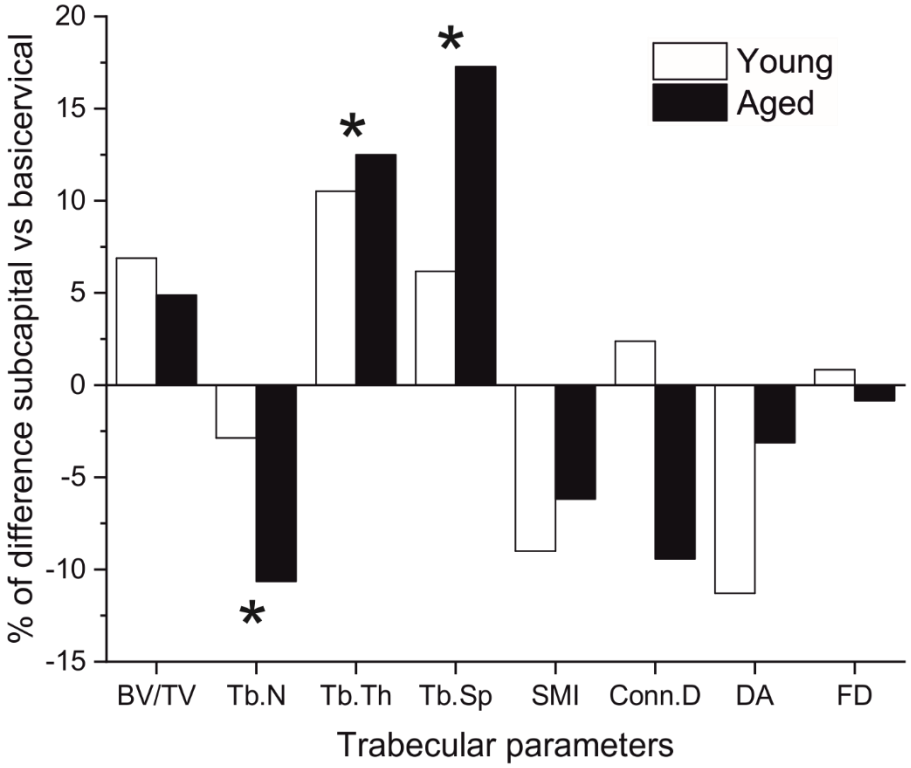

Figure 3. Trabecular microarchitecture: percentage of difference between subcapital and basicervical regions of the superolateral neck in young and aged groups (* p<0.05 between the regions)

5.4.2. Cortical bone microarchitecture

Basicervical region showed significantly higher values in cortical BV/TV (p<0.001) and pore spacing (p=0.004), while the values of open porosity and total porosity were significantly reduced compared to the subcapital region (p<0.001). We did not observe any differences in Po.N/BV (p=0.545), closed porosity (p=0.921), SD of pore separation (p=0.425) and SD of pore diameter (p=0.308) (Table 2, Figure 2, 4). Cortical BV/TV showed the highest values in basicervical region in the young group compared to the same region in aged group and subcapital regions of both age groups, but the differences did not reach significance (p=0.142). Interaction of age and region for Po.Sp (p=0.008) revealed inter-site heterogeneity in young individuals (higher Po.Sp in basicervical than in subcapital), in contrast to Po.Sp homogeneity between two subregions in the aged group. Po.Sp was significantly lower in the subcapital region, but statistical significance was not reached between age groups (p=0.068). Pore diameter did not reach significant difference between the regions, although pores tended to be larger in the subcapital region (p=0.069); likewise, increase in pore size with advanced age approached statistical significance (p=0.074). Basicervical cortex was significantly thicker compared to the subcapital region (p=0.02), whereas the difference between young and aged groups was not significant (p=0.099). However, there was a tendency to age-specific pattern of cortical thickness

distribution between the subregions, since subcapital cortex did not undergo major changes in cortical thickness during aging, while basicervical cortical thickness tended to decline in aged men but without reaching significance level (p=0.073); nevertheless, basicervical cortex maintains higher thickness than subcapital in aged individuals.

Table 2. Cortical microarchitectural parameters of subcapital and basicervical regions in young and aged group**.**

Parameter	***Location***	***n***	***Mean***	***SD***	***p-value***
Total porosity [%]	Subcapital young	10	19.48	5.40	Site*Group p=0.142
	Subcapital aged	10	21.45	5.11	
	Basicervical young	10	13.60	4.05	Site p<0.001*
	Basicervical aged	10	18.49	5.68	Group p=0.115
Bone surface to volume ratio [1/mm]	Subcapital young	10	80.52	5.40	Site*Group p=0.142
	Subcapital aged	10	78.55	5.11	
	Basicervical young	10	86.40	4.05	Site p<0.001*
	Basicervical aged	10	81.51	5.68	Group p=0.115
Pore diameter [mm]	Subcapital young	10	0.20	0.04	Site*Group p=0.953
	Subcapital aged	10	0.24	0.06	
	Basicervical young	10	0.17	0.05	Site p=0.069
	Basicervical aged	10	0.20	0.07	Group p=0.074
Pore spacing [mm]	Subcapital young	10	0.29	0.04	Site*Group p=0.008*
	Subcapital aged	10	0.27	0.03	
	Basicervical young	10	0.32	0.04	Site p=0.004*
	Basicervical aged	10	0.27	0.03	Group p=0.068
Pore number per bone volume [1/mm^3]	Subcapital young	10	41.46	50.64	Site*Group p=0.426
	Subcapital aged	10	25.66	11.65	
	Basicervical young	10	31.36	9.96	Site p=0.545
	Basicervical aged	10	27.04	10.87	Group p=0.318
Open porosity [%]	Subcapital young	10	19.30	5.51	Site*Group p=0.147
	Subcapital aged	10	21.27	5.20	
	Basicervical young	10	13.41	4.11	Site p<0.001*
	Basicervical aged	10	18.30	5.76	Group p=0.121
Closed porosity [%]	Subcapital young	10	0.22	0.16	Site*Group p=0.967
	Subcapital aged	10	0.22	0.14	
	Basicervical young	10	0.21	0.08	Site p=0.921
	Basicervical aged	10	0.22	0.11	Group p=0.870
Cortical thickness [mm]	Subcapital young	10	0.30	0.08	Site*Group p=0.073
	Subcapital aged	10	0.27	0.08	
	Basicervical young	10	0.36	0.08	Site p=0.02*
	Basicervical aged	10	0.28	0.07	Group p=0.099

*Repeated-measures ANOVA: * p< 0.05*

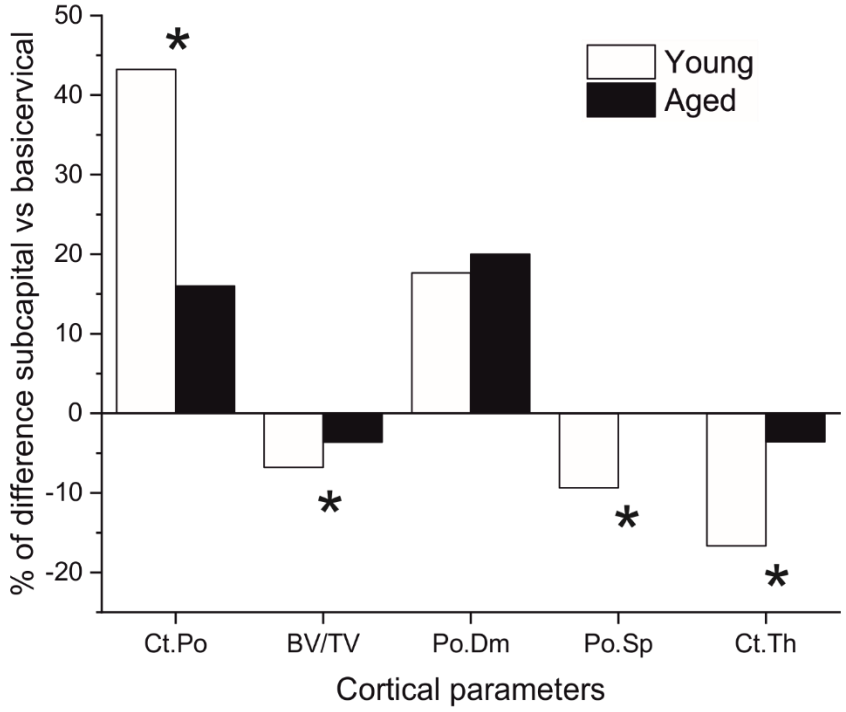

Figure 4. Cortical microarchitecture: percentage of difference between subcapital and basicervical regions of the superolateral neck in young and aged groups (* $p<0.05$ between the regions)

5.5. Discussion

Our microarchitectural assessment revealed that the femoral neck microarchitecture is not uniform, which may be one of the main reasons for observed differential rates of fracture occurrence between the basicervical and subcapital regions of the superolateral neck.

Specifically, our results showed that the trabecular bone of the basicervical region presented with an overall greater number of trabeculae that were more densely packed compared to fewer trabeculae with higher trabecular separation in the subcapital region; yet, trabecular bone fraction did not differ between two regions, and showed an age-related decline in both regions. Ciarelli et al. (Ciarelli et al. 2000) used micro-CT to analyze cubes from the region immediately below the epiphyseal line in the proximal femora and showed significantly higher trabecular number in the group without fractures, whereas hip fracture group was characterized by less numerous and thicker trabeculae. Other authors also gave advantage to trabecular number over trabecular thickness for bone strength and mechanical resistance, highlighting that once critical number of trabeculae is lost any subsequent thickening of trabeculae with drugs cannot restore full bone strength even if BT/TV is fully recovered (Guo and Kim 2002). Therefore, considering similar BV/TV in both regions in our study, it is likely mechanically advantageous to have more trabeculae than thicker trabeculae, suggesting higher trabecular bone strength at the basicervical region. We did not observe any changes in shape of trabeculae (SMI) between the sites or during aging, although other studies showed significant increases in SMI values at the mid-region of the femoral neck in males (Djuric et al. 2010). Yet, trabecular bone of those two regions of the superolateral neck was not previously analyzed.

Our study showed that the cortical bone of the basicervical region was thicker and less porous compared to the subcapital region in both age groups. Previous studies using high-resolution peripheral quantitative computed tomography (HR-pQCT) of the subtrochanteric femur or distal tibia recognized

high cortical porosity and low cortical thickness as independent strong predictors of osteoporotic fracture (Kral et al. 2017; Sundh et al. 2015; Sundh et al. 2017; Zebaze and Seeman 2015). Therefore, our results indicated that, in addition to likely mechanically weaker trabecular bone, subcapital region also features a weaker cortex. Based on previous finite element analysis studies, the sideways fall loads all three anatomical parts of the superolateral neck (basicervical, mid-cervical and subcapital) with the force of the same intensity (Rolvien et al. 2018); hence, the preference to subcapital fracture must be largely driven by its weaker microarchitecture as revealed in our study.

We are not aware of any study that analyzed 3D microarchitecture of the superolateral neck cortex in men. In contrast, the inferomedial neck received some attention by Chen et al. (Chen et al. 2010), who demonstrated that its porosity increased with aging in men. It has been shown recently that the inferomedial neck has a significantly thicker cortex compared with the superolateral neck (Rolvien et al. 2018). Moreover, the inferomedial cortex and superolateral cortex do not "behave" identically during aging or between sexes. Namely, while the superolateral neck gets thinner with aging in females, the inferomedial cortical thickness increases (Mayhew et al. 2005) or decreases (Chen et al. 2010), depending on the study. In men, cortical thickness of both regions is reportedly not subject to significant changes during aging (Johannesdottir et al. 2011; Mayhew et al. 2005), while in Japanese population an age-related decrease in cortical thickness was noted in the inferomedial neck (Chen et al. 2010). Our findings of unchanged cortical thickness with aging in males are in agreement with previous studies (Johannesdottir et al. 2011; Mayhew et al. 2005), although it should be noted that those studies measured the thickness of mid-portion of the neck (including the mid-portion of the superolateral neck) while here we evaluated the subcapital and basicervical regions. Despite lack of significant change in overall cortical thickness with aging, our results showed that the difference in cortical thickness between young and aged group was higher in basicervical than in subcapital region.

During the sideways fall, major part of the load is carried by the cortical bone, which is even more pronounced in the superolateral neck in the osteoporotic femur (Verhulp et al. 2008). Considering that we also found mechanically less resistant trabeculae in the subcapital region, mechanically weaker cortex of subcapital region would be more stricken by the force produced by the fall than the basicervical region. A previous study on the relative contribution of cortical and trabecular bone to the femoral strength pointed out the minor contribution of trabecular bone (Holzer et al. 2009); nevertheless, Manske et al. (Manske et al. 2009) examined relative contribution to bone strength of both cortical and trabecular bone among all four quadrants (inferomedial, superolateral, anterior, and posterior) and found that in the superolateral femoral neck of individuals between 36–92 years both compartments significantly contribute to failure load during mechanical testing. Johannesdottir et al. (Johannesdottir et al. 2017) reported that in young adults both compartments contribute significantly, while in aged people due to trabecular deterioration much more force has to be accommodated by the cortical bone. Indeed, our study showed more pronounced trabecular bone deterioration in aged individuals, suggesting that the condition of the cortical bone is essential for fracture resistance.

Rolvien et al. (Rolvien et al. 2018) showed that besides microarchitecture, other parameters such as lower osteocyte lacunar density and higher mineralization heterogeneity also contribute to particularly high fracture susceptibility of the superolateral neck. As osteocytes are crucial orchestrators of bone remodeling (Rolvien et al. 2018), variations in bone microarchitecture between basicervical and subcapital regions may reflect differences in osteocyte network characteristics. However, here we did not examine the differences in mineralization distribution and osteocyte lacunar density among the superolateral neck subregions, and their contribution to subcapital fractures.

In conclusion, as microarchitectural profile of basicervical region showed better performances by most cortical and trabecular parameters, our study highlights the following relationships between the microarchitecture and fracture risk in the proximal femur of men:

- If hip fracture is to occur in a young adult after strong impact force, it is more likely that subcapital region will break first.
- In aged individuals, deterioration of both regions is significant during aging, but because of better "starting" position of the basicervical region, the subcapital fractures are also more likely in advanced age.
- Trabecular microarchitecture seems to follow the cortical characteristics of the corresponding region (high-quality cortex in basicervical region is supported with microarchitectualy more resistant trabecular bone, whereas beneath poorer quality cortex of the subcapital region less resistant trabeculae are situated).

Our study reveals the microarchitectural basis for empirical observations of subcapital fractures in males occurring much more commonly than basicervical and also for rarity of basicervical fractures in general. Here, we examined physiological inter-site variations and microarchitectural changes between young and aged individuals in a fundamentally important region of the skeleton (superolateral femoral neck). It should be borne in mind that here we examined individuals who did not sustain a hip fracture; it is possible that individuals with hip fracture have different patterns of age-related changes, as previously shown for cortical bone (Bell et al. 1999; Power et al. 2018) and trabecular bone (Milovanovic et al. 2012) of the femur. Nevertheless, unraveling physiological inter-site variations in bone microarchitecture as well as differences between young and aged individuals can help us better understand the risk of fracture at specific locations within the femoral neck.

SECTION 6

Three-dimensional mapping of cortical porosity and thickness along the superolateral femoral neck in older women

The results presented in this Section were first published in *Open Access* in: Cirovic A, Cirovic A, Djukic D, Djonic D, Zivkovic V, Nikolic S, Djuric M, Milovanovic P. Three-dimensional mapping of cortical porosity and thickness along the superolateral femoral neck in older women. Sci Rep. 2022 Sep 15;12(1):15544. doi: 10.1038/s41598-022-19866-2, so no permission is needed from the original publisher.

6.1. Abstract

Although several studies have analyzed inter-individual differences in the femoral neck cortical microstructure, intra-individual variations have not been comprehensively evaluated. By using microCT, we mapped cortical pore volume fraction (Ct.Po) and thickness (Ct.Th) along the superolateral femoral neck in 14 older women (age: 77.1±9.8 years) to identify subregions and segments with high porosity and/or low thickness—potential "critical" spots where a fracture could start. We showed that Ct.Po and Ct.Th significantly differed between basicervical, midcervical, and subcapital subregions of the femoral neck (p<0.001), where the subcapital subregion showed the lowest mean Ct.Th and the highest mean Ct.Po. These cortical parameters also varied substantially with age and with the location of the analyzed microsegments along the individual's neck (p<0.001), showing multiple microsegments with high porosity and/or low thickness. Although the highest ratio of these microsegmentswas found in the subcapital subregion, they were also present at other examined subregions, which may provide an anatomical basis for explaining the fracture initiation at various sites of the superolateral neck. Given that fractures likely start at structurally and mechanically weaker spots, intra-individual variability in Ct.Po and Ct.Th should be considered and the average values for the entire femoral neck should be interpreted with caution.

Keywords: bone, microarchitecture, hip fractures, cortical pore volume fraction, variability

6.2. Introduction

Hip fracture is one of the main age-related health concerns, of which about 70% occurs in women (Cooper et al. 1992; Williamson et al. 2017). Specifically, it is estimated that about 3.7 times more women above 50 years will sustain hip fracture in 2050 compared with 1990, reaching approximately 4.5 million fractures worldwide (Cooper et al. 1992). The already high costs for hip fracture treatment are also expected to rise in the next years (Svedbom et al. 2013). Approximately one quarter of women with hip fracture dies within the first year, while survivors face the consequences in both physical and psychosocial dimensions of life (Gjertsen et al. 2016; Peeters et al. 2016). Therefore, it is of great importance to understand the basis for hip fractures, so that fracture risk can be detected early and appropriate preventive and therapeutic measures can be undertaken.

Bone microarchitecture deteriorates with aging, and numerous studies have demonstrated negative effects of age on cortical and trabecular structure at the femoral neck (Chen et al. 2010; Djuric et al. 2010; Milovanovic et al. 2012; Rolvien et al. 2018a; Thomas et al. 2009). If unrecognized and untreated, these age-related changes may result in hip fracture. The superolateral neck of the femur is a known fracture-initiating location in older individuals when a sudden impact from a sideways fall exceeds inherent fracture resistance of this bony region (de Bakker et al. 2009; Milovanovic et al. 2012; Milovanovic et al. 2014; Tang et al. 2018; Zani et al. 2015a). During a sideways fall, force produced by the impact is generated at the greater trochanter and afterwards transmitted to the femoral neck. Fleps et el. found that soft tissue, including muscles, absorbed most of the force, and protected the greater trochanter to a certain degree (Fleps et al. 2018). Nevertheless, the femoral neck is devoid of muscles and only relies on its bone structural properties (e.g., cortical pore volume fraction and thickness) to resist compressive stress produced by the fall.

In anatomical terms, there are three main types of hip fractures: basicervical, transcervical (midcervical), and subcapital fractures of the femoral neck (Koval and Zuckerman 2000; Sheehan et al. 2015). Among these types, subcapital type is considered the most common (Jo et al. 2016a; Shoda et al. 2017), while basicervical type occurs more rarely (Saarenpää et al. 2002; Shoda et al. 2017). However, it is still not sufficiently understood why different anatomical types of the neck fractures occur even with similar fracture mechanism. It is possible that various regions of the superolateral neck cortex deteriorate differently with aging, which makes some parts more prone to initiating fracture than others.

While previous studies examined the microstructural basis for hip fractures, either at the level of trabecular or cortical bone (Bell et al. 2000; Bell et al. 1999a; Bell et al. 1999b; Fratzl-Zelman et al. 2009; Milovanovic et al. 2012; Milovanovic et al. 2014; Tang et al. 2018), they either ignored variations within the femoral neck (Fratzl-Zelman et al. 2009; Gauthier et al. 2018; Lochmüller et al. 2008), or focused on structural variation within the neck's cross-section, usually identifying the superolateral quadrant as a critical area, but disregarding any potential variations along the superolateral neck (Bell et al. 1999b; Djuric et al. 2010; Malo et al. 2013; Rolvien et al. 2018a; Thomas et al. 2009).

Since cortical pore volume fraction and cortical thickness are main determinants of bone strength (Sundh et al. 2015; Sundh et al. 2017; Zebaze and Seeman 2015), we hypothesized that these two microstructural parameters are not uniform along the superolateral femoral neck and that there must be multiple "critical" spots—spots with high porosity and/or low cortical thickness. Therefore, the aim of our study was to map cortical pore volume fraction and cortical thickness along the superolateral femoral neck of older female individuals to identify the micro-locations in which microstructure suggests higher susceptibility to fracture.

6.3. Materials and methods

The entire femoral neck was obtained at autopsy from 14 older women (age: 77.1±9.8 years) without history of hip fracture. Neither of the included individuals had malignant diseases, or local neoplastic or degenerative diseases of the femoral neck. Neither of them used medications known to significantly deteriorate bone structure. The collection of the sample was approved by the Ethics Committee of the Faculty of Medicine, University of Belgrade (No. 29/IX-10). All methods were performed following the relevant guidelines and regulations.

By using a water-cooled, low-speed, diamond saw, the superolateral region—the region where a typical osteoporotic fracture starts—was removed from the rest of the neck. Subsequently, the entire superolateral neck was scanned using Skyscan 1172 micro-computed tomography system (Bruker microCT, Skyscan, Belgium). For scanning we used the following system parameters: 80 kV, 124 µA, exposure time of 1200 ms, aluminum and copper filter, 2K camera binning with isotropic voxel size of 10 µm, rotation step of 0.40°, and triple frame averaging. The reconstruction of the projection images was performed in NRecon software (Bruker microCT, Belgium) on InstaRecon platform (InstaRecon, USA) with suitable thermal drift correction, misalignment compensation, Gaussian smoothing of 3, and appropriate ring artifact and beam hardening corrections.

To allow mapping of cortical pore volume fraction and thickness, we divided the entire superolateral neck length (average length 19.75±2.03 mm) to a number of smaller segments. The thickness of the cortical segments was 500 µm to ensure that they are small enough to allow capturing gradients along the femoral neck, but large enough to capture a meaningfully large volume. Such a thickness was arbitrarily selected, keeping in mind to have segments that are formed by an integer number of slices (50 slices, resolution 10 µm), and provided a compromise between convenience, computer hours, and representative volumes.

In each of the segments, the cortical region of interest (ROI) was marked manually, and global threshold of 95/255 was used to distinguish between mineralized bone and marrow spaces. Cortical bone was manually and rigorously separated from trabecular bone, and transitional zone was excluded from the ROI (Figure 2). Cortical pore volume fraction (Ct.Po, %) and cortical thickness (Ct.Th, mm) were evaluated using CT Analyzer version 1.16.4.1 Bruker, Belgium. As for cortical thickness, all cortical pores were removed based on a custom-made algorithm with Boolean operators so that cortical thickness could be evaluated automatically. Since the determination of structure thickness in 3D is based on fitting a sphere in the VOI, the thickness of the VOI lower than the actual cortical thickness would result in Ct.Th values that actually reflect the thickness of the VOI rather than the thickness of

the cortex. To avoid this error, we performed 2D assessment of all slices and determined the mean Ct.Th by fitting circles in the ROI.

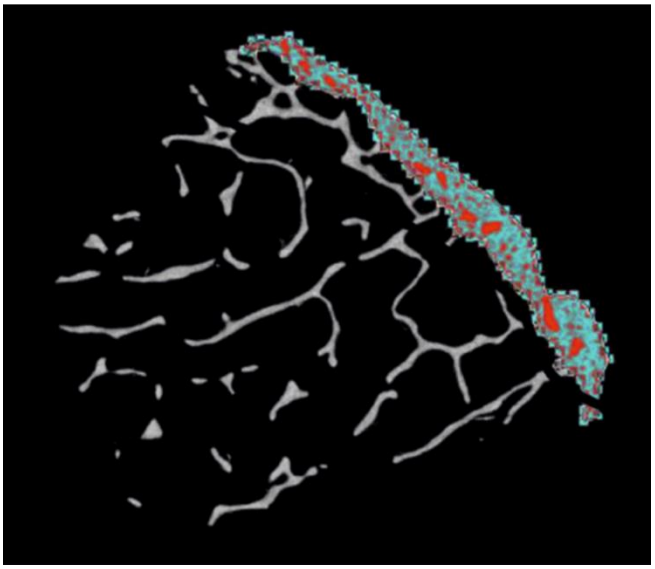

Figure 1. Manual segmentation of the cortical bone: Delineating a region of interest (ROI)

Based on the idea to look for "critical" spots among the segments along the neck in each individual separately, color-coded schemes of the cortical pore volume fraction and thickness values were created to visualize the distribution of "critical" points along the femoral neck (intra-individual differences). We also generated color-coded images based on the range of porosity or thickness values pooled for all individuals (inter-individual differences). Considering that the femoral neck length differed between the individuals, the data were standardized to the unit length to allow inter-individual comparisons.

SPSS version 15 was used for descriptive statistics, repeated-measures ANOVA, multiple regression analysis, and linear mixed-model analysis. Normality of data distribution was assessed by the Kolmogorov–Smirnov test. Repeated-measures ANOVA was applied to assess differences in Ct.Th or Ct.Po between the basicervical, midcervical, and subcapital regions, with post-hoc tests with Bonferroni correction for multiple testing. Multiple linear regression (method: Enter) was conducted to analyze the relationship between segmental cortical pore volume fraction or thickness values with segments' locations and individual age, where arbitrary numbering of the segment locations started from the base of the neck. Linear mixed model was applied, where Ct.Po or Ct.Th was selected as a dependent variable, site (location of the cortical segment, i.e., segment number) and age group (<80 years and ≥80 years) as fixed factors, and individual as a random factor. Results were considered significant if p values were lower than 0.05.

Microsoft Excel, version 2007, was used to prepare color-coded maps of cortical pore volume fraction and cortical thickness among the segments along the femoral neck (Figure 2). Specifically, cortical pore volume fraction and cortical thickness values of each segment were color-coded based on their numerical values. To this end, we used the Conditional formatting option and selected Color scales; 3-Color scale was chosen, and three colors were set based on the three cutoff points of the numerical values of Ct.Po and Ct.Th as follows: red = maximum porosity, minimum thickness; yellow = 50% percentile porosity, 50% percentile thickness; green = minimum porosity, maximum thickness. Segments with porosity or thickness values between these three cutoff values were automatically assigned an appropriate color code proportionate to their value by the software. In color-coded maps (Figure 1), each column represents the length of the femoral neck of one individual (P1–P14).

Considering that the lengths of the femoral neck were not equal in each individual, they were normalized to the unit length to facilitate comparisons. Two types of color-coded maps were prepared. One type was based on the range of porosities and thicknesses of each individual, meaning that e.g. red segments mark the positions of each individual's potentially most critical spots (high porosity; low cortical thickness) (Figure 2A, C); nevertheless, such maps do not take into consideration the individual's porosity or thickness values in relation to other individuals. Therefore, we also prepared color-coded maps based on the pooled range of porosities and thicknesses of all of the individuals (Figure 2B, D), illustrating the distributions of porosity and thicknesses within individual and inter-individual differences in these parameters. Horizontal lines in the maps denote arbitrary boundaries between basicervical, mid-cervical, and subcapital subregions of the femoral neck (20%:60%:20%).

6.4. Results

Our microarchitectural assessment of the segments of the superolateral femoral neck showed within and between-individual variability in cortical pore volume fraction and cortical thickness along the femoral neck of older females, even within the subregions usually considered uniform (basicervical, mid-cervical, and subcapital) (Tables 1 and 2).

Repeated-measures ANOVA between the basicervical, midcervical, and subcapital subregions showed that Ct.Po and Ct.Th significantly depended on the subregion (both $p<0.001$). Specifically, post-hoc tests showed that the subcapital subregion had significantly higher Ct.Po than the midcervical subregion ($p=0.001$) and the basicervical subregion ($p=0.001$); and significantly lower Ct.Th than the midcervical subregion ($p<0.001$) and the basicervical subregion ($p<0.001$). Moreover, the basicervical subregion showed significantly higher Ct.Th than the midcervical subregion ($p=0.001$).

Multiple linear regression analysis showed that segmental Ct.Po was associated with segments' location ($p<0.001$) and individual age ($p=0.03$) ($R^2=0.174$). Specifically, Ct.Po values increased from the base of the neck towards the femoral head, and increased with the increasing age. Segmental Ct.Th was associated with segments' location ($p<0.001$) and individual age ($p<0.001$) ($R^2=0.426$). Specifically, Ct.Th values decreased from the base of the neck towards the femoral head, and decreased with the increasing age.

To verify the effects of the segment's location along the femoral neck on its Ct.Po or Ct.Th values, we also applied linear mixed-model analysis, where Ct.Po or Ct.Th was selected as a dependent variable, site (location of the cortical segment, i.e., segment number) and age group (<80 years and ≥80 years) as fixed factors, and individual as a random factor. The results confirmed that site was significantly associated both with Ct.Po and Ct.Th ($p<0.001$ for both).

Table 1. Descriptive statistics of cortical pore volume fraction among 500-µm-thick cortical segments of the superolateral femoral neck. Data are presented for the entire neck and for each subregion of the entire sample (basicervical, midcervical, and subcapital) (N=14).

	Cortical pore volume fraction [%]				**Cortical thickness [mm]**			
Name of examined region	**Mean**	**SD**	**Minimum**	**Maximum**	**Mean**	**SD**	**Minimum**	**Maximum**
Entire superolateral neck	24.1	9.6	7.4	72.2	0.24	0.06	0.09	0.36
Basicervical[a] subregions	19.4	6.7	7.4	36.9	0.28	0.03	0.2	0.36
Midcervical[a] subregions	22.6	7.6	8.4	61.1	0.25	0.5	0.09	0.35
Subcapital[a] subregions	32.4	12.3	12.6	72.2	0.17	0.04	0.09	0.26
Dependence on the subregion	$P < 0.001$ [x, y]				$P < 0.001$ [x, y, z]			

Note. N, total number of included individuals;
a, basicervical subregion encompassed 20% of segments close to the base of the neck, subcapital subregion encompassed 20% of cortical segments close to the femoral head, and midcervical subregion encompassed the middle 60% of cortical segments;x, subcapital vs midcervical p<0.05; y, subcapital vs basicervical P<0.05; z, midcervical vs basicervical p<0.05.

Figure 2 illustrates considerable individual variability in cortical pore volume fraction (Figure 2A, B) and cortical thickness (Figure 1C, D) between the subregions, but also within the subregions (basicervical, midcervical, and subcapital). Figure 1A displays the segments of the superolateral femoral neck color-coded per value of cortical pore volume fraction and illustrates such variability along the neck. It was observed that there were potentially "critical" points (segments) in various cortical subregions within an individual, but majority of these points were located closer to the femoral head, and less often in the mid-neck, or at the base of the neck (Figure 2A). It was also notable that there were inter-individual differences in the distribution of "critical" regions. Specifically, Figure 2B shows color-coded distribution of cortical pore volume fraction in relation to the pooled values from all of the individuals, further illustrating inter-individual differences in cortical microstructure. Of note, although P9 and P14 have red spots in panels A and C, panels B and D show that most segments in P9 and P14 were in green to yellow range and there were no red segments, suggesting that these individuals have lower Ct.Po and Ct.Th than other individuals and possibly a lower fracture risk.
Along the length of the superolateral neck, cortical thickness varied substantially within each individual, but majority of thinner segments were located closer to the femoral head (Figure 2C). Within the whole sample (all 500-µm-thick segments in all 14 specimens), cortical thickness varied considerably (Figure 2D) (Table 2).

Table 2. Cortical pore volume fraction and cortical thickness per individual.

Case number	Age [years]	Femoral length [mm]	Cortical pore volume fraction [%]				Cortical thickness [mm]			
			Mean	SD	Min	Max	Mean	SD	Min	Max
P1	80	19.5	25.83	8.45	12.15	50.80	0.25	0.05	0.16	0.33
P2	62	19.5	17.38	9.11	7.36	49.62	0.26	0.03	0.16	0.30
P3	89	19.5	19.50	7.58	9.42	45.10	0.26	0.04	0.17	0.33
P4	87	19.5	30.13	16.89	9.07	72.17	0.18	0.06	0.09	0.29
P5	89	18	29.03	5.63	17.05	38.22	0.18	0.04	0.12	0.24
P6	82	22.5	28.70	7.21	15.31	47.71	0.22	0.05	0.14	0.30
P7	80	22.5	21.75	9.07	10.54	60.34	0.24	0.06	0.12	0.31
P8	85	21	22.74	5.56	12.13	37.68	0.22	0.04	0.15	0.28
P9	68	21	16.46	4.24	8.85	26.67	0.29	0.05	0.17	0.36
P10	68	18	27.03	6.27	10.58	40.51	0.25	0.05	0.13	0.31
P11	64	18	24.97	8.93	14.15	45.10	0.27	0.06	0.13	0.36
P12	64	15.5	29.30	9.80	16.22	49.76	0.19	0.04	0.13	0.29
P13	80	22.5	26.53	8.83	13.57	52.50	0.21	0.06	0.09	0.32
P14	82	19.5	17.71	5.15	10.21	35.25	0.29	0.04	0.19	0.35

6.5. Discussion

In this study, we demonstrated increased cortical pore volume fraction and lower cortical thickness in the subcapital subregion compared with the midcervical and basicervical subregions of the superolateral femoral neck. The midcervical subregion had lower thickness than the basicervical subregion. The subcapital and midcervical subregions particularly showed heterogeneous spatial distribution of cortical pore volume fraction. As shown by Granke et al. (Granke et al. 2016), heterogeneous spatial distribution of cortical porosities is associated with a decrease in fracture toughness properties. Increased intra-cortical pore volume fraction is considered an essential indicator of increased risk of bone fracture (Bell et al. 1999a; McCalden et al. 1993a; Sundh et al. 2015; Sundh et al. 2017; Ural and Vashishth 2007). Previous studies showed regional differences in cortical pore

volume fraction within the cross-section of the femoral neck (Bell et al. 1999a; Rolvien et al. 2018a). Specifically, Bell et al. divided the full circumference of the femoral neck in four regions: anterior, posterior, medial, and lateral, and showed that the lateral neck was the most porous region in women (Bell et al. 1999a). Together with other indicators of bone fragility (Milovanovic et al. 2014; Tang et al. 2018)and biomechanical reasons, this observation may explain why the lateral (superolateral) neck is the most common place for start of a fracture during the sideways fall (de Bakker et al. 2009; Kheirollahi and Luo 2015; Zani et al. 2015a).Indeed, considering that cortical bone is the first to resist force caused by the impact during the fall, and is the principal contributor to the femoral neck strength (Holzer et al. 2009a), increased pore volume fraction likely reduces bone strength (Sundh et al. 2017), and it was shown by mechanical testing that three quarters of the entire cortical bone strength were attributable to its porosity (McCalden et al. 1993b). Therefore, the particularly increased cortical pore volume fraction in the subcapital subregion may explain why fractures are most common there; moreover, its heterogeneous spatial distribution of cortical porosities is associated with a decrease in fracture toughness properties, as shown by Granke et al. (Granke et al. 2016).

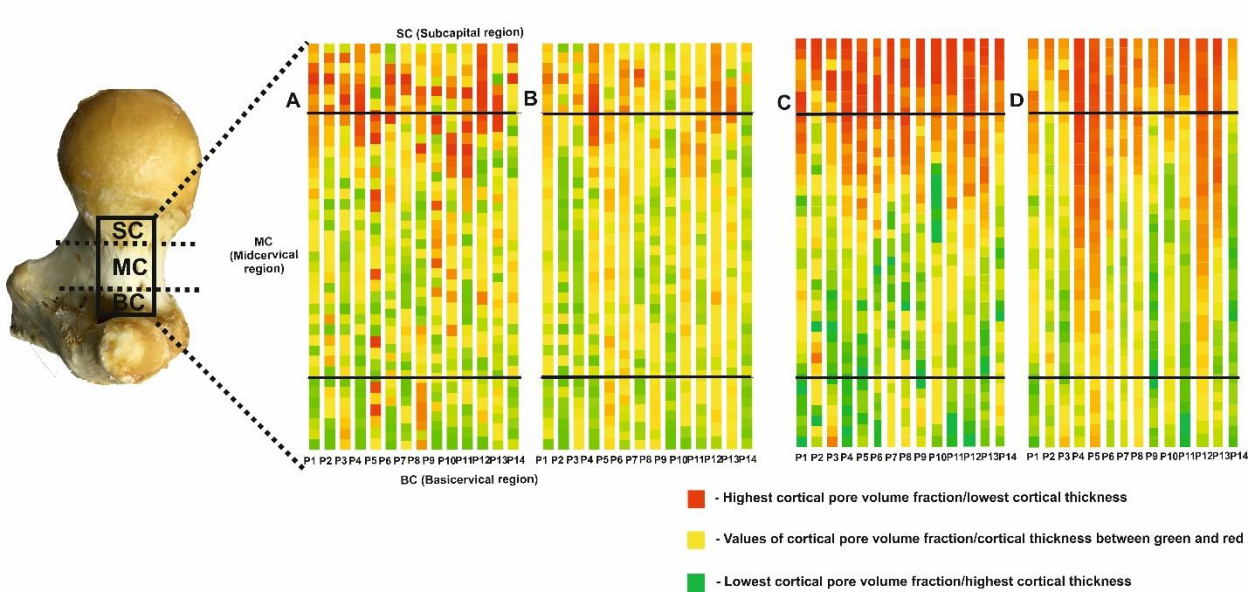

Figure 2. Color-coded maps of distribution of cortical pore volume fraction and thickness along the superolateral femoral neck in all individuals. Each column represents the femoral neck of one individual (P1–P14) normalized to the same length to facilitate comparisons. Color codes of cortical segments along the superolateral femoral neck range from green (the lowest porosity or highest thickness) via yellow (middle range values for both parameters) to red (highest porosity or lowest thickness). (A and C) Color codes based on the range of Ct.Po (A) and Ct.Th (C) of each individual separately. (B and D) Color codes based on the pooled range of Ct.Po (B) and Ct.Th (D) of all individuals, illustrating the distributions of Ct.Po (B) and Ct.Th (D) within individual and inter-individual differences in these parameters. Horizontal black lines are arbitrary boundaries between basicervical, midcervical, and subcapital subregions of the femoral neck.

Recently, Cirovic et al. analyzed microarchitectural parameters of two subregions of the superolateral neck in young and aged men, and reported that the basicervical subregion was significantly less porous than the subcapital region (Cirovic et al. 2020). Bousson et al. investigated porosity of the medial neck in women aged between 72 and 103 years, and showed that cortical pore volume fraction varied considerably between subjects, from 4.96% to 38.87% (Bousson et al. 2004). Our study showed inter-individual differences in porosity, but also highlighted substantial variation in

porosity along the entire superolateral neck of women (between 7.4% and 72.4%) (Table 1). Moreover, our results showed that average values of porosity were two- to three times lower than maximum values (depending on the region); the spots with maximum porosity (or close to maximum) are more likely the "critical" spots for fracture initiation. However, in all previous studies, the clinical implications for fracture risk were based on the assumption that the examined regions were structurally uniform (Bell et al. 1999c; Bousson et al. 2004; Cirovic et al. 2020; Rolvien et al. 2018b). Studies that applied µFE modeling provided some insights into the distributions of maximal principal and average tissue-level principal strain magnitudes at the entire femoral neck; however, they were based on poorer resolution and did not distinguish between the subregions of the superolateral femoral neck (Iori et al. 2020; Van Rietbergen et al. 2003a; Verhulp et al. 2008).

Although subregions of the femoral neck (inferomedial, superolateral; basicervical, midcervical, and subcapital) are taken as homogenous, the results of our study highlighted substantial variability in cortical pore volume fraction and thickness along the superolateral femoral neck of an individual. There were critical points in various cortical regions within an individual, majority of which were located closer to the femoral head, and less often in the mid-neck, or at the base of the neck, especially for cortical pore volume fraction. Inter-individual variability in the distribution of "critical" segments might explain fracture initiation at different sites of the superolateral femoral neck among different individuals, assuming that the strains and stresses are similar along the femoral neck. These findings may corroborate previous observations that strain magnitudes in osteoporotic bone are less uniformly distributed (Van Rietbergen et al. 2003b). Nevertheless, it was evident that the highest concentration of "weak" spots was in the subcapital region. This corresponds to the literature data about higher occurrence of subcapital fractures compared with transcervical and basicervical (Jo et al. 2016b; Magu et al. 2014). Our findings suggest that consideration of the average porosity and thickness of the entire neck or even its main subregions may not reliably reflect the actual microarchitecture of the cortical bone, partly masking the real critical spots of the femoral neck. Our study had a great advantage to analyze a number of smaller segments (each 500-µm-thick) in a representative set of individuals (older females).

Our study was limited by a cross-sectional study design. Another issue is that we did not perform any mechanical testing; in this context, to make a significant step towards quantitative prediction of failure load and location based on imaging data alone, it may be beneficial to conduct such tests and finite element studies in the future. In addition, in this study we focused only on cortical bone; nevertheless, cortical bone is the first one to accept the mechanical load and is considered crucial for the mechanical integrity of the proximal femur (Holzer et al. 2009b). The location of a fracture depends also on the mechanism of fracture (Faisal and Luo 2016), but it is generally believed that this is more or less similar in individuals who fall onto the greater trochanter, which puts the superolateral neck at a sudden high stress (Zani et al. 2015b). Although there are still scarce data, some FE studies showed high stress concentration at the subcapital subregion during sideways fall, and confirmed high frequency of subcapital fractures among femoral neck fractures (Jia et al. 2014; Keyak 2001; Koivumäki et al. 2010). Moreover, FE simulation of sideway fall showed that soft tissue absorbed some impact and reduced the force transferred through the neck (Fleps et al. 2018); nevertheless, the force is obviously sufficiently high to cause the fracture of the neck at the least resistant region. Moreover, further FE studies will have to account for the here-reported, evident, segmental variability in the femoral neck, and examine more closely whether differences in characteristics of a fall put particular strain on specific segments along the femoral neck. However, presence of structurally weak spots is a prerequisite for a fracture in any given segment area, and our study provides important clues for further evaluations of the fracture risk. Nevertheless, it should be acknowledged that cortical porosity and thickness are not the only parameters relevant for bone strength, so further studies should also examine other microarchitectural parameters (such as orientation of cortical pores) and matrix

mineralization; however, as for degree of anisotropy of the cortical pores, if the selected VOI is too thin (narrow), which was the case with our 500-μm-thick segments, the value of degree of anisotropy would probably reflect the choice of the thin VOI rather than the actual spatial arrangement of the cortical pores as suggested by Tassani and Perilli for trabecular bone (Tassani and Perilli 2013).

Although our study provides clinically relevant data, it may be useful to perform an HR-pQCT study in a similar way to further verify clinical relevance of our findings. However, the resolution of HR-pQCT is approximately 40–80 μm, and that resolution is blind for many of the cortical pores, which is a major weakness of clinical bone microarchitecture assessment by HR-pQCT.

In conclusion, our results revealed tremendous diversity of cortical pore volume fraction as well as cortical thickness values among the segments in each examined region of the superolateral femoral neck. While the highest ratio of critical to non-critical spots was observed in the subcapital subregion, we observed a number of critical spots in other subregions as well, which offers the explanation for the microstructural basis of hip fractures in various regions of the femoral neck. Our results also emphasize that the assessments of large femoral regions that give the average values of cortical pore volume fraction or thickness may not be fully representative of the actual microarchitecture and fracture risk, as they may mask some critical spots with other "better" spots in the neighborhood. Moreover, our results suggest that more attention should be directed to heterogeneity of bone structure and heterogeneous skeletal effects of aging and diseases; considering that fracture follows the path of least resistance, the presence of particularly weak spots is more important for bone fragility than the average values.

SECTION 7

Altered osteocyte lacunar density pattern, trabecular mineralization imbalance in the femoral neck, and decreased trabecular microhardness in the trabeculae of the femoral head as microstructural indicators of higher fracture risk in individuals with type 2 diabetes mellitus

The results presented in this Section are being prepared for publication. The list of authors involved in the work presented is as follows: Cirovic A, Schmidt FN, Jadzic J, Vujacic M, Sihota P, Petrovic B, Djukic D, Zivkovic V, Bascarevic Z, Nikolic S, Djonic D, Djuric M, Busse B, Milovanovic P.

7.1. Abstract

Despite previous efforts, our understanding of why individuals with type 2 diabetes mellitus (T2DM) are more susceptible to fractures remains limited. In this study, we examined bone mineral density distribution, osteocyte lacunar density, and microhardness in the femoral head trabeculae (18 T2DM and 25 controls; 30 women and 5 men, mean age: 77 years) and osteocyte lacunar density in the regions of superolateral femoral neck (8 T2DM and 8 controls; 16 men, mean age: 61years). Individuals with T2DM had a lower femoral head trabecular Ca width, while none of the osteocyte lacunar density parameters did not vary between examined groups (Lc.N/B.Ar, Mn.Lc.N/B.Ar and total- Lc.N/B.Ar). We found lower nonmineralized lacunar number per bone area (Lc.N/B.Ar) in the endocortical and periosteal regions of the superolateral femoral neck of T2DM subjects compared with controls ($p=0.006$, $p=0.004$), while mineralized lacunar number per bone area (Mn.Lc.N/B.Ar) was similar between the investigated groups ($p=0.172$, $p=0.262$). Mn.Lc.N/B.Ar was the highest in the periosteal and endocortical compartments of the transcervical region ($p=0.015$, $p=0.069$, respectively) compared with other regions of the superolateral femoral neck. Total-Lc.N/B.Ar in the periosteal region did not significantly vary between the examined groups ($p=0.078$). A higher percent of mineralized lacunae was found in the endocortical ($p<0.05$) and periosteal subregions ($p=0.062$) of T2DM subjects compared with controls. The control group had higher trabecular bone microhardness than the T2DM group ($p=0.038$). The observed changes in osteocyte lacunar density, mineralization, and hardness might explain the increased hip fracture susceptibility in individuals with T2DM.

Key words: Type 2 diabetes mellitus; backscattered electron imaging, Ca width, microhardness, osteocyte lacunar density.

7.2. Introduction

In 2017, it was estimated that 6.28% of the world's population had diabetes mellitus (DM), and over one million deaths were associated with diabetes mellitus (DM) (Khan et al. 2020). If current trends continue, it is expected that more than 10% of the world's population will have DM by 2030 (Saeedi et al. 2019). Poor glycemic control is associated with accelerated development of diabetic complications (Fasil et al. 2018), which further reduces quality of life (Huang et al. 2007; Quah et al. 2011) and increases treatment expenses. More than half of the costs for medical treatment are spent on managing diabetic complications (von Ferber et al. 2007). Osteoporosis is another rapidly expanding public health problem worldwide. According to current estimates, over 27 million individuals in the European Union have osteoporosis (Hernlund et al. 2013). The mortality rate in patients with hip fracture is higher in those with coexisting DM compared with non-DM subjects (Gulcelik et al. 2011; Martinez-Laguna et al. 2017; Tebe et al. 2019).

In the absence of a better tool, dual-energy X-ray absorptiometry (DXA) is mostly used in clinical setting to assess individual risk of fracture. However, many studies have emphasized that individuals with type 2 DM (T2DM) frequently have higher bone mineral density (BMD) (Nilsson et al. 2017; Rakic et al. 2006; Schwartz et al. 2002; van Daele et al. 1995) than controls; however, T2DM patients are still at an increased risk for sustaining a hip fracture (Dede et al. 2014; Fan et al. 2016; Forsén et al. 1999; Janghorbani et al. 2007; Rathmann and Kostev 2015; Tebe et al. 2019; Vestergaard et al. 2009). Many studies have confirmed an increased risk of fracture in individuals with DM (Bonds et al. 2006; Melton et al. 2008; Valderrabano and Linares 2018), especially of the hip, foot, and spine (Bonds et al. 2006). A study conducted on 5285 women with T2DM and 88120 postmenopausal women without DM showed a 20% higher risk for sustaining any fracture in women with T2DM (Bonds et al. 2006). Although the basis of the increased fracture risk in DM individuals has frequently been evaluated, the reported results are often conflicting and there is not yet a firm conclusion. For example, it has been reported that bone microarchitecture in DM subjects may be worse, equally good,

or even better compared with that in non-DM subjects (Burghardt et al. 2010; Samakkarnthai et al. 2020). Based on the results of microindentation testing (microhardness)/bone material strength index (BMSi), bone material properties may be deteriorated in T2DM individuals compared with controls (Cirovic et al. 2022a), but it is now always the case (Samakkarnthai et al. 2020). Higher levels of advanced glycation end products (AGEs) are associated with the increased fracture risk in DM subjects, but AGEs levels could also be similar between DM subjects and controls. Recently, we have shown lower femoral neck cortical and trabecular microhardness in T2DM subjects in both compartments (cortical and trabecular)(Cirovic et al. 2022a); however, this study was conducted on a limited sample size (T2DM, n=8).

Aside from bone microarchitecture, microindentation testing, and examination of AGEs, other relevant bone characteristics have not yet been well evaluated in subjects with DM subjects. These include bone mineral density distribution, i.e., the degree of mineralization, and osteocyte lacunar density. As individuals age, osteocyte lacunar density decreases, while the number of highly mineralized osteocyte lacunae increases(Busse et al. 2010). Since elderly men and women, in particular, are prone to fractures, alterations in osteocyte lacunar density due to T2DM may be a factor contributing to the fracture risk (Busse et al. 2010). Kolibová et al. have recently found an increased number of mineralized osteocyte lacunae in the cortex of the femoral diaphysis in subjects with type 1 DM compared with controls (Kolibová et al. 2023). Lower mean matrix mineralization and higher mineralization heterogeneity have been found in individuals who sustained a fracture in a quantitative backscattered electron Imaging (qBEI) study (Hofstaetter et al. 2012). Wölfel et al. analyzed the mid-shaft of the femur in T2DM subjects post-mortem and found lower osteon density, lower peak frequency, and broader calcium width in the endocortical and periosteal regions in a fraction of T2DM subjects (those with high cortical porosity) (Wölfel et al. 2020b).

In this study, we analyzed several indicators of bone quality in cortical and trabecular compartments of the superolateral femoral neck and trabecular compartment of the femoral head. Specifically, osteocyte lacunar density, bone mineral density distribution (i.e., the degree of mineralization), and bone material properties were examined in individuals with T2DM and controls. We hypothesized that the superolateral femoral neck's cortical bone in T2DM may display impaired osteocyte lacunar density and lower osteon density. We also hypothesized that the femoral head trabeculae in subjects with T2DM have altered trabecular mineralization pattern, impaired trabecular osteocyte lacunar density, and reduced bone material properties.

7.3. Materials and methods

7.3.1 Study design

For the purpose of this study, femoral neck samples were collected from a tertiary-level orthopedic university hospital (Institute for Orthopedic Surgery "Banjica," Belgrade), while post-mortem samples of proximal femora were obtained from autopsy in collaboration with the Institute of Forensic Medicine, Faculty of Medicine, University of Belgrade. Specifically, femoral head samples were obtained at the Institute for Orthopedic Surgery "Banjica" from 18 T2DM subjects who sustained unilateral low-energy femoral neck fracture. At the Institute of Forensic Medicine, we collected superolateral femoral neck samples from individuals with T2DM; superolateral femoral neck samples from non-DM subjects, which served as controls; and femoral head samples from non-DM individuals, which served as controls for the specimens obtained at the Institute for Orthopedic Surgery "Banjica." Detailed inclusion and exclusion criteria were listed in our previous publications (Cirovic et al. 2022a; Cirovic et al. 2022b).

Specifically, for the first part of the study, we collected eight femoral neck specimens from individuals with T2DM diagnosed prior to death and eight proximal femora from non-DM individuals at the Institute of Forensic Medicine. For the second part of the study, we obtained 18 specimens (15

women and 3 men) of the femoral head from individuals with T2DM at the Institute for Orthopedic Surgery "Banjica" and 25 femoral head specimens (20 women and 5 men) from individuals without T2DM at the Institute of Forensic Medicine (Table 1).

Table 1. Demographic data and BMI.

Region of interest	***Number of specimen and sex distribution***	***Mean age***	***BMI***
Superolateral femoral neck	16 men (8 T2DM and controls)	61±10 years	T2DM: 26.83±2.81 CTL: 23.42±4.6
Femoral head trabeculae	38 (30 women and 5 men); 14 T2DM and 19 controls	77.18years	T2DM: 25.77 ± 3 CTL: 27.5 ± 4.6

7.3.2. Microindentation testing

To evaluate the micromechanical properties of the femoral head trabecular bone, we utilized a Vickers microhardness tester (HMV-G version, Schimadzu, Japan). The measurements were carried out in line with the previously established conditions for microhardness measurements (Cirovic et al. 2022a). A load of 50 g and an indentation time of 12 s were applied to various trabecular regions. Prior to the microindentation testing, all samples were embedded in resin and polished. Using a 40× magnifying lens, we conducted five separate and valid measurements of the trabecular compartment in each specimen, and the average values were utilized for intergroup comparisons. In order to avoid boundary effects, we ensured that the indentations were at least 2.5 diagonals from the margins, and there were at least 2.5 diagonals between adjacent indentations to prevent overlapping of artificial depressions from one indentation to another (Yin et al. 2019). The measurements were carried out independently by two researchers, and the average value was used for the analysis.

7.3.3. Bone mineral density distribution and osteocyte lacunar density

To examine the bone mineral density distribution (BMDD) and perform a 2D morphological analysis of osteocyte lacunae, quantitative backscattered electron imaging was utilized. The resin-embedded specimens underwent coplanar grinding and were subsequently polished and carbon-coated before imaging. A scanning electron microscope (Crossbeam 340, GeminiSEM, Zeiss AG, Oberkochen, Germany) was operated in backscattered electron mode at 20 keV with a constant working distance of 20 mm. To control the current beam, a Faraday cup was utilized, and grayscale values were calibrated using an aluminum–carbon standard. Cortical specimens were evaluated using scanning electron microscope (LEO435 VP; LEO Electron Microscopy Ltd., Cambridge, UK) operated at 20 kV and 680 pA using a constant working distance of 20 mm (BSE Detector, Type 202; K.E. Developments Ltd., Cambridge, UK). During imaging, all parameters were monitored and kept at a constant level. Images were acquired at a magnification of 100x. Four to five images per specimen were captured for the assessment of BMDD (mean calcium weight percentage (mean Ca, wt %); most frequent calcium weight percentage (peak Ca, wt %); standard deviation of the calcium content curve, displaying the heterogeneity of mineralization content (width Ca, wt %); percentage of bone area mineralized below the 5th percentile of the reference range of the control group (Ca low, % bone area); percentage of bone area containing calcium concentration above the 95th percentile of the control group (Ca high, % bone area)) and osteocyte lacunar morphology analysis. All examined regions (trabecular and cortical compartments) were evaluated for the following parameters: number of mineralized lacunae per bone area (Mn.Lc.N/B.Ar), number of non-mineralized lacunae per bone area (Lc.N/B.Ar), and total number of lacunae per bone area (total-Lc.N/B.Ar) using ImageJ/Fiji (1.53t). We also calculated percent of mineralized and non-mineralized lacunae by dividing the total number of lacunae per bone

area with the percent of mineralized lacunae per bone area (%Mn.Lc; [%]) and the number of non-mineralized lacunae per bone area (Lc.N; [%]) separately. All the parameters of the BMDD (Ca Mean, wt%) were evaluated from the backscattered electron images using a custom-made MATLAB code (MATLAB, Natick, Massachusetts).

In the part of our study in which we examined the superolateral neck of the femur, we analyzed the density of osteocyte lacunae along the entire length of the bone, from the junction of the head and neck to the greater trochanter. To perform more detailed analyses, we divided the full length of the superolateral neck into three subdivisions as follows: subcapital, transcervical, and basicervical regions. We have previously discussed this subdivision in greater depth in our previous paper (Cirovic et al. 2020). By doing so, we were able to distinguish all three subregions along the longitudinal axis of the superolateral femoral neck. Moreover, on the transverse section of each subregion (subcapital, transcervical, and basicervical), the two parts, endocortical and periosteal, were clearly distinguishable. Therefore, in the final analysis of osteocyte lacunae in the superolateral femoral neck cortex, we included the endocortical and periosteal parts of the subcapital region, the endocortical and periosteal parts of the transcervical region, and the endocortical and periosteal parts of the basicervical region.

7.3.4. Statistical analysis

The Kolmogorov–Smirnov test was used to verify that all of the measured parameters complied with normal distribution. The *t* test for independent samples was used to check for differences in age, BMI, the parameters of BMDD, Lc.N/B.Ar, Mn.Lc.N/B.Ar, Total-Lc.N/B.Ar, and microhardness between the investigated groups (T2DM and controls). Analysis of variance (ANOVA) for repeated measurements, with Bonferroni post-hoc correction, was performed to check for the effects of the group, region (three regions of the superolateral femoral neck), and their interaction on osteocyte lacunar density parameters. All analyses were performed two-tailed in SPSS software ver. 15 at the significance level of 0.05.

7.4. Results

7.4.1. Femoral head trabeculae

T2DM and control subjects did not differ in age ($p>0.5$) or BMI ($p=0.8$). There were no significant differences in Ca low, mean Ca, and peak Ca between T2DM and controls ($p=0.115$, $p=0.352$, $p=0.236$, respectively). Ca width was significantly higher in the controls, while Ca high was lower in T2DM subjects, but the significance level was not reached ($p=0.074$) (Figure 1). Mn.Lc.N/B.Ar, Lc.N/B.Ar and total-Lc.N/B.Ar did not differ between T2DM subjects and controls ($p>0.05$).

7.4.2. Microindentation testing

Control specimens had higher trabecular bone microhardness than T2DM specimens ($p=0.0381$).

7.4.3. Osteocyte lacunae density

As for the trabeculae of the femoral head,Lc.N/B.Ar, Mn.Lc.N/B.Ar did not vary between the examined groups ($p=0.169$, $p=0.183$). Osteon density did not vary between the examined groups ($p>0.05$).

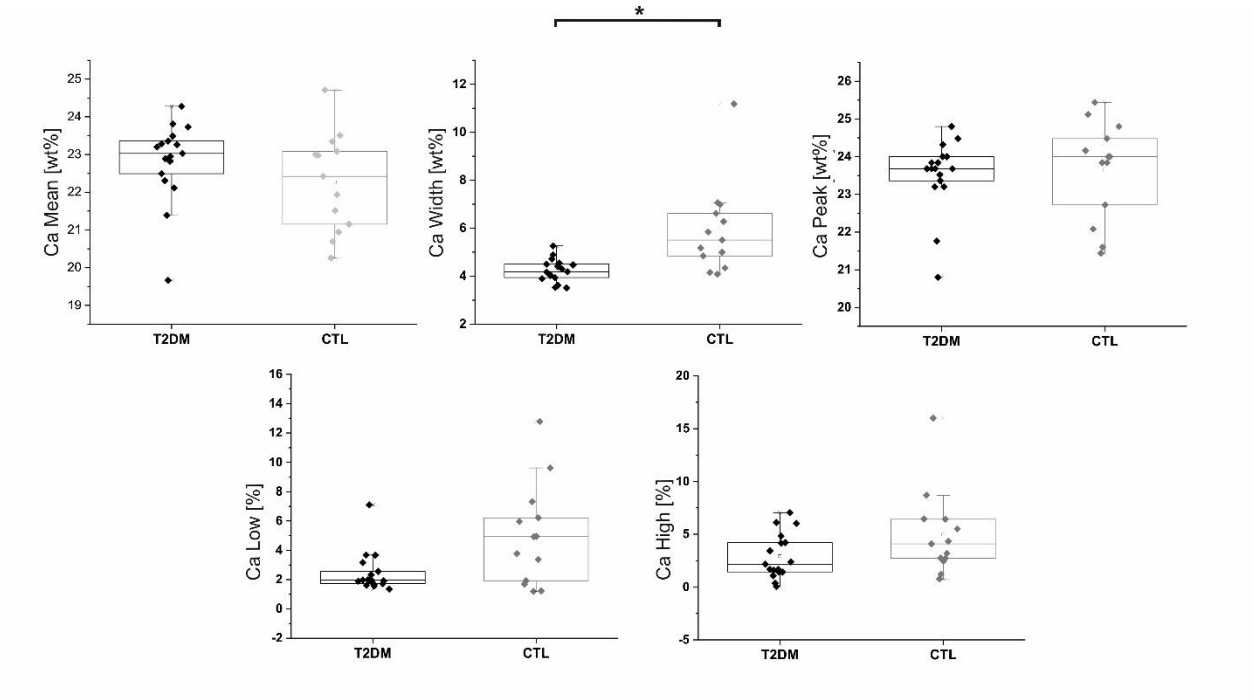

Figure 1. Mineralization parameters of the femoral head trabeculae in T2DM and controls.

7.4.4. Superolateral femoral neck

T2DM and control subjects were similar in age (p=0.605) and BMI (p=0.114). We found lower Lc.N/B.Ar in the endocortical and periosteal regions of the superolateral femoral neck in the T2DM group compared with the corresponding regions in the control group (p=0.006, p=0.004, respectively), while Mn.Lc.N/B.Ar was similar between the investigated groups (p=0.172, p=0.262 respectively). Mn.Lc.N/B.Ar tended to be higher in the endocortical compartment of transcervical region (p=0.069) compared with subcapital and basicervical regions. The periosteal compartment of the transcervical region had significantly higher Mn.Lc.N/B.Ar than other regions of the superolateral femoral neck (p=0.015). Total-N.Lc/B.Ar did not vary significantly among the examined groups (T2DM and controls) in the periosteal region (p=0.078). Higher %Mn.Lc was found in the endocortical ($p<0.05$) and periosteal subregions (p=0.062) of T2DM subjects compared with the controls. As for the trabecular bone, all of the examined parameters were similar in the two groups ($p>0.05$). An interaction of site and group remained insignificant for all of the examined parameters (Lc.N/B.Ar, Mn.Lc.N/B.Ar, and Total- Lc.N/B.Ar) both endocortically and periosteally (all $p>0.05$). A summary of the results in shown in Figure 2.

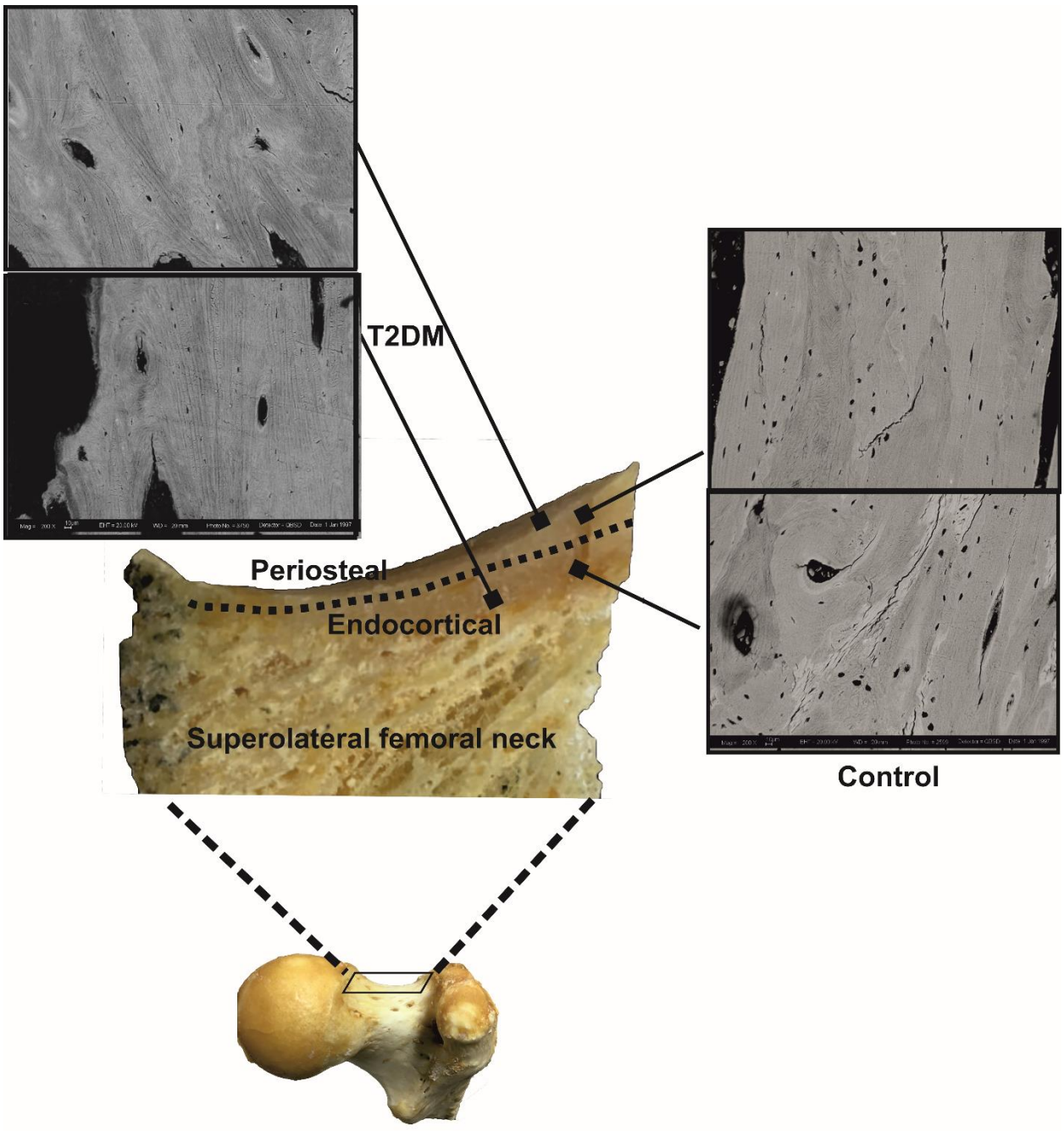

Figure 2. Osteocyte lacunar parameters in T2DM and controls at the superolateral femoral neck.

7.5. Discussion

In this study, we analyzed the density of osteocyte lacunae, microhardness, and degree of mineralization of the trabeculae of the femoral head. In the superolateral femoral neck, we evaluated the density of osteocyte lacunae and osteonal density. We obtained lower microhardness and a lower Ca width in the femoral head trabeculae, indicating that T2DM may induce changes in the bone matrix mineralization, leading to a decreased mechanical bone resistance. On the other hand, fracture initiation is associated with unfavorable properties of the cortex of the superolateral femoral neck, and we found an altered pattern of the osteocyte lacunae density within it.

Wölfel et al. examined the mineralization profile of the cortex of the femoral diaphysis in three groups of individuals postmortem: subjects with T2DM, T2DM subjects with pronounced cortical porosity, and controls. They found higher calcium width in the endocortical region of T2DM individuals with pronounced cortical porosity (Wölfel et al. 2020a). Although the results reported by Wölfel et al. are in contrast with ours, there are two main differences. Firstly, Wölfel et al. analyzed femora diaphysis, and secondly, the focus of the study was cortical bone. So, this could explain why the results from Wölfel et al. are somewhat opposite to ours. Pritchard et al. (Pritchard et al. 2013) also evaluated the degree of mineralization in T2DM individuals. They collected femoral neck specimens obtained after surgery due to osteoarthritis and analyzed the trabecular compartment. The authors found higher mean calcium and lower calcium width in individuals and suggested that this could be explained by altered bone remodeling (Pritchard et al. 2013). Misof et al. analyzed bone mineralization in transiliac bone biopsy specimens obtained from 26 young (premenopausal) women. In that study, neither cancellous nor cortical BMDD parameters from these individuals were significantly different from reference BMDD (Misof et al. 2022). However, the study had several limitations, such as including only premenopausal women and utilizing specimens from the iliac bone. Rolvien et al. analyzed various aspects of BMDD in femoral diaphysis of 51 female donors post-mortem. They found similar values of calcium width between young and osteoporosis groups, while aged individuals had lower calcium width compared with both groups (Rolvien et al. 2020). Moreover, apart from BMDD parameters, Rolvien et al. performed an osteocyte lacunar density evaluation based on the qBEI images and found that aged subjects had significantly lower Lc.N/B.Ar and higher Mn.Lc.N/B.Ar compared with young subjects. In contrast, individuals with osteoporosis did not differ from controls for either of these parameters. Taking BMDD and osteocyte lacunar density evaluation into consideration, it is reasonable to speculate that T2DM and osteoporosis have adverse effects on bone quality but in a different manner. T2DM subjects more commonly experience hip and humerus fractures, while wrist fractures are common among individuals with osteoporosis, however it is not always the case (Schousboe et al. 2022; Viggers et al. 2023). It is possible that T2DM accelerates bone aging, as evidenced by advanced glycation end products (AGEs) accumulation in bone tissue [39]. Lower calcium width indicates more homogeneous mineralization, which ensures relatively uniform mechanical properties and facilitates crack propagation in the shortest trajectory. In cases where regions with higher calcium quantities are present in the bone, they are avoided by the trajectory of the fracture, leading to gradual loss of fracture energy and the appearance of incomplete fractures.

Recently, we have measured the microhardness of the superolateral femoral neck's cortical and trabecular compartments in eight subjects with diabetes and eight controls and obtained lower microhardness (Cirovic et al. 2022a) of both compartments in T2DM subjects. This study represents a significant step forward in better understanding the mechanisms involved in the increased hip fracture risk in T2DM individuals.

Farr et al. reported a lower BMSi at the tibia mid-shaft in 30 T2DM women compared with non-DM controls. Nonetheless, Samakkarnthai et al. found no difference in BMSi at the same site in a larger cohort that included 171 T2DM patients and 108 age-matched non-DM subjects of both sexes (Samakkarnthai et al. 2020). Holloway-Kew also determined a BMSi using OsteoProbe in 340 men

(234 controls, 59 subjects with impaired fasting glucose, and 47 T2DM subjects). When all three groups were statistically analyzed with ANCOVA, no differences were observed (Holloway-Kew et al. 2021); however, when the authors fused controls with subjects with impaired fasting glucose as a non-DM group and compared them with T2DM individuals, significance appeared. More precisely, T2DM subjects had a lower BMSi. The main advantage of this and our previous study (Cirovic et al. 2022a) is that we examined the microhardness of the typical fracture site in T2DM, while all three studies were focused on the tibia, which is not frequently fractured in T2DM patients (Viggers et al. 2023).

7.6. Conclusion

Our study yielded two significant findings. Firstly, individuals with T2DM exhibit an altered pattern of osteocyte lacunar density in the cortex of the superolateral femoral neck. This alteration has the potential to reduce cortical bone strength and increase the likelihood of fractures. Secondly, a decreased femoral head trabecular calcium width results in a more uniform trabecular bone structure. This uniformity may contribute to the propagation of fractures over shorter distances.

SECTION 8

Discussion

Type 2 diabetes mellitus (T2DM) is a chronic metabolic disorder that affects millions of individuals worldwide. One of the major complications of T2DM is the increased risk of bone fractures, which can lead to significant morbidity and mortality. In this study, we aimed to investigate how T2DM affects the trabecular bone quality at the femoral head and the trabecular and cortical bone characteristics at the superolateral femoral neck.

In summary, this thesis highlights the complex relationship between T2DM and femoral neck bone propertie (Summary figure). In the cortical compartment, we found that individuals with T2DM had lower cortical porosity and thickness, as well as lower cortical microhardness and reduced number of osteocyte lacunae per bone area, compared with controls. Interestingly, the endocortical region of the superolateral femoral neck showed a higher percent of mineralized lacunae in T2DM individuals than in controls. These findings suggest that diabetes alters cortical bone quality in different ways, which may lead to a gradual deterioration in bone fracture resistance and increase the risk of fractures. It is important to note that cortical bone is the first line of defense against opposing forces produced by a same-level fall.

The results of our analysis regarding the trabecular bone are comparable with previous relevant research. Trabecular microarchitecture was very similar between T2DM and control groups, although control cases had a higher structure model index (SMI) (the only microarchitectural parameter that varied among the groups) than T2DM subjects. However, it is noteworthy that the trabeculae in both groups were predominantly plate-shaped, which indicates that they may not be more susceptible to fractures. Although T2DM did not influence trabecular microarchitecture, T2DM-related vascular complications such as carotid artery disease were linked to particular alterations in some trabecular microarchitectural parameters, such as Tb.N and Tb.Sp; namely, T2DM individuals with vascular complications had a lower trabecular number and higher trabecular separation than other T2DM individuals (without vascular complications). A previous, large prospective study, conducted over a follow-up period of almost 5 years, investigated the potential association between high-resolution peripheral quantitative CT (HR-pQCT) findings and the appearance of major osteoporotic fractures; authors revealed that trabecular number at the distal radius was among the best predictors of wrist fracture occurrence (Samelson et al. 2019). Therefore, our results may indicate that the higher fracture risk in T2DM is particularly related to vascular complications. Considering that T-score and FRAX did not differ between these two groups of T2DM individuals, it seems plausible that the presence of vascular complications in individuals with T2DM could be a helpful indicator of a particularly high fracture risk; however, although this may be a very promising indicator for the evaluation of fracture risk in clinical practice, further studies in clinical setting are necessary to demonstrate the usefulness of the presence of vascular complications as an independent predictor of fracture risk and also its usefulness for the decisions regarding the anti-osteoporosis therapy.

In contrast to the cortical compartment, where we obtained lower number of non-mineralized lacunae per bone area in the endocortical and periosteal regions of the superolateral femoral neck in the T2DM group compared with the corresponding regions in the control group, trabecular osteocyte lacunar density parameters such as the number of non-mineralized lacunae per bone area, total number of osteocyte lacunae per bone area, and number of mineralized lacunae per bone area remained unchanged under the influence of T2DM. Nevertheless, both our studies and previous research (Samakkarnthai et al. 2020) showed lower microhardness in trabecular bone specimens obtained from T2DM subjects compared with controls. Additionally, in individuals with T2DM, the calcium width was lower in trabeculae, suggesting that less hypermineralized zones may be linked with a straighter projection of the fracture line.

In summary, our study suggests that T2DM affects bone quality in different ways, depending on whether we consider the cortical or trabecular compartment. The deterioration of cortical bone

mechanical resistance may increase the risk of fractures, and our findings highlight the importance of treatment and prevention strategies for individuals with T2DM.

Our results also demonstrated high diversity of cortical thickness and porosity along the cortex of the superolateral femoral neck. Loundagin et al. analyzed association between various aspects of bone quality (microarchitecture and mineralization parameters) and mechanical testing outcome (Instron Electropuls E3000 test frame) in 36 cortical bone specimens from five donors. Their findings implied that stressed volume (the volume of material above yield stress) strongly correlated with cortical bone porosity (Loundagin et al. 2021). Since cortical porosity may vary manifold without the presence of diabetes and we showed that diabetes may increase cortical porosity and decease cortical thickness, a detailed mapping of the superolateral femoral neck was necessary for further evaluation of the increased fracture risk in T2DM individuals. Based on our results in control specimens, we concluded that the division of the superolateral femoral neck to the subcapital, midcervical, and basicervical subregions is meaningful for fracture risk stratification; and interaction between diabetes and superolateral neck subregions at various levels bone quality (e.g. bone mineral density distribution) remains to be examined in the future.

Yadav et al. conducted a series of analyses, including micro-CT, finite element analyses, nanoindentation and compression tests, in three groups of femoral head trabecular core specimens, namely, T2DM, osteoporosis, and osteopenia. They demonstrated lower toughness in the T2DM group compared with the osteoporosis group (Yadav et al. 2021). In CT-based finite element analysis, Rotman et al. obtained lower bone strength parameters in T2DM subjects who sustained fragility fracture compared with those without fracture (Rotman et al. 2021).

Exploring the adverse effects of diabetes on bone health is crucial for understanding the clinical implications of diabetes and developing targeted interventions to prevent or treat diabetes-induced bone quality impairment. By addressing bone health in individuals with diabetes, healthcare professionals can help improve the quality of life, reduce healthcare costs, and ultimately improve overall health outcomes.

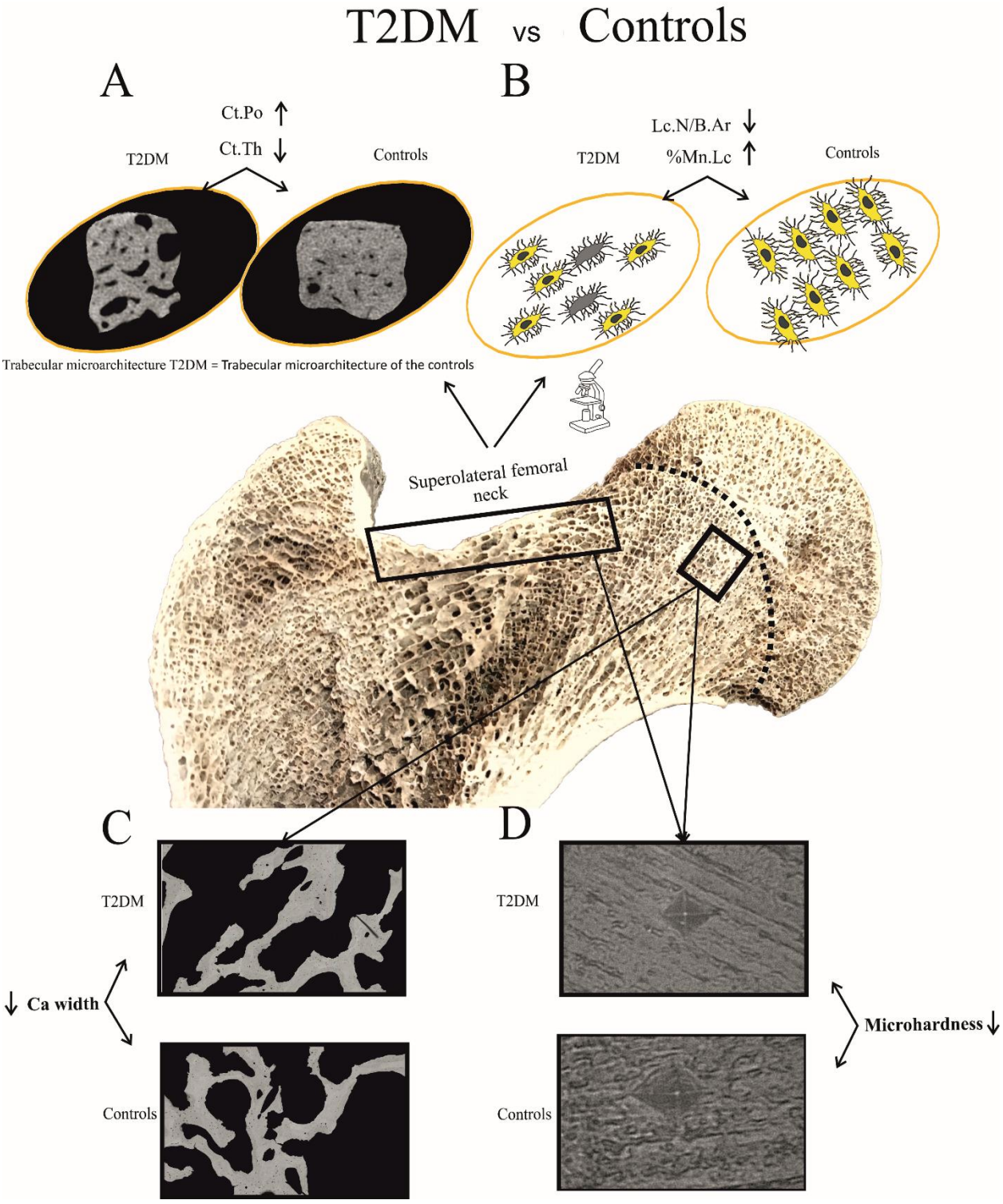
T2DM vs Controls
A
Ct.Po ↑
Ct.Th ↓
T2DM
Controls
B
Lc.N/B.Ar ↓
%Mn.Lc ↑
T2DM
Controls
Trabecular microarchitecture T2DM = Trabecular microarchitecture of the controls
Superolateral femoral neck
C
T2DM
↓ Ca width
Controls
D
T2DM
Microhardness ↓
Controls

Summary figure: Summary of the methodological approach and main results. The methods employed for bone sample analysis included micro-computed tomography, backscattered electron imaging, examination of bone mineral density distribution, and microhardness evaluation at two distinct sites within the femoral head and neck. We evaluated the trabeculae and cortex of the superolateral femoral neck and the trabeculae at the femoral head region. Our findings revealed the following: A) We observed a deteriorated cortical microarchitecture in the superolateral femoral neck, while no significant variation was detected in trabecular microarchitecture in any of the examined sites. B) Additionally, we found a lower density of non-mineralized osteocyte lacunae in the endocortical and subperiosteal compartments of the superolateral femoral neck cortex, accompanied by an increased percentage of mineralized osteocyte lacunae. C) Furthermore, we identified an altered pattern of trabecular mineralization in individuals with type 2 diabetes mellitus (T2DM), along with D) lower trabecular and cortical microhardness.

Figure legend:

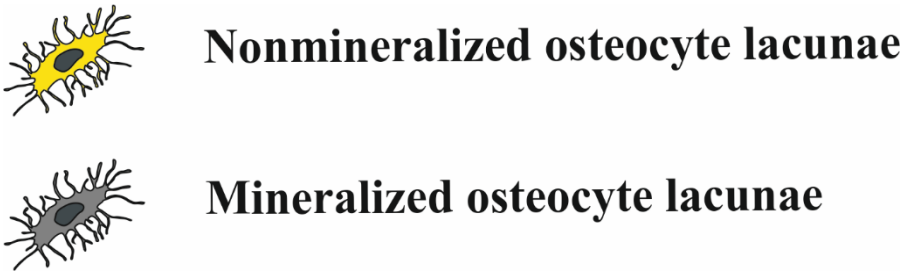

SECTION 9

Conclusions

Our study revealed the following key findings regarding the femoral neck quality in individuals with T2DM compared with controls:

- The microarchitecture of the trabecular bone in the femoral neck was found to be similar between individuals with T2DM and the control group; the presence of vascular complications led to the deterioration of trabecular microarchitecture.
- Compared with the control group, the individuals with T2DM exhibited lower cortical thickness and higher cortical porosity in the superolateral femoral neck region. This suggests potential weakening of the cortical bone in T2DM individuals.
- T2DM subjects had lower osteocyte lacunar number per bone area in the endocortical and periosteal regions of the superolateral femoral neck compared with the corresponding regions in the control group. However, osteonal density was similar between the two groups. This indicates a difference in osteocyte lacunar distribution without a significant change in osteonal density.
- T2DM individuals had lower trabecular calcium width in the femoral neck compared with controls. However, other trabecular mineralization parameters were similar between the individuals with T2DM and the control group.
- Significant variations were observed in the cortical and trabecular microarchitecture along the superolateral femoral neck in the controls.

Overall, these findings provide insights into the specific alterations in the femoral neck bone quality associated with T2DM, including changes in cortical thickness, cortical porosity, osteocyte lacunar density, and mineralization pattern. Understanding these variations can contribute to a better understanding of bone health and fracture risk in individuals with T2DM.

SECTION 10

References

Alswat, K.A. 2017. Gender disparities in osteoporosis. J Clin Med Res 9, 382.

Alzaheb, R.A. and Altemani, A.H. 2018. The prevalence and determinants of poor glycemic control among adults with type 2 diabetes mellitus in Saudi Arabia. Diabetes Metab Syndr Obes 11, 15-21.

Aschner, P., Karuranga, S., James, S., Simmons, D., Basit, A., Shaw, J.E., et al. 2021. The International Diabetes Federation's guide for diabetes epidemiological studies. Diabetes Res Clin Pract 172:108630.

Bell, K., Loveridge, N., Jordan, G., Power, J., Constant, C. and Reeve, J. 2000. A novel mechanism for induction of increased cortical porosity in cases of intracapsular hip fracture. Bone 27, 297-304.

Bell, K.L., Loveridge, N., Power, J., Garrahan, N., Meggitt, B.F. and Reeve, J. 1999a. Regional differences in cortical porosity in the fractured femoral neck. Bone 24, 57-64.

Bell, K., Loveridge, N., Power, J., Garrahan, N., Stanton, M., Lunt, M. et al. 1999b. Structure of the femoral neck in hip fracture: cortical bone loss in the inferoanterior to superoposterior axis. J Bone Miner Res. 14, 111-119.

Bellows, C.G., Reimers, S.M. and Heersche, J.N.M. 1999. Expression of mRNAs for type-I collagen, bone sialoprotein, osteocalcin, and osteopontin at different stages of osteoblastic differentiation and their regulation by 1,25 dihydroxyvitamin D3. Cell Tissue Res 297, 249-259.

Boivin, G., Bala, Y., Doublier, A., Farlay, D., Ste-Marie, L.G., Meunier, P.J. et al. 2008. The role of mineralization and organic matrix in the microhardness of bone tissue from controls and osteoporotic patients. Bone 43, 532-538.

Bonds, D.E., Larson, J.C., Schwartz, A.V., Strotmeyer, E.S., Robbins, J., Rodriguez, B.L., et al. 2006. Risk of fracture in women with type 2 diabetes: the Women's Health Initiative Observational Study. J Clin Endocrinol Metab 91, 3404-3410.

Busse, B., Djonic, D., Milovanovic, P., Hahn, M., Püschel, K., Ritchie, R.O., et al. 2010. Decrease in the osteocyte lacunar density accompanied by hypermineralized lacunar occlusion reveals failure and delay of remodeling in aged human bone. Aging Cell 9, 1065-1075.

Bousson, V., Peyrin, F., Bergot, C., Hausard, M., Sautet, A. and Laredo, J.D. 2004. Cortical bone in the human femoral neck: three-dimensional appearance and porosity using synchrotron radiation. J Bone Miner Res 19, 794-801.

Burghardt, A.J., Issever, A.S., Schwartz, A.V., Davis, K.A., Masharani, U., Majumdar, S. et al. 2010. High-resolution peripheral quantitative computed tomographic imaging of cortical and trabecular bone microarchitecture in patients with type 2 diabetes mellitus. J Clin Endocrinol Metab 95, 5045-5055.

Chen, C.-Y., Chiu, F.-Y., Chen, C.-M., Huang, C.-K., Chen, W.-M. and Chen, T.-H. 2008. Surgical treatment of basicervical fractures of femur—a prospective evaluation of 269 patients. J Trauma 64, 427-429.

Chen, H., Zhou, X., Shoumura, S., Emura, S. and Bunai, Y. 2010. Age-and gender-dependent changes in three-dimensional microstructure of cortical and trabecular bone at the human femoral neck. Osteoporos Int 21, 627-636.

Chudyk, A.M., Ashe, M.C., Gorman, E., Al Tunaiji, H.O. and Crossley, K.M. 2012. Risk of hip fracture with hip or knee osteoarthritis: a systematic review. Clin Rheumatol 31, 749-757.

Ciarelli, T.E., Fyhrie, D.P., Schaffler, M.B. and Goldstein, S.A. 2000. Variations in three-dimensional cancellous bone architecture of the proximal femur in female hip fractures and in controls. J Bone Miner Res 15, 32-40.

Cirovic, A., Cirovic, A., Djonic, D., Zivkovic, V., Nikolic, S., Djuric, M. et al. 2020. Three-dimensional microstructural basis for differential occurrence of subcapital versus basicervical hip fractures in men. Calcif Tissue Int 107, 240-248.

Cirovic, A., Jadzic, J., Djukic, D., Djonic, D., Zivkovic, V., Nikolic, S., et al. 2022a. Increased Cortical Porosity, Reduced Cortical Thickness, and Reduced Trabecular and Cortical Microhardness of the Superolateral Femoral Neck Confer the Increased Hip Fracture Risk in Individuals with Type 2 Diabetes. Calcif Tissue Int 111, 457-465.

Cirovic, A., Vujacic, M., Petrovic, B., Cirovic, A., Zivkovic, V., Nikolic, S., et al. 2022. Vascular Complications in Individuals with Type 2 Diabetes Mellitus Additionally Increase the Risk of Femoral Neck Fractures Due to Deteriorated Trabecular Microarchitecture. Calcif Tissue Int 110, 65-73.

Cirovic A and Milovanovic P. Mikroarhitekturni aspekti povećane koštane fragilnosti osoba sa dijabetesom tipa 2. Med Podm 2023; DOI 10.5937/mp75-44905.

Cooper, C., Campion, G. and Melton, L., 3rd. 1992. Hip fractures in the elderly: a world-wide projection. Osteoporos Int 2, 285-289.

Conway, B.N., Long, D.M., Figaro, M.K. and May, M.E. 2016. Glycemic control and fracture risk in elderly patients with diabetes. Diabetes research and clinical practice 115, 47-53.

Cui, W.-Q., Won, Y.-Y., Baek, M.-H., Lee, D.-H., Chung, Y.-S., Hur, J.-H. and Ma, Y.-Z. 2008. Age- and region-dependent changes in three-dimensional microstructural properties of proximal femoral trabeculae. Osteoporos Int 19, 1579-1587.

de Bakker, P.M., Manske, S.L., Ebacher, V., Oxland, T.R., Cripton, P.A. and Guy, P. 2009. During sideways falls proximal femur fractures initiate in the superolateral cortex: evidence from high-speed video of simulated fractures. J Biomech 42, 1917-1925.

Dede, A.D., Tournis, S., Dontas, I. and Trovas, G. 2014. Type 2 diabetes mellitus and fracture risk. Metabolism 63, 1480-1490.

Dedrick, D.K., Mackenzie, J.R. and Burney, R.E. 1986. Complications of femoral neck fracture in young adults. J Trauma Acute Care Surg 26, 932-937.

Djuric, M., Djonic, D., Milovanovic, P., Nikolic, S., Marshall, R., Marinkovic, J. and Hahn, M. 2010. Region-specific sex-dependent pattern of age-related changes of proximal femoral cancellous bone and its implications on differential bone fragility. Calcif Tissue Int 86, 192-201.

Djuric, M., Zagorac, S., Milovanovic, P., Djonic, D., Nikolic, S., Hahn, M., et al. 2013. Enhanced trabecular micro-architecture of the femoral neck in hip osteoarthritis vs. healthy controls: a micro-computer tomography study in postmenopausal women. Int. Orthop 37, 21-26.

Dubey, A., Aharonoff, G.B., Zuckerman, J.D. and Koval, K.J. 2000. The effects of diabetes on outcome after hip fracture. Bull Hosp Jt Dis 59, 94-98.

Durlak, J.A. 2009. How to Select, Calculate, and Interpret Effect Sizes. J Pediatr Psychol 34, 917-928.

Endo, D., Ogami-Takamura, K., Imamura, T., Saiki, K., Murai, K., Okamoto, K. and Tsurumoto, T. 2020. Reduced cortical bone thickness increases stress and strain in the female femoral diaphysis

analyzed by a CT-based finite element method: Implications for the anatomical background of fatigue fracture of the femur. Bone Rep 13, 100733-100733.

Faisal, T.R. and Luo, Y. 2016. Study of stress variations in single-stance and sideways fall using image-based finite element analysis. Biomed Mater Eng 27, 1-14.

Fan, Y., Wei, F., Lang, Y. and Liu, Y. 2016. Diabetes mellitus and risk of hip fractures: a meta-analysis. Osteoporos Int 27, 219-228.

Farr, J.N., Drake, M.T., Amin, S., Melton, L.J., 3rd, McCready, L.K. and Khosla, S. 2014. In vivo assessment of bone quality in postmenopausal women with type 2 diabetes. J Bone Miner Res 29, 787-795.

Fasil, A., Biadgo, B. and Abebe, M. 2018. Glycemic control and diabetes complications among diabetes mellitus patients attending at University of Gondar Hospital, Northwest Ethiopia. Diabetes Metab Syndr Obes 12, 75-83.

Fleps, I., Enns-Bray, W.S., Guy, P., Ferguson, S.J., Cripton, P.A. and Helgason, B. 2018. On the internal reaction forces, energy absorption, and fracture in the hip during simulated sideways fall impact. PLoS one 13, e0200952.

Forsén, L., Meyer, H.E., Midthjell, K. and Edna, T.H. 1999. Diabetes mellitus and the incidence of hip fracture: results from the Nord-Trøndelag Health Survey. Diabetologia 42, 920-925.

Franklin, J., Englund, M., Ingvarsson, T. and Lohmander, S. 2010. The association between hip fracture and hip osteoarthritis: a case-control study. BMC Musculoskelet Disord 11, 274-274.

Fratzl-Zelman, N., Roschger, P., Gourrier, A., Weber, M., Misof, B., Loveridge, N., et al. 2009. Combination of nanoindentation and quantitative backscattered electron imaging revealed altered bone material properties associated with femoral neck fragility. Calcif Tissue Int 85, 335-343.

Furst, J.R., Bandeira, L.C., Fan, W.W., Agarwal, S., Nishiyama, K.K., McMahon, D.J., et al. 2016. Advanced Glycation Endproducts and Bone Material Strength in Type 2 Diabetes. J Clin Endocrinol Metab 101, 2502-2510.

Gauthier, R., Langer, M., Follet, H., Olivier, C., Gouttenoire, P.J., Helfen, L., et al. 2018. 3D micro structural analysis of human cortical bone in paired femoral diaphysis, femoral neck and radial diaphysis. J Struct Biol 204, 182-190.

Gjertsen, J.-E., Baste, V., Fevang, J.M., Furnes, O. and Engesæter, L.B. 2016. Quality of life following hip fractures: results from the Norwegian hip fracture register. BMC musculoskeletal disorders 17, 1-8.

Granke, M., Makowski, A.J., Uppuganti, S. and Nyman, J.S. 2016. Prevalent role of porosity and osteonal area over mineralization heterogeneity in the fracture toughness of human cortical bone. J Biomech 49, 2748-2755.

Gulcelik, N.E., Bayraktar, M., Caglar, O., Alpaslan, M. and Karakaya, J. 2011. Mortality after hip fracture in diabetic patients. Exp Clin Endocrinol Diabetes 119, 414-418.

Guo, X. and Kim, C. 2002. Mechanical consequence of trabecular bone loss and its treatment: a three-dimensional model simulation. Bone 30, 404-411.

Hanusch, B.C., Tuck, S.P., McNally, R.J.Q., Wu, J.J., Prediger, M., Walker, J., Tang, J., Piec, I., Fraser, W.D., Datta, H.K. and Francis, R.M. 2017. Does regional loss of bone density explain low trauma distal forearm fractures in men (the Mr F study)? Osteoporos Int 28, 2877-2886.

Hernlund, E., Svedbom, A., Ivergard, M., Compston, J., Cooper, C., Stenmark, J., et al. 2013. Osteoporosis in the European Union: medical management, epidemiology and economic burden. A report prepared in collaboration with the International Osteoporosis Foundation (IOF) and the European Federation of Pharmaceutical Industry Associations (EFPIA). Arch Osteoporos 8, 136.

Hofstaetter, J.G., Hofstaetter, S.G., Nawrot-Wawrzyniak, K., Hiertz, H., Grohs, J.G., Trieb, K., et al. 2012. Mineralization pattern of vertebral bone material following fragility fracture of the spine. Journal of Orthopaedic Research 30, 1089-1094.

Holloway-Kew, K.L., Betson, A., Rufus-Membere, P.G., Gaston, J., Diez-Perez, A., Kotowicz, M.A. and Pasco, J.A. 2021. Impact microindentation in men with impaired fasting glucose and type 2 diabetes. Bone 142, 115685.

Holzer, G., Von Skrbensky, G., Holzer, L.A. and Pichl, W. 2009. Hip fractures and the contribution of cortical versus trabecular bone to femoral neck strength. J Bone Miner Res 24, 468-474.

Huang, E.S., Brown, S.E., Ewigman, B.G., Foley, E.C. and Meltzer, D.O. 2007. Patient perceptions of quality of life with diabetes-related complications and treatments. Diabetes care 30, 2478-2483.

Hunt, H.B., Torres, A.M., Palomino, P.M., Marty, E., Saiyed, R., Cohn, M., et al. 2019. Altered Tissue Composition, Microarchitecture, and Mechanical Performance in Cancellous Bone From Men With Type 2 Diabetes Mellitus. J Bone Miner Res 34, 1191-1206.

Iori, G., Peralta, L., Reisinger, A., Heyer, F., Wyers, C., van den Bergh, J., et al. 2020. Femur strength predictions by nonlinear homogenized voxel finite element models reflect the microarchitecture of the femoral neck. Med Eng Phys 79, 60-66.

Jadzic, J., Milovanovic, P., Cvetkovic, D., Ivovic, M., Tomanovic, N., Bracanovic, M., et al. 2021. Mechano-structural alteration in proximal femora of individuals with alcoholic liver disease: Implications for increased bone fragility. Bone 150, 116020.

Janghorbani, M., Van Dam, R.M., Willett, W.C. and Hu, F.B. 2007. Systematic review of type 1 and type 2 diabetes mellitus and risk of fracture. Am J Epidemiol 166, 495-505.

Jia, W., Wu, J., Gao, D. and Sun, M. 2014. Characteristics of Skin-Electrode Impedance for a Novel Screw Electrode. Proc IEEE Annu Northeast Bioeng Conf 2014, 1-2.

Jiang, C., Giger, M.L., Kwak, S.M., Chinander, M.R., Martell, J.M. and Favus, M.J. 2000. Normalized BMD as a predictor of bone strength. Acad Radiol 7, 33-39.

Johannesdottir, F., Poole, K.E., Reeve, J., Siggeirsdottir, K., Aspelund, T., Mogensen, B., et al. 2011. Distribution of cortical bone in the femoral neck and hip fracture: a prospective case-control analysis of 143 incident hip fractures; the AGES-REYKJAVIK Study. Bone 48, 1268-1276.

Johannesdottir, F., Thrall, E., Muller, J., Keaveny, T.M., Kopperdahl, D.L. and Bouxsein, M.L. 2017. Comparison of non-invasive assessments of strength of the proximal femur. Bone 105, 93-102.

Jo, S., Lee, S.H. and Lee, H.J. 2016. The correlation between the fracture types and the complications after internal fixation of the femoral neck fractures. Hip & pelvis 28, 35-42.

Karim, L., Moulton, J., Van Vliet, M., Velie, K., Robbins, A., Malekipour, F., et al. 2018. Bone microarchitecture, biomechanical properties, and advanced glycation end-products in the proximal femur of adults with type 2 diabetes. Bone 114, 32-39.

Katayama, Y., Akatsu, T., Yamamoto, M., Kugai, N. and Nagata, N. 1996. Role of nonenzymatic glycosylation of type I collagen in diabetic osteopenia. J Bone Miner Res 11, 931-937.

Kazley, J.M., Banerjee, S., Abousayed, M.M. and Rosenbaum, A.J. 2018. Classifications in brief: Garden classification of femoral neck fractures. Clin Orthop Relat Res 476, 441 -445.

Keyak, J.H. 2001. Improved prediction of proximal femoral fracture load using nonlinear finite element models. Med Eng Phys 23, 165-173.

Khan, M.A.B., Hashim, M.J., King, J.K., Govender, R.D., Mustafa, H. and Al Kaabi, J. 2020. Epidemiology of Type 2 Diabetes - Global Burden of Disease and Forecasted Trends. J Epidemiol Glob Health 10, 107-111.

Kheirollahi, H. and Luo, Y. 2015. Identification of high stress and strain regions in proximal femur during single-leg stance and sideways fall using QCT-based finite element model. Int J Med Health Biomed Bioeng Pharm Eng 9, 633-640.

Khosla, S., Samakkarnthai, P., Monroe, D.G. and Farr, J.N. 2021. Update on the pathogenesis and treatment of skeletal fragility in type 2 diabetes mellitus. Nat Rev Endocrinol 17, 685-697.

Kida, Y., Saito, M., Shinohara, A., Soshi, S. and Marumo, K. 2019. Non-invasive skin autofluorescence, blood and urine assays of the advanced glycation end product (AGE) pentosidine as an indirect indicator of AGE content in human bone. BMC Musculoskelet Disord 20, 627.

Kim, S.Y., Schneeweiss, S., Liu, J., Daniel, G.W., Chang, C.-L., Garneau, K. and Solomon, D.H. 2010. Risk of osteoporotic fracture in a large population-based cohort of patients with rheumatoid arthritis. Arthritis Res Ther 12, R154.

Koivumäki, J.E., Thevenot, J., Pulkkinen, P., Salmi, J.A., Kuhn, V., Lochmüller, E.M., et al. 2010. Does femoral strain distribution coincide with the occurrence of cervical versus trochanteric hip fractures? An experimental finite element study. Med Biol Eng Comput 48, 711-717.

Kolibová, S.D., Wölfel, E.M., Hemmatian, H., Milovanovic, P., Mushumba, H., Wulff, B., et al. 2023. Osteocyte apoptosis and cellular micropetrosis signify skeletal aging in type 1 diabetes. Acta Biomater 162:254-265.

Koval, K. and Zuckerman, J. 2000. Hip fractures: a practical guide to management, Springer Science & Business Media.

Kral, R., Osima, M., Borgen, T.T., Vestgaard, R., Richardsen, E. and Bjørnerem, Å. 2017. Increased cortical porosity and reduced cortical thickness of the proximal femur are associated with nonvertebral fracture independent of Fracture Risk Assessment Tool and Garvan estimates in postmenopausal women. PloS one 12, e0185363.

Leanza, G., Maddaloni, E., Pitocco, D., Conte, C., Palermo, A., Maurizi, A.R., Pantano, A.L., Suraci, C., Altomare, M., Strollo, R., Manfrini, S., Pozzilli, P., Schwartz, A.V. and Napoli, N. 2019. Risk factors for fragility fractures in type 1 diabetes. Bone 125, 194-199.

Lee, R.H., Sloane, R., Pieper, C., Lyles, K.W., Adler, R.A., Van Houtven, C., LaFleur, J. and Colon-Emeric, C. 2019. Glycemic Control and Insulin Treatment Alter Fracture Risk in Older Men With Type 2 Diabetes Mellitus. J Bone Miner Res 34, 2045-2051.

Lipscombe, L.L., Jamal, S.A., Booth, G.L. and Hawker, G.A. 2007. The risk of hip fractures in older individuals with diabetes: a population-based study. Diabetes care 30, 835-841.

Lochmüller, E.M., Matsuura, M., Bauer, J., Hitzl, W., Link, T.M., Müller, R. Et al. 2008. Site-specific deterioration of trabecular bone architecture in men and women with advancing age. J Bone Miner Res 23, 1964-1973.

Loundagin, L. L., Pohl, A. J., & Edwards, W. B. 2021. Stressed volume estimated by finite element analysis predicts the fatigue life of human cortical bone: the role of vascular canals as stress concentrators. Bone, 143, 115647.

Ly, F.S., Proctor, A., Hoffseth, K., Yang, H.T. and Hansma, P.K. 2020. Significant correlation of bone material strength index as measured by the OsteoProbe with Vickers and Rockwell hardness. Rev Sci Instrum 91, 084102.

Magu, N.K., Magu, S., Rohilla, R.K., Batra, A., Jaipuria, A. and Singh, A. 2014. Computed tomographic evaluation of the proximal femur: A predictive classifcation in displaced femoral neck fracture management. Indian J Orthop 48, 476-483.

Maillard, C., Berruyer, M., Serre, C.M., Dechavanne, M. and Delmas, P.D. 1992. Protein-S, a vitamin K-dependent protein, is a bone matrix component synthesized and secreted by osteoblasts. Endocrinology 130, 1599-1604.

Malo, M., Rohrbach, D., Isaksson, H., Töyräs, J., Jurvelin, J., Tamminen, I., et al. 2013. Longitudinal elastic properties and porosity of cortical bone tissue vary with age in human proximal femur. Bone 53, 451-458.

Manske, S.L., Liu-Ambrose, T., Cooper, D.M., Kontulainen, S., Guy, P., Forster, B.B. et al. 2009. Cortical and trabecular bone in the femoral neck both contribute to proximal femur failure load prediction. Osteoporos Int 20, 445-453.

Martinez-Laguna, D., Nogues, X., Abrahamsen, B., Reyes, C., Carbonell-Abella, C., Diez-Perez, A. et al. 2017. Excess of all-cause mortality after a fracture in type 2 diabetic patients: a population-based cohort study. Osteoporos Int 28, 2573-2581.

Mayhew, P.M., Thomas, C.D., Clement, J.G., Loveridge, N., Beck, T.J., Bonfield, W., et al. 2005. Relation between age, femoral neck cortical stability, and hip fracture risk. Lancet 366, 129-135.

McCalden, R.W., McGeough, J.A., Barker, M.B. and Court-Brown, C.M. 1993. Age-related changes in the tensile properties of cortical bone. The relative importance of changes in porosity, mineralization, and microstructure. J Bone Joint Surg Am 75, 1193-1205.

Melton, L.J., 3rd, Leibson, C.L., Achenbach, S.J., Therneau, T.M. and Khosla, S. 2008. Fracture risk in type 2 diabetes: update of a population-based study. J Bone Miner Res 23, 1334-1342.

Miao, J., Brismar, K., Nyren, O., Ugarph-Morawski, A. and Ye, W. 2005. Elevated hip fracture risk in type 1 diabetic patients: a population-based cohort study in Sweden. Diabetes care 28, 2850-2855.

Milovanovic, P., Rakocevic, Z., Djonic, D., Zivkovic, V., Hahn, M., Nikolic, S., et al. 2014. Nano-structural, compositional and micro-architectural signs of cortical bone fragility at the superolateral femoral neck in elderly hip fracture patients vs. healthy aged controls. Exp Gerontol 55, 19-28.

Milovanovic, P., Djonic, D., Marshall, R.P., Hahn, M., Nikolic, S., Zivkovic, V., et al. 2012. Micro-structural basis for particular vulnerability of the superolateral neck trabecular bone in the postmenopausal women with hip fractures. Bone 50, 63-68.

Milovanovic, P., Zimmermann, E.A., Riedel, C., vom Scheidt, A., Herzog, L., Krause, M., et al. 2015. Multi-level characterization of human femoral cortices and their underlying osteocyte network reveal trends in quality of young, aged, osteoporotic and antiresorptive-treated bone. Biomaterials 45, 46-55.

Misof, B.M., Blouin, S., Andrade, V.F., Roschger, P., Borba, V.Z., Hartmann, M.A., et al. 2022. No evidence of mineralization abnormalities in iliac bone of premenopausal women with type 2 diabetes mellitus. J Musculoskelet Neuronal Interact 22, 305-315.

Napoli, N., Chandran, M., Pierroz, D.D., Abrahamsen, B., Schwartz, A.V. and Ferrari, S.L. 2017. Mechanisms of diabetes mellitus-induced bone fragility. Nat Rev Endocrinol 13, 208-219.

Nilsson, A.G., Sundh, D., Johansson, L., Nilsson, M., Mellström, D., Rudäng, R., et al. 2017. Type 2 Diabetes Mellitus Is Associated With Better Bone Microarchitecture But Lower Bone Material Strength and Poorer Physical Function in Elderly Women: A Population-Based Study. J Bone Miner Res 32, 1062-1071.

Odetti, P., Rossi, S., Monacelli, F., Poggi, A., Cirnigliaro, M., Federici, M. and Federici, A. 2005. Advanced glycation end products and bone loss during aging. Ann N Y Acad Sci 1043, 710-717.

Oren, T.W., Botolin, S., Williams, A., Bucknell, A. and King, K.B. 2011. Arthroplasty in veterans: analysis of cartilage, bone, serum, and synovial fluid reveals differences and similarities in osteoarthritis with and without comorbid diabetes. J Rehabil Res Dev 48, 1195-1210.

Osima, M., Kral, R., Borgen, T.T., Høgestøl, I.K., Joakimsen, R.M., Eriksen, E.F. et al. 2017. Women with type 2 diabetes mellitus have lower cortical porosity of the proximal femoral shaft using low-resolution CT than nondiabetic women, and increasing glucose is associated with reduced cortical porosity. Bone 97, 252-260.

Oyen, J., Brudvik, C., Gjesdal, C.G., Tell, G.S., Lie, S.A. and Hove, L.M. 2011. Osteoporosis as a risk factor for distal radial fractures: a case-control study. J Bone Joint Surg Am 93, 348-356.

Panula, J., Pihlajamäki, H., Mattila, V.M., Jaatinen, P., Vahlberg, T., Aarnio, P. and Kivelä, S.-L. 2011. Mortality and cause of death in hip fracture patients aged 65 or older-a population-based study. BMC Musculoskelet Disord 12, 1-6.

Patsch, J.M., Burghardt, A.J., Yap, S.P., Baum, T., Schwartz, A.V., Joseph, G.B. and Link, T.M. 2013. Increased cortical porosity in type 2 diabetic postmenopausal women with fragility fractures. J Bone Miner Res 28, 313-324.

Peeters, C.M., Visser, E., Van de Ree, C.L., Gosens, T., Den Oudsten, B.L. and De Vries, J. 2016. Quality of life after hip fracture in the elderly: a systematic literature review. Injury 47, 1369-1382.

Piccoli, A., Cannata, F., Strollo, R., Pedone, C., Leanza, G., Russo, F., et al. 2020. Sclerostin Regulation, Microarchitecture, and Advanced Glycation End-Products in the Bone of Elderly Women With Type 2 Diabetes. J Bone Miner Res 35, 2415-2422.

Poole, K.E., Treece, G.M., Mayhew, P.M., Vaculík, J., Dungl, P., Horák, M., Štěpán, J.J. and Gee, A.H. 2012. Cortical thickness mapping to identify focal osteoporosis in patients with hip fracture. PLoS One 7, e38466.

Power, J., Loveridge, N., Kröger, H., Parker, M. and Reeve, J. 2018. Femoral neck cortical bone in female and male hip fracture cases: Differential contrasts in cortical width and sub-periosteal porosity in 112 cases and controls. Bone 114, 81-89.

Pritchard, J., Papaioannou, A., Tomowich, C., Giangregorio, L., Atkinson, S., Beattie, K., Adachi, J., et al. 2013. Bone mineralization is elevated and less heterogeneous in adults with type 2 diabetes and osteoarthritis compared to controls with osteoarthritis alone. Bone 54, 76-82.

Quah, J.H., Luo, N., Ng, W.Y., How, C.H. and Tay, E.G. 2011. Health-related quality of life is associated with diabetic complications, but not with short-term diabetic control in primary care. Ann Acad Med Singap 40, 276-286.

Rakic, V., Davis, W.A., Chubb, S.A., Islam, F.M., Prince, R.L. and Davis, T.M. 2006. Bone mineral density and its determinants in diabetes: the Fremantle Diabetes Study. Diabetologia 49, 863-871.

Rathmann, W. and Kostev, K. 2015. Fracture risk in patients with newly diagnosed type 2 diabetes: a retrospective database analysis in primary care. J Diabetes Complications 29, 766-770.

Rolvien, T., Milovanovic, P., Schmidt, F.N., von Kroge, S., Wölfel, E.M., Krause, M., et al. 2020. Long-term immobilization in elderly females causes a specific pattern of cortical bone and osteocyte deterioration different from postmenopausal osteoporosis. J Bone Miner Res 35, 1343-1351.

Rolvien, T., Vom Scheidt, A., Stockhausen, K.E., Milovanovic, P., Djonic, D., Hubert, J., et al. 2018. Inter-site variability of the osteocyte lacunar network in the cortical bone underpins fracture susceptibility of the superolateral femoral neck. Bone 112, 187-193.

Rotman, D., Ariel, G., Lievano, J. R., Schermann, H., Trabelsi, N., Salai, M., et al. 2021. Assessing hip fracture risk in type-2 diabetic patients using CT-based autonomous finite element methods: a feasibility study. Bone Joint J 103(9), 1497-1504.

Saarenpää, I., Partanen, J. and Jalovaara, P. 2002. Basicervical fracture–a rare type of hip fracture. Arch Orthop Trauma Surg 122, 69-72.

Saeedi, P., Petersohn, I., Salpea, P., Malanda, B., Karuranga, S., Unwin, N., et al. Global and regional diabetes prevalence estimates for 2019 and projections for 2030 and 2045: Results from the International Diabetes Federation Diabetes Atlas, 9(th) edition. Diabetes Res Clin Pract 157, 107843.

Samakkarnthai, P., Sfeir, J.G., Atkinson, E.J., Achenbach, S.J., Wennberg, P.W., Dyck, P.J., Tweed, A.J., Volkman, T.L., Amin, S., Farr, J.N., Vella, A., Drake, M.T. and Khosla, S. 2020. Determinants of Bone Material Strength and Cortical Porosity in Patients with Type 2 Diabetes Mellitus. J Clin Endocrinol Metab 105, e3718-3729.

Samelson, E. J., Broe, K. E., Xu, H., Yang, L., Boyd, S., Biver, E., ... & Bouxsein, M. L. 2019. Cortical and trabecular bone microarchitecture as an independent predictor of incident fracture risk in older women and men in the Bone Microarchitecture International Consortium (BoMIC): a prospective study. Lancet Diabetes Endocrinol 7(1), 34-43.

Sanguineti, R., Storace, D., Monacelli, F., Federici, A. and Odetti, P. 2008. Pentosidine effects on human osteoblasts in vitro. Ann N Y Acad Sci 1126, 166-172.

Sassi, F., Buondonno, I., Luppi, C., Spertino, E., Stratta, E., Di Stefano, M., Ravazzoli, M., Isaia, G., Trento, M., Passera, P., Porta, M., Isaia, G.C. and D'Amelio, P. 2018. Type 2 diabetes affects bone cells precursors and bone turnover. BMC Endocr Disord 18(1), 1-8.

Schousboe, J.T., Morin, S.N., Kline, G.A., Lix, L.M. and Leslie, W.D. 2022. Differential risk of fracture attributable to type 2 diabetes mellitus according to skeletal site. Bone 154, 116220.

Schwartz, A.V., Hillier, T.A., Sellmeyer, D.E., Resnick, H.E., Gregg, E., Ensrud, K.E., Schreiner, P.J., Margolis, K.L., Cauley, J.A., Nevitt, M.C., Black, D.M. and Cummings, S.R. 2002. Older women with diabetes have a higher risk of falls: a prospective study. Diabetes Care 25, 1749-1754.

Sell, D.R. and Monnier, V.M. 1989. Structure elucidation of a senescence cross-link from human extracellular matrix. Implication of pentoses in the aging process. J Biol Chem 264, 21597-21602.

Shanbhogue, V.V., Hansen, S., Frost, M., Jørgensen, N.R., Hermann, A.P., Henriksen, J.E. and Brixen, K. 2016. Compromised cortical bone compartment in type 2 diabetes mellitus patients with microvascular disease. Eur J Endocrinol 174, 115-124.

Sheehan, S.E., Shyu, J.Y., Weaver, M.J., Sodickson, A.D. and Khurana, B. 2015. Proximal femoral fractures: what the orthopedic surgeon wants to know. Radiographics 35, 1563-1584.

Shoda, E., Kitada, S., Sasaki, Y., Hirase, H., Niikura, T., Lee, S.Y., Sakurai, A., Oe, K. and Sasaki, T. 2017. Proposal of new classification of femoral trochanteric fracture by three-dimensional computed tomography and relationship to usual plain X-ray classification. J Orthop Surg 25(1):2309499017692700.

Sihota, P., Yadav, R.N., Dhaliwal, R., Bose, J.C., Dhiman, V., Neradi, D., Karn, S., Sharma, S., Aggarwal, S., Goni, V.G., Mehandia, V., Vashishth, D., Bhadada, S.K. and Kumar, N. 2021. Investigation of Mechanical, Material, and Compositional Determinants of Human Trabecular Bone Quality in Type 2 Diabetes. J Clin Endocrinol Metab 106, e2271-e2289.

Sundh, D., Mellström, D., Nilsson, M., Karlsson, M., Ohlsson, C. and Lorentzon, M. 2015. Increased Cortical Porosity in Older Men With Fracture. J Bone Miner Res 30, 1692-1700.

Sundh, D., Nilsson, A.G., Nilsson, M., Johansson, L., Mellstrom, D. and Lorentzon, M. 2017. Increased cortical porosity in women with hip fracture. J Intern Med 281, 496-506.

Svedbom, A., Hernlund, E., Ivergård, M., Compston, J., Cooper, C., Stenmark, J., et al. 2013. Osteoporosis in the European Union: a compendium of country-specific reports. Arch Osteoporos 8, 1-218.

Tang, T., Cripton, P.A., Guy, P., McKay, H.A. and Wang, R. 2018. Clinical hip fracture is accompanied by compression induced failure in the superior cortex of the femoral neck. Bone 108, 121-131.

Tanner, D.A., Kloseck, M., Crilly, R.G., Chesworth, B. and Gilliland, J. 2010. Hip fracture types in men and women change differently with age. BMC Geriatr 10, 1-4.

Tassani, S. and Perilli, E. 2013. On local micro-architecture analysis of trabecular bone in three dimensions. Int Orthop 37, 1645-1646.

Tebe, C., Martinez-Laguna, D., Carbonell-Abella, C., Reyes, C., Moreno, V., Diez-Perez, A., Collins, G.S. and Prieto-Alhambra, D. 2019. The association between type 2 diabetes mellitus, hip fracture, and post-hip fracture mortality: a multi-state cohort analysis. Osteoporos Int 30, 2407-2415.

Valderrabano, R.J. and Linares, M.I. 2018. Diabetes mellitus and bone health: epidemiology, etiology and implications for fracture risk stratification. Clin Diabetes Endocrinol 25;4:9.

Valentini, A., Cianfarani, M.A., De Meo, L., Morabito, P., Romanello, D., Tarantino, U., Federici, M. and Bertoli, A. 2018. FRAX tool in type 2 diabetic subjects: the use of HbA(1c) in estimating fracture risk. Acta Diabetol 55, 1043-1050.

Verhulp, E., van Rietbergen, B. and Huiskes, R. 2008. Load distribution in the healthy and osteoporotic human proximal femur during a fall to the side. Bone 42, 30-35.

Vestergaard, P., Rejnmark, L. and Mosekilde, L. 2009. Diabetes and its complications and their relationship with risk of fractures in type 1 and 2 diabetes. Calcif Tissue Int 84, 45-55.

Thomas, C.D.L., Mayhew, P.M., Power, J., Poole, K.E., Loveridge, N., Clement, J.G., Burgoyne, C.J. and Reeve, J. 2009. Femoral neck trabecular bone: loss with aging and role in preventing fracture. J Bone Miner Res 24, 1808-1818.

Ural, A. and Vashishth, D. 2007. Effects of intracortical porosity on fracture toughness in aging human bone: a μ CT-based cohesive finite element study. J Biomech Eng 129(5):625-31.

van Daele, P.L., Stolk, R.P., Burger, H., Algra, D., Grobbee, D.E., Hofman, A., Birkenhäger, J.C. and Pols, H.A. 1995. Bone density in non-insulin-dependent diabetes mellitus. The Rotterdam Study. Ann Intern Med 122, 409-414.

Van Rietbergen, B., Huiskes, R., Eckstein, F. and Rüegsegger, P. 2003b. Trabecular bone tissue strains in the healthy and osteoporotic human femur. J Bone Miner Res 18, 1781-1788.

Vestergaard, P., Rejnmark, L. and Mosekilde, L. 2009. Diabetes and its complications and their relationship with risk of fractures in type 1 and 2 diabetes. Calcif Tissue Int 84, 45-55.

Viggers, R., Starup-Linde, J. and Vestergaard, P. 2023. Discrepancies in type of first major osteoporotic fracture and anti-osteoporotic therapy in elderly people with type 2 diabetes mellitus: A retrospective Danish cohort study. Bone 171, 116745.

Vogt, M.T., Cauley, J.A., Tomaino, M.M., Stone, K., Williams, J.R. and Herndon, J.H. 2002. Distal radius fractures in older women: a 10-year follow-up study of descriptive characteristics and risk factors. The study of osteoporotic fractures. J Am Geriatr Soc 50, 97-103.

von Ferber, L., Köster, I. and Hauner, H. 2007. Medical costs of diabetic complications total costs and excess costs by age and type of treatment results of the German CoDiM Study. Exp Clin Endocrinol Diabetes. 115, 97-104.

Warriner, A.H., Patkar, N.M., Curtis, J.R., Delzell, E., Gary, L., Kilgore, M. and Saag, K. 2011. Which fractures are most attributable to osteoporosis? J Clin Epidemiol 64, 46-53.

Williamson, S., Landeiro, F., McConnell, T., Fulford-Smith, L., Javaid, M.K., Judge, A. and Leal, J. 2017. Costs of fragility hip fractures globally: a systematic review and meta-regression analysis. Osteoporos Int 28, 2791-2800.

Wölfel, E.M., Jähn-Rickert, K., Schmidt, F.N., Wulff, B., Mushumba, H., Sroga, G.E., Püschel, K., Milovanovic, P., Amling, M., Campbell, G.M., Vashishth, D. and Busse, B. 2020. Individuals with type 2 diabetes mellitus show dimorphic and heterogeneous patterns of loss in femoral bone quality. Bone 140, 115556.

Wright, N.C., Saag, K.G., Curtis, J.R., Smith, W.K., Kilgore, M.L., Morrisey, M.A., Yun, H., Zhang, J. and Delzell, E.S. 2012. Recent trends in hip fracture rates by race/ethnicity among older US adults. J Bone Miner Res 27, 2325-2332.

Yadav, R. N., Sihota, P., Uniyal, P., Neradi, D., Bose, J. C., Dhiman, V.et al. 2021. Prediction of mechanical properties of trabecular bone in patients with type 2 diabetes using damage based finite element method. J Biomech 123, 110495.

Yin, B., Guo, J.L., Wang, J.Z., Li, S., Liu, Y.K. and Zhang, Y.Z. 2019. Bone Material Properties of Human Phalanges Using Vickers Indentation. Orthop Surg 11, 487-492.

Yokomoto-Umakoshi, M., Kanazawa, I., Kondo, S. and Sugimoto, T. 2017. Association between the risk of falls and osteoporotic fractures in patients with type 2 diabetes mellitus. Endocr J 64, 727-734.

Zani, L., Erani, P., Grassi, L., Taddei, F. and Cristofolini, L. 2015. Strain distribution in the proximal Human femur during in vitro simulated sideways fall. J Biomech 48, 2130-2143.

Zebaze, R. and Seeman, E. 2015. Cortical bone: a challenging geography. J Bone Miner Res 30, 24-29.

Zimmermann, E.A., Schaible, E., Bale, H., Barth, H.D., Tang, S.Y., Reichert, P., et al. 2011. Age-related changes in the plasticity and toughness of human cortical bone at multiple length scales. Proc Natl Acad Sci U S A 108, 14416-14421.

Publications and conference abstracts derived from the thesis:

In extenso original papers:

1. Cirovic A, Vujacic M, Petrovic B, Cirovic A, Zivkovic V, Nikolic S, Djonic D, Bascarevic Z, Djuric M, Milovanovic P. Vascular complications in individuals with type 2 diabetes mellitus additionally increase the risk of femoral neck fractures due to deteriorated trabecular microarchitecture. Calcif Tissue Int. 2022;110(1):65-73. doi: 10.1007/s00223-021-00894-5. **M22, IF 4.333**
2. Cirovic A, Jadzic J, Djukic D, Djonic D, Zivkovic V, Nikolic S, Djuric M, Milovanovic P. Increased cortical porosity, reduced cortical thickness, and reduced trabecular and cortical microhardness of the superolateral femoral neck confer the increased hip fracture risk in individuals with type 2 diabetes. Calcif Tissue Int. 2022;111(5):457-465. doi: 10.1007/s00223-022-01007-6 **M22, IF 4.333**
3. Cirovic A, Cirovic A, Djonic D, Zivkovic V, Nikolic S, Djuric M, Milovanovic P. Three-dimensional microstructural basis for differential occurrence of subcapital versus basicervical hip fractures in men. Calcif Tissue Int. 2020;107(3):240-248. doi: 10.1007/s00223-020-00717-z. **M22, IF 4.33**
4. Cirovic A, Cirovic A, Djukic D, Djonic D, Zivkovic V, Nikolic S, Djuric M, Milovanovic P. Three-dimensional mapping of cortical porosity and thickness along the superolateral femoral neck in older women. Sci Rep. 2022;12(1):15544. doi: 10.1038/s41598-022-19866-2. **M21 IF 4.997**
5. Cirovic A, Schmidt NF, Jadzic J, Vujacic M, Sihota P, Petrovic B, Djukic D, Zivkovic V, Bascarevic Z, Nikolic S, Djonic D, Djuric M, Busse B, Milovanovic P. Altered osteocyte lacunar density pattern, trabecular mineralization imbalance in the femoral neck, and decreased trabecular microhardness in the trabeculae of the femoral head as microstructural indicators of higher fracture risk in individuals with type 2 diabetes mellitus –*submitted*
6. Cirovic A, Milovanovic P. Mikroarhitekturni aspekti povećane koštane fragilnosti osoba sa dijabetesom tipa 2. Medicinski podmladak 2023; DOI 10.5937/mp75-44905. **M52**

Abstracts presented at a congresses:

1. Cirovic A, Djukic D, Cirovic A, Zivkovic V, Djonic D, Nikolic S, Djuric M, Milovanovic P. Microstructural alterations of superolateral femoral neck cortical bone in men with diabetes as a possible basis for fragility fractures: a cadaveric study. ECTS 2022, Helsinki, Bone Reports, Volume 16, Supplement, May 2022, 101341.
2. Cirovic A, Cirovic A, Vujacic M, Bascarevic Z, Djonic D, Djuric M, Milovanovic P. Distinct phenotypes of bone fragility in patients with type 2 diabetes mellitus depending on the presence of vascular complications: A study of three-dimensional trabecular microarchitecture. Abstracts of the ECTS Congress 2021, 48th European Calcified Tissue Society Congress, ECTS 2021 Digital Congress, 6-8 May 2021; Bone Rep 2021; 14S.
3. Cirovic A, Cirovic A, Zivkovic V, Nikolic S, Milovanovic P, Djuric M, Djonic D. High-resolution three-dimensional microstructural analysis of cortex of the superolateral femoral neck in men reveals critical subregion. Abstracts of the ECTS Congress 2021, 48th European Calcified Tissue Society Congress, ECTS 2021 Digital Congress, 6-8 May 2021; Bone Rep 2021; 14S.

4. Ćirović A. Femoral trabecular microarchitecture, mineralization, and microhardness in individuals with type 2 diabetes mellitus and healty controls subjects. 7th Congress of Serbian Anatomical Society of Serbia. Belgrade, 9-11th December, 2021
5. Cirovic A, Jadzic J, Djukic D, Zivkovic V, Djonic D, Nikolic S, Djuric M, Busse B, Milovanovic P. Altered pattern of osteocyte number, distribution, and viability as a potential contributor to increased fragility at the femoral neck of individuals with type 2 diabetes. Abstracts of the ECTS Congress 2023, 50th European Calcified Tissue Society Congress 15 – 18 April 2023.

Кратка биографија аутора

Др Александар Ћировић је рођен 17. јула 1990. године у Београду. Основну школу као и природно-математички смер гимназије завршио је у Трстенику. Медицински факултет Универзитета у Београду уписао је школске 2009/10, а дипломирао је 15. 10. 2015. са просечном оценом 9,39.

Докторске студије, на модулу Биологија скелета, уписао је на Медицинском факултету Универзитета У Београду школске 2016/17. У звање сарадника у настави на катедри за ужу област Анатомија изабран је 13.07.2016. а реизабран 13.07.2017. Од 2018. ради на Институту за Анатомију као асистент. Добитник је награде "*Central Eastern Europe Travel Award* (2022)" коју додељује Евроско удружење за калцификована ткива (*European Calcified Tissue Society*). Учествовао је или активно учествује у два пројекта Фонда за Науку Републике Србије, "Effects of diabetes mellitus on osteocytic, neural and vascular networks in bone: implications for increased fracture susceptibility at the proximal femur - DiaBoNet" и " Changes in bone structure and composition leading to increased fracture risk in aged population with chronic comorbidities - BoFraM". Александар Ћировић је аутор и коаутор у више радова публикованих у часописима индексимарим у Journal Citation Reports (JCR) листи.

Author's Brief Biography

Dr. Aleksandar Ćirović was born on July 17, 1990, in Belgrade. He completed his primary education as well as the gymnasium in Trstenik. He enrolled in the Medical Faculty of the University of Belgrade in the academic year 2009/10 and graduated on October 15, 2015, with an average grade of 9.39.

He entered doctoral studies at the Faculty of Medicine (Module: Skeletal biology) of the University of Belgrade in the academic year 2016/17. He was elected as a teaching assistant in the Department of Anatomy on July 13, 2016, and re-elected on July 13, 2017. Since 2018, he has been working at the Institute of Anatomy as an assistant. He received the "Central Eastern Europe Travel Award (2022)" awarded by the European Calcified Tissue Society. He has participated or is actively participating in two projects funded by the Science Fund of the Republic of Serbia: "Effects of diabetes mellitus on osteocytic, neural, and vascular networks in bone: implications for increased fracture susceptibility at the proximal femur - DiaBoNet" and "Changes in bone structure and composition leading to increased fracture risk in the aged population with chronic comorbidities - BoFraM." Aleksandar Ćirović is an author and co-author of multiple papers published in journals indexed in the Journal Citation Reports (JCR) list.

образац изјаве о ауторству

Изјава о ауторству

Име и презиме аутора: Александар Ћировић

Број индекса: 5001/16

Изјављујем

да је докторска дисертација под насловом

Промене у микроструктури као основа повећане фрагилности врата бутне кости особа са тип 2 дијабетесом
(енгл. Microstructural basis of increased bone fragility in the femoral neck of individuals with type 2 diabetes mellitus)

- резултат сопственог истраживачког рада;
- да дисертација у целини ни у деловима није била предложена за стицање друге дипломе према студијским програмима других високошколских установа;
- да су резултати коректно наведени и
- да нисам кршио/ла ауторска права и користио/ла интелектуалну својину других лица.

Потпис аутора

У Београду, 04.09.2023.

_____

образац изјаве о истоветности штампане и електронске верзије докторског рада

Изјава о истоветности штампане и електронске верзије докторског рада

Име и презиме аутора: Александар Ћировић

Број индекса: 5001/16

Студијски програм: Докторксе Академске Студије,Молуд: Биологија скелета
Наслов рада: Промене у микроструктури као основа повећане фрагилности врата бутне кости особа са тип 2 дијабетесом
(енгл. Microstructural basis of increased bone fragility in the femoral neck of individuals with type 2 diabetes mellitus)

Ментор: проф. др Петар Миловановић

Изјављујем да је штампана верзија мог докторског рада истоветна електронској верзији коју сам предао ради похрањивања у **Дигиталном репозиторијуму Универзитета у Београду.**

Дозвољавам да се објаве моји лични подаци везани за добијање академског назива доктора наука, као што су име и презиме, година и место рођења и датум одбране рада.

Ови лични подаци могу се објавити на мрежним страницама дигиталне библиотеке, у електронском каталогу и у публикацијама Универзитета у Београду.

Потпис аутора

У Београду, 04.09.2023.

_____

образац изјаве о коришћењу

Изјава о коришћењу

Овлашћујем Универзитетску библиотеку „Светозар Марковић“ да у Дигитални репозиторијум Универзитета у Београду унесе моју докторску дисертацију под насловом:

Промене у микроструктури као основа повећане фрагилности врата бутне кости особа са тип 2 дијабетесом
(енгл. Microstructural basis of increased bone fragility in the femoral neck of individuals with type 2 diabetes mellitus)

која је моје ауторско дело.

Дисертацију са свим прилозима предао/ла сам у електронском формату погодном за трајно архивирање.

Моју докторску дисертацију похрањену у Дигиталном репозиторијуму Универзитета у Београду и доступну у отвореном приступу могу да користе сви који поштују одредбе садржане у одабраном типу лиценце Креативне заједнице (Creative Commons) за коју сам се одлучио/ла.

1. Ауторство (CC BY)

2. Ауторство – некомерцијално (CC BY-NC)

3. Ауторство – некомерцијално – без прерада (CC BY-NC-ND)

4. Ауторство – некомерцијално – делити под истим условима (CC BY-NC-SA)

5. Ауторство – без прерада (CC BY-ND)

6. Ауторство – делити под истим условима (CC BY-SA)

(Молимо да заокружите само једну од шест понуђених лиценци. Кратак опис лиценци је саставни део ове изјаве).

Потпис аутора

У Београду, 04.09.2023.

_____